

Muzhikyan, Aramazd et al.

Article

The 2017 ISO New England System Operational Analysis and Renewable Energy Integration Study (SOARES)

Energy Reports

Provided in Cooperation with:

Elsevier

Suggested Citation: Muzhikyan, Aramazd et al. (2019) : The 2017 ISO New England System Operational Analysis and Renewable Energy Integration Study (SOARES), Energy Reports, ISSN 2352-4847, Elsevier, Amsterdam, Vol. 5, pp. 747-792, <https://doi.org/10.1016/j.egy.2019.06.005>

This Version is available at:

<https://hdl.handle.net/10419/243627>

Standard-Nutzungsbedingungen:

Die Dokumente auf EconStor dürfen zu eigenen wissenschaftlichen Zwecken und zum Privatgebrauch gespeichert und kopiert werden.

Sie dürfen die Dokumente nicht für öffentliche oder kommerzielle Zwecke vervielfältigen, öffentlich ausstellen, öffentlich zugänglich machen, vertreiben oder anderweitig nutzen.

Sofern die Verfasser die Dokumente unter Open-Content-Lizenzen (insbesondere CC-Lizenzen) zur Verfügung gestellt haben sollten, gelten abweichend von diesen Nutzungsbedingungen die in der dort genannten Lizenz gewährten Nutzungsrechte.

Terms of use:

Documents in EconStor may be saved and copied for your personal and scholarly purposes.

You are not to copy documents for public or commercial purposes, to exhibit the documents publicly, to make them publicly available on the internet, or to distribute or otherwise use the documents in public.

If the documents have been made available under an Open Content Licence (especially Creative Commons Licences), you may exercise further usage rights as specified in the indicated licence.



<https://creativecommons.org/licenses/by-nc-nd/4.0/>



Research paper

The 2017 ISO New England System Operational Analysis and Renewable Energy Integration Study (SOARES)



Aramazd Muzhikyan, Steffi O. Muhanji, Galen D. Moynihan, Dakota J. Thompson, Zachary M. Berzolla, Amro M. Farid*

Thayer School of Engineering at Dartmouth, 14 Engineering Drive Hanover, NH 03755, USA

ARTICLE INFO

Article history:

Received 11 December 2018
Received in revised form 8 March 2019
Accepted 19 June 2019
Available online xxxx

Keywords:

Renewable energy integration
Operating reserves
Unit commitment
Economic dispatch
ISO New England
Enterprise control

ABSTRACT

The bulk electric power system in New England is fundamentally changing. The representation of nuclear, coal and oil generation facilities is set to dramatically fall, and natural gas, wind and solar facilities will come to fill their place. The introduction of variable energy resources (VERs) like solar and wind, however, necessitates fundamental changes in the power grid's dynamic operation. VER forecasts are uncertain, and their profiles are intermittent; thus requiring greater quantities of operating reserves. This paper describes the methodology and the key findings of the 2017 ISO New England System Operational Analysis and Renewable Energy Integration Study (SOARES). This study was commissioned by the ISO New England stakeholders to investigate the effect of several scenarios of varying generation mix on normal operating reserves. The project was conducted using the holistic assessment approach called the Electric Power Enterprise Control System (EPECS) simulator. The study finds a minimal impact on current normal operating conditions in the ISO-NE system for scenarios with relatively low penetration of VERs. Nevertheless, for scenarios with a significant presence of VERs, the system may require additional amounts of both upward and downward load following reserves and upward and downward ramping reserves to effectively maintain reliable operations. In these scenarios, the curtailment of semi-dispatchable resources also becomes an integral part of balancing performance; in part to complement operating reserves and in part to mitigate the topological limitations of the system. Indeed, the integration of significant amounts of VERs in relatively remote regions significantly increases the potential of congestion on several key interfaces. In many of these scenarios, the system experiences heavy saturations of regulation reserves and their increase would enhance the response to residual imbalances. The concludes with final insights into the emerging roles of curtailment, energy storage, and demand response as integral parts of normal balancing performance.

© 2019 Published by Elsevier Ltd. This is an open access article under the CC BY-NC-ND license (<http://creativecommons.org/licenses/by-nc-nd/4.0/>).

1. Introduction

1.1. ISO New England's rapidly evolving resource mix

The resource mix of ISO New England (ISO-NE) is rapidly changing. Fig. 1 shows the evolution of its generation mix from 2000 to 2017 (van Welie, 2018). As of 2015, over 9% of the total generation came from renewable energy sources where 3.2% was from wind and 0.9% from solar PV (ISO New England, 2017a). This percentage is expected to grow as the levelized cost of

solar PV and wind installations continues to fall (UVIG, 2017). In the meantime, the representation of nuclear, coal, and oil plants in the generation portfolio is set to dramatically fall for two complementary reasons. First, the emergence of low cost natural gas generation in recent years (IEA, 2017) has partially supplanted these facilities in the economic merit order. Second, these facilities have an average age of over 30 years (ISO New England, 2016c) and are likely to be retired in the coming years. For example, nuclear retirements are expected to bring down the percentage of nuclear generation to 10% (ISO New England, 2017d) by 2025 as compared to the 31% in 2017 (van Welie, 2018). These retirements are likely to be replaced by more wind and natural gas resources in the overall resource mix. The percentage of natural gas powered generation is expected to account for over 56% of the overall generation in 2025 (ISO New England, 2017d). Furthermore, renewable portfolio requirements of various member states have also driven the ISO-NE resource mix to include more VERs (Rourke, 2015). These requirements vary by state.

* Corresponding author.

E-mail addresses: aramazd.muzhikyan.th@dartmouth.edu (A. Muzhikyan), steffi.o.muhanji.th@dartmouth.edu (S.O. Muhanji), galen.d.moynihan.th@dartmouth.edu (G.D. Moynihan), dakota.j.thompson.th@dartmouth.edu (D.J. Thompson), zachary.m.berzolla.th@dartmouth.edu (Z.M. Berzolla), amfarid@dartmouth.edu (A.M. Farid).

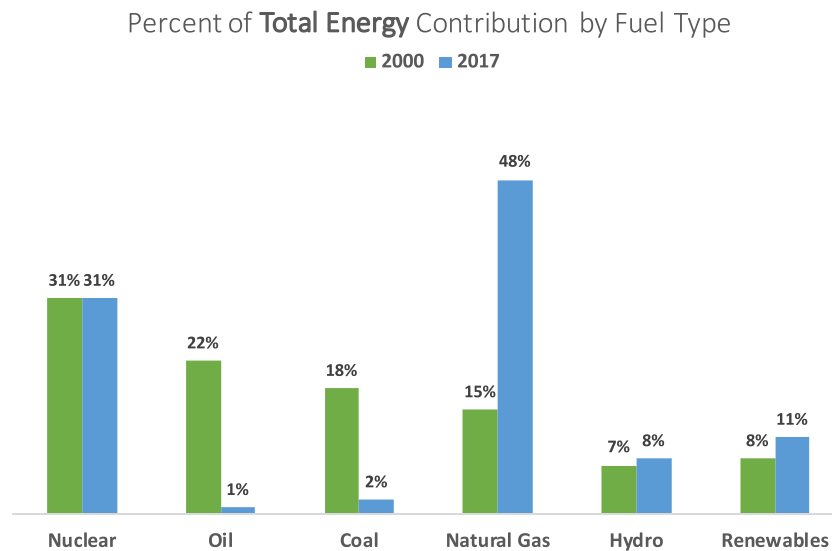


Fig. 1. ISO New England generation mix in 2000 and 2017 (van Welie, 2018).

Some states, like Vermont, require up to 75% of renewable energy generation including large-scale hydro (van Welie, 2018). This supply-side change in resource mix is occurring simultaneously with demand-side investment in energy efficiency measures. It is estimated that over \$7.1 billion (Rourke, 2015) will be invested in energy efficiency between 2019 and 2024 in addition to over \$4.9 billion already spent between 2009 and 2013 (van Welie, 2018).

This changing resource mix, and particularly the introduction of VERs, is set to cause fundamental changes in the power grid's dynamic operations (Farid et al., 2015). As shown in Fig. 2, traditional power systems have often been built on the basis of an electrical energy value chain which consists of relatively few, centralized, and actively controlled thermal power generation facilities (von Meier, 2006; Schavemaker and Van der Sluis, 2008). These serve a relatively large number of distributed, stochastic electrical loads (von Meier, 2006; Schavemaker and Van der Sluis, 2008). Furthermore, the dominant operating paradigm and goal for these operators and utilities was to always serve the consumer demanded load with maximum reliability at whatever the production cost (Gellings, 1985). Over the years, system operators and utilities have improved their methods to achieve this task (Wood and Wollenberg, 2014; Gomez-Exposito et al., 2008). Generation dispatch, reserve management and automatic control has matured. Load forecasting techniques have advanced significantly to bring forecast errors to as low as a couple of percent. System security procedures and their associated standards have evolved equally.

The introduction of VERs evolves this status quo. As they are added into the grid, the picture of the generation and demand portfolio gains a third quadrant as shown in the bottom half of Fig. 2. From the perspective of dispatchability, VERs are non-dispatchable in the traditional sense: the output depends on external conditions and are not controllable by the grid operator¹ (Kassakian et al., 2011); except in a downward direction for curtailment. As VERs displace thermal generation units in the overall generation mix, the overall dispatchability of the generation fleet decreases. In regards to forecastability, VERs increase

the uncertainty level in the system (Kassakian et al., 2011). Relative to traditional load, VER forecast accuracy is low, even in the short term (Giebel et al., 2011). The decreased dispatchability coupled with decreased forecastability summarized by Fig. 2 calls for holistic assessment of the electric power system as it evolves.

The integration of VERs will bring about fundamental changes that will necessitate a structured and holistic view for assessing the power system as it evolves. While existing regulatory codes and standards will continue to apply (Anonymous et al., 2012; Mohseni and Islam, 2012; Diaz-Gonzalez et al., 2014), it is less than clear how the holistic behavior of the grid will change or how reliability will be assured. Furthermore, it is important to assess the degree to which control, automation, and information technology are truly necessary to achieve the desired level of reliability. Thirdly, it is unclear what value for cost these technical integration decisions can bring. From a societal perspective, and beyond simply variable energy integration, smart grid initiatives have been priced at several tens of billions of dollars in multiple regions (Gellings et al., 2011; Easton et al., 2012). Therefore, there is a need to thoughtfully quantify and evaluate the steps taken in such a large scale technological migration of the existing power grid.

1.2. The need for holistic techno-economic assessment methods

This work, thus, argues that a future electricity grid with a high penetration of VERs requires holistic assessment methods. This argument is structured as shown in Fig. 3. On one axis, the electrical power grid is viewed as a cyber-physical system. That is, assessing the physical integration of VERs *must* be taken in the context of the control, automation, and information technologies that would be added to mitigate and coordinate their effects. On another, it is an energy value chain spanning generation and demand. On the third axis, it contains dispatchable as well as stochastic energy resources. These axes holistically define the scope of the power grid system which must meet competing techno-economic objectives. Power grid technical objectives are often viewed as balancing operations, line congestion management and voltage management (Gomez-Exposito et al., 2008). Economically speaking, the investment decision for a given technology, be it VERs or their associated control, must be assessed against the changes in reliability and operational cost. These economic and control technologies will later be viewed from the lens of dynamic properties including dispatchability, flexibility and

¹ In recent years, significant efforts in both academic and industrial research and development have advanced the potential for variable energy resources to provide ancillary services (Diaz-Gonzalez et al., 2014; Mohseni and Islam, 2012; Anonymous et al., 2012). However, these technologies have yet to become mainstream in the existing fleet of solar and wind generation facilities. This work, therefore, assumes that VERs are truly variable.



Past:	Generation/Supply	Load/Demand
	Thermal Units: (Few, Well-Controlled, Dispatchable Resources)	Conventional Loads: (Fairly Slow Moving, Highly Predictable, Always Served)
Future:	Generation/Supply	Load/Demand
	Well-Controlled & Dispatchable Thermal Units: (Potential Erosion of Capacity Factor) 	Conventional Loads: (Fairly Slow Moving, Highly Predictable, Always Served)
	Stochastic/ Forecasted Solar & Wind Generation: (Variability can cause unmanaged grid imbalances) 	

Fig. 2. The evolution of the power system (Farid and Muzhikyan, 2013).

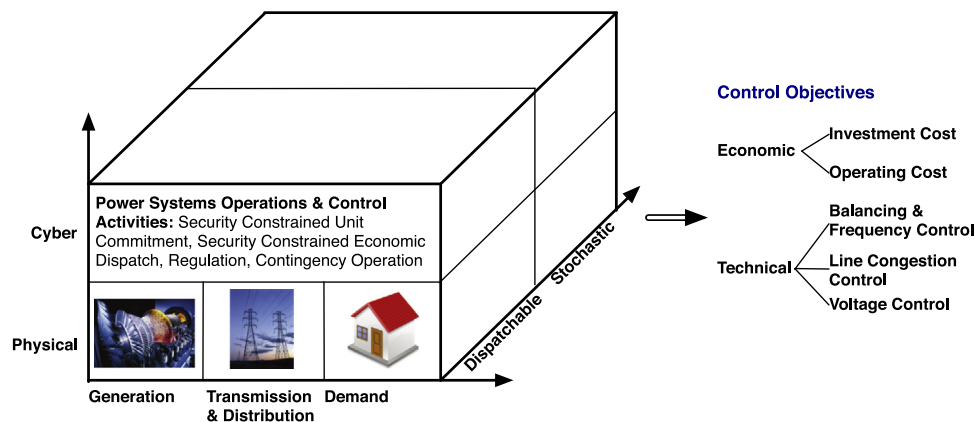


Fig. 3. Enterprise control as guiding assessment structure for power grids.

forecastability. Naturally, such holistic assessment methods will represent an evolution of existing methods. This work thus seeks to draw from the trends and recommendations in the existing literature and frame them within the structure of Fig. 3.

This ongoing evolution of the power grid can already be viewed through the lens of “enterprise control”. Originally, the concept of enterprise control (Martin, 2012; ANSI-ISA, 2005) was developed in the manufacturing sector out of the need for greater agility (Sanchez and Nagi, 2001; Gunasekaran, 1998) and flexibility (Beach et al., 2000; De Toni and Tonchia, 1998; Pels et al., 1997) in response to increased competition, mass-customization and short product life cycles. Automation became viewed as a technology to not just manage the fast dynamics of manufacturing processes but also to integrate (Lapalus et al., 1995) that control with business objectives. Over time, a number of integrated enterprise system architectures (Williams et al., 2001; Kosanke et al., 1999) were developed coalescing in the current ISA-S95 standard (ANSI-ISA, 2000, 2005). Analogously, recent work on power grids has been proposed to update operation control center architectures (Wu et al., 2005) and integrate the associated communication architectures (Yan et al., 2013). The recent NIST interoperability initiatives further demonstrate the trend towards integrated and holistic approaches to power grid operation (Anonymous, 2010). These initiatives form the foundation for further and more advanced holistic control of the grid (Amin, 2001, 2006, 2008, 2011; McArthur et al., 2012).

Given the emergence of these trends in New England, ISO-NE has initiated the 2017 System Operational Analysis and Renewable Energy Integration Study (SOARES). This project serves as the last of three Phase II projects of the 2016 Economic Study (Henderson, 2016; Coste, 2016). Given their extensive publications on

the topic, ISO-NE has selected the Laboratory for Intelligent Integrated Networks for Engineering Systems (LIINES) at the Thayer School of Engineering at Dartmouth to conduct the study. This report describes the project’s methodology as a whole emphasizing a novel, but now extensively published (Muzhikyan et al., 2015b,a, 2016b, 2014b, 2015c,d, 2016a, 2014a), holistic assessment approach called the Electric Power Enterprise Control System (EPECS) simulator. It also situates this new approach relative to the existing renewable energy integration literature. To maintain continuity, the project specifically seeks to study ISO-NE operations in the years 2025 and 2030 for the six scenarios identified during Phase I of the 2016 Economic Study request. The study will specifically address quantifying operating reserve requirements, ramp rates over hourly and sub-hourly periods, and identify periods of insufficient operating reserves.

1.3. Research scope and questions

This study was commissioned by ISO New England as a means of addressing the reliability concerns presented by the evolving generation base within the region. The scope of this study addresses six 2025 *hypothetical* scenarios and six 2030 *hypothetical* scenarios that were agreed upon consensually among ISO New England stakeholders. These scenarios provide further analysis for ISO-NE stakeholders without necessarily reflecting ISO-NE’s prediction of the future New England electric power systems. They are described in Section 4. The study includes the following research questions that are answered in Section 5 entitled Results. What is the impact of the 12 predefined scenarios on:

- ...the resulting quantities of load following reserves?

- ...the resulting ramping reserves?
- ...the curtailment of semi-dispatchable resources?
- ...the interface and tie-line performance?
- ...the regulation reserves?
- ...the balancing performance?

This study fits within the three critical roles ISO New England performs to ensure reliable electricity at competitive prices (van Welie, 2018):

- **Grid Operation:** Coordinate and direct the flow of electricity over the region's high voltage transmission system.
- **Market Administration:** Design, run, and oversee the markets where wholesale electricity is bought and sold.
- **Power System Planning:** Study, analyze, and plan to make sure New England's electricity needs will be met over the next 10 years.

As such, the focus of the study is to inform stakeholders in regards to these agreed upon scenarios.

In light of the ISO New England mission, this study is *not* meant to promote renewable energy resources or any other single type of energy resource. This report does *not* seek to answer resource-specific questions such as:

- What is the maximum penetration rate of renewable energy resources that can be reliably integrated in the New England region?
- How much natural gas generation is required to achieve a desired level of system-wide flexibility (i.e. ramp rate)?
- How does the inflexibility of nuclear generation limit reliable balancing operations?

Each of these questions, due to their resource-specificity, imply a certain preference for one type of energy resource over another. Instead, this report focuses on the system-level results pertaining to the 12 scenarios mentioned above. From such a presentation, the reader may conclude whether certain resource *mixes* are more or less likely to lead to reliable operation.

1.4. Report outline

The rest of this report is structured as follows. Section 2 provides a review of the methodological adequacy of existing renewable energy integration studies and the methodological characteristics of the EPECS simulator. Section 3 presents the implementation technical details of the EPECS simulator. Section 4 describes the ISO New England data used for this study, and Section 5 analyzes the case study results. Finally, the report is brought to a conclusion in Section 6.

2. Background

This section describes the methodological characteristics of the 2016 ISO New England Economic Study, the enterprise control assessment method used in this study and other existing renewable energy integration studies found in the literature.

2.1. Methodological characteristics of the 2016 ISO New England economic study

The 2016 ISO New England Economic Study was conducted at the request of the New England Power Pool (NEPOOL), and examines resource-expansion scenarios of the regional power system and the potential effects of these different future changes on resource adequacy, operating and capital costs, and options for meeting environmental policy goals (ISO New England, 2017b).

The study presents a common framework for NEPOOL participants, regional electricity market stakeholders, policymakers, and consumers, information, analyses, and observations on the following:

- The potential impacts on the ISO New England markets of implementing public policies in the New England states
- Projected energy market revenues, and the contribution of these revenues to the generic fixed costs of new generation, for various generation types under particular sets of assumptions
- The potential impacts, under the status-quo forecast and compared with the public policy overlay, on system reliability and operability, resource costs and revenues, total cost of supplying load, and emissions in New England

The metrics studied include production costs, load-serving entity (LSE) energy expenses, locational marginal prices (LMPs), generic capital costs and annual carrying charges (ACCs) for each resource type, transmission-expansion costs, generation by fuel type and the emissions associated with each type, and the effects of transmission-interface constraints that may bind economic power flows.

The analyses were conducted using ABB's GridView program that calculates least-cost transmission-security-constrained unit commitment and economic dispatch under differing sets of assumptions and minimizes production costs for a given set of unit characteristics (ABB Inc. Electric Systems Consulting). The program can explicitly model a full network, but the New England study model used a "pipe and bubble" format, with "pipes" representing transmission interfaces connecting the "bubbles" representing the various planning areas. The ISO New England system was modeled as a constrained single area for unit commitment, and regional resources were economically dispatched in the simulations to respect the assumed transmission system security constraints under normal and contingency conditions. Depending on the case, the model dispatched up to 900 units (new and existing) in New England. For each scenario's set of resources (with their various operating characteristics), the simulation "dispatched" power plants to meet different levels of customer demand in every hour of the year being analyzed. These simulations established a wide array of hypothetical data about how the electric power system "performed" in terms of reliability, economics, and environmental indicators and the effects of transmission system constraints.

2.2. Methodological characteristics of existing renewable energy integration studies

A review of existing renewable energy integration studies is conducted from the perspective of the guiding structure found in Fig. 3. Collectively, the renewable energy integration studies have many similarities (Ela et al., 2009; Holttinen et al., 2012a, 2013; Brouwer et al., 2014; Daniel et al., 2015; Hannele, 2018; Holttinen, 2018; IEA, 2018; Bloom et al., 2016). They generally apply combined unit-commitment and economic dispatch (UCED) models to assess the additional operating costs of renewable energy integration (GE Energy, 2010; Lew et al., 2013; GE Energy, 2013; PACIFICORP, 2010; Shlatz et al., 2011; GE-Energy, 2010; Corporation and Association, 2010; Johnson et al., 2014; University of Hawaii and Anonymous, 2011; EnerNex and Corporation, 2010; Report et al., 2012; EWIS, 2010; Hoflich et al., 2010). Fewer studies add a model of regulation as a separate ancillary service. These three enterprise control layers are conducted primarily to assess the additional operating cost of renewable energy integration and are not integrated with a model of the physical grid to calculate technical variables such as potential power

grid imbalances (Brooks et al., 2002; Ummels, 2009; Brouwer et al., 2014). One often cited concern is that these simulations do not correspond to the existing enterprise control practice. For example, time steps, market structure and physical constraints should correspond to the operating reality (Georgilakis, 2008; Soder et al., 2008; Holttinen et al., 2012a, 2013; Brouwer et al., 2014). In the case of market time step, it has been confirmed both numerically (Bird et al., 2012; Holttinen et al., 2012a, 2013; Muzhikyan et al., 2015a,b) as well as analytically (Muzhikyan et al., 2016a, 2014b, 2015d,c) to affect power grid imbalances and costs. Such a conclusion inextricably ties power system operation and control to their associated policies and regulations.

In contrast, the assessment of additional operating reserve requirements is mostly done by using statistical methods (Ela et al., 2009; Holttinen et al., 2012a, 2013; Brouwer et al., 2014) that are generally some variation on the theme found in Holttinen et al. (2008). The differences between these approaches has been classified by Brouwer et al. (2014). In general, the standard deviation σ of potential imbalances is calculated using the probability distribution of net load or forecast error. The load following and regulation reserve requirements are then defined to cover appropriate confidence intervals of the distribution based on the experience of power system operators and existing standards. A detailed discussion on the definition and types of operating reserves is provided in Section 3.3. Normally, load following is taken to equal to 2σ (Holttinen et al., 2008; Robitaille et al., 2012) to comply with the North American Electric Reliability Corporation (NERC) balancing requirements: NERC defines the minimum score for Control Performance Requirements 2 (CPS2) equal to 90% (NERC, 2012). Other integration studies have used a 3σ confidence interval (Aigner et al., 2012; Ummels et al., 2007) to correspond to the industry standard of 95% (Halamay et al., 2011). Based on the experience of power system operators, regulation is normally taken to be between 4σ and 6σ (Holttinen et al., 2008; Robitaille et al., 2012; Hansen and Papalexopoulos, 2012).

With respect to timescales, not all studies consider multiple timescales of operation. However, in order to characterize a power system's imbalances accurately, it is necessary to use a multi-timescale analysis. A single timescale would only capture part of the variability of the net load and leave out either slower or faster phenomena. For example, Halamay et al. (2011) does not consider regulation because the available data has 10 min resolution. Luickx et al. (2009), Albadi and El-Saadany (2011) implement only unit commitment models, according to the assumption that wind integration has the biggest impact on unit commitment. Furthermore, another concern is the usage and treatment of different power system timescales in the integration studies. Load following and regulation reserves operate at different but overlapping timescales. Net load variability as a property exists in all timescales, although with changing magnitudes. Forecast error, on the other hand, appears in two timescales: 1 h (day-ahead forecast error) and 5–15 min (short term forecast error). Thus, VER intra-hour variability and day-ahead forecast error are relevant to load following reserve requirements. Meanwhile, 5–15 min variations and short-term forecast error are relevant to regulation reserve requirements. This division of impacts is not carefully addressed in the literature.

In conclusion, renewable energy integration studies, as a collective body of literature, give a much more holistic understanding of the power grid and its potential evolution in the future. While these studies continue to evolve, they may require incorporation of certain methodological changes to better reflect the current need for more holistic assessment methods. Particularly, in regards to balancing operation, they use statistical methods for which there is a lack of consensus and which are based

upon questionable assumptions. It is likely that the assessment of reserves will ultimately shift to simulation-based and analytical methods. UCED simulations form an integral piece of most integration studies and are likely to remain so. However, several authors have already advocated for the need to maintain the coherence between market operating procedures and the simulations.

2.3. Methodological characteristics of enterprise control assessment

The methodological limitations of the existing renewable energy integration literature described in the previous section can be addressed by a framework for holistic power grid enterprise control assessment. In such a way, the variability of renewable energy resources can be viewed as an input disturbance which the (enterprise) power system systematically manages to deliver attenuated power system imbalances. Consequently, the power from renewable energy sources is modeled in terms of its key characteristics, namely penetration level, forecast errors, and variability. Such an approach is in agreement with several recommendations in the literature for integrated approaches (Ummels, 2009; Soder et al., 2008; Holttinen et al., 2012a, 2013). Furthermore, one work advocates the role of custom-built simulators to assess the future electricity grid (Podmore and Robinson, 2010). Gathering the discussions from the previous section, such an approach fulfills the following requirements:

- allows for an evolving mixture of generation and demand as energy resources; be they dispatchable, semi-dispatchable, variable, or must-run.
- allows for the simultaneous study of generation, transmission and load
- allows for the time domain simulation of the convolution of relevant grid enterprise control functions
- allows for the time domain simulation of changes to the power grid topology in the operations time scale
- specifically addresses the holistic dynamic properties of dispatchability, flexibility and forecastability
- represents potential changes in enterprise grid control functions as impacts on these dynamic properties
- accounts for the consequent changes in operating cost and the required investment costs

The first four of these requirements are basically associated with the nature of the power grid itself as it evolves. In the meantime, the next two are associated with the behavior of the power grid in the operations time scale. Finally, the last requirement contextualizes the simulation with cost accounting.

The EPECS simulator used for this study is developed in accordance with such an enterprise control assessment framework. While it is not feasible to incorporate all power system operation processes within a single model, the EPECS simulator captures the ones most relevant to ISO New England balancing operations, namely day-ahead resource scheduling, same-day resource scheduling, real-time balancing operations and regulation service. Most fundamentally, the EPECS methodology is *integrated* and *techno-economic*. Consequently, it has the ability to provide clear techno-economic trade-offs for any changes to the physical power system and its associated layers of control. The detailed description of the EPECS simulator different control layers is presented in Section 3.

3. Methodology: Electric power enterprise control system simulator for ISO New England

3.1. Overview of electric power enterprise control system simulation

This section introduces the Electric Power Enterprise Control System (EPECS) simulator customized for ISO New England's

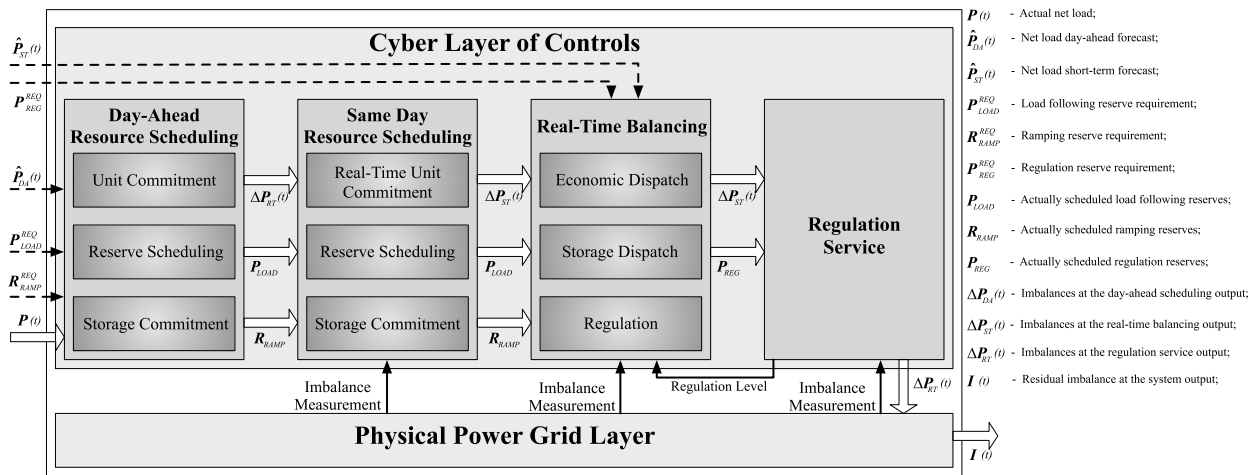


Fig. 4. Architecture of the Electric Power Enterprise Control System (EPECS) simulator customized for ISO New England operations.

operations. Its architecture is graphically depicted in Fig. 4 and may be viewed as an extension of several enterprise control works (Farid et al., 2015; Farid and Muzhikyan, 2013) involving variable energy integration (Muzhikyan et al., 2015a,b, 2016a, 2013a,b, 2014b, 2015d,c, 2016), energy storage (Muzhikyan et al., 2016b, 2014a), and demand response (Jiang et al., 2015b,d,a,c). The simulator includes a physical power grid layer and several layers of primary, secondary, and tertiary enterprise control functions as shown in Fig. 4. These include day-ahead resource scheduling, same-day resource scheduling, real-time balancing, and the regulation service. Such an approach has several advantages. First, the net load $P(t)$ may be viewed as a system disturbance which is systematically rejected by forecasting and relevant enterprise control functions to give a highly attenuated system imbalance time domain signal $I(t)$. Second, it can address the recommendations in the literature (Georgilakis, 2008) to assess the impact of variable generation on operating reserve requirements. Such an approach helps lay the methodological foundation for understanding renewable energy integration independent of the particularities of a physical power system in a given region (Holtinen et al., 2013). Finally, the EPECS simulator is quite flexible. Its layers are modular and may be modified as necessary to assess the impact of a given control function or technology on the time domain simulation.

This section now explains each of the layers in EPECS simulator in detail; focusing on the specific characteristics of ISO-NE's operations. First, Sections 3.2 and 3.3 introduce several fundamental definitions in order to facilitate the usage of the EPECS simulator across different power systems and introduce greater objectivity in this study's methodology. Section 3.4 describes the day-ahead resource scheduling at ISO-NE in the form of a Security Constrained Unit Commitment (SCUC). Section 3.5 then describes same-day resource scheduling in the form of a Real-Time Unit Commitment (RTUC). Section 3.6 then describes real-time balancing operations in the form of a Security Constrained Economic Dispatch (SCED). Section 3.7 describes a pseudo-steady state model of the regulation service. Finally, Section 3.8 describes the physical power grid model.

3.2. Fundamental definitions on variable energy resources

The EPECS simulator has several types of energy resources; including variable, dispatchable, semi-dispatchable, and must-run resources.

Definition 3.2.1 (Variable Resources). Resources that have a stochastic and intermittent power output. Normally, these include wind, solar, run-of-river hydro, and tie-lines are assumed to be variable resources. In this study, all variable resources served as semi-dispatchable resources.

Definition 3.2.2 (Semi-Dispatchable Resources). Energy resources that can be dispatched downwards (i.e curtailed) from their uncurtailed power injection value. When curtailment is allowed for variable resources, they become dispatchable. In this study, wind, solar, run-of-river hydro, and tie-lines are assumed to be semi-dispatchable resources.

Definition 3.2.3 (Must-Run Resources). Energy resources that must run all the time at their maximum output. In this study, nuclear generation units are assumed to be must-run resources.

Definition 3.2.4 (Dispatchable Resources). Energy resources that can be dispatched up and down from their current value of power injection. In this study, all other resources are assumed to be dispatchable.

Within the EPECS simulator, variable energy resources are modeled as a time-dependent exogenous spatially-distributed quantity that contributes directly to the net load. They are described in terms of a number of non-dimensional quantities.

Definition 3.2.5 (Penetration Level (π)). The (aggregated) installed VER capacity P_V^{max} normalized by the system peak load P_L^{peak} (Wang et al., 2012):

$$\pi = \frac{P_V^{max}}{P_L^{peak}} \quad (1)$$

Definition 3.2.6 (VER Capacity Factor (γ)). The average VER power output $P_V(t)$ (e.g., over 1 year period) per installed capacity (Muzhikyan et al., 2014b):

$$\gamma = \frac{\overline{P_V(t)}}{P_V^{max}} \quad (2)$$

Next, it is important to introduce the concept of variability as it is applied to the VERs, the load, and/or the net load. The variability of each of these plays a significant role in balancing operations. Intuitively speaking, variability is associated with the change rates of a given output. In this paper, it is defined as:

Definition 3.2.7 (Variability (A)). Given the choice of the output $P(t)$ (e.g. the VER generation, the load, the net load), the variability is the root-mean-square of that output's rate normalized by the root-mean-square of that output (Muzhikyan et al., 2014b):

$$A = \frac{\text{rms}(dP(t)/dt)}{\text{rms}(P(t))} \quad (3)$$

Since the power spectra of the VER and load have distinctive shapes (Apt, 2007; Curtright and Apt, 2008), the way to change the variability of the profile without distorting its spectral shape is temporal scaling (Muzhikyan et al., 2014b). Assume that a default profile $P_0(t)$ has a variability A_0 and $P(t)$ is related to it in the following way:

$$P(t) = P_0(\alpha t) \quad (4)$$

According to (3), the variability of $P(t)$ is:

$$A = \frac{\text{rms}(dP_0(\alpha t)/dt)}{\text{rms}(P_0(\alpha t))} = \alpha \cdot \frac{\text{rms}(dP_0(\alpha t)/d(\alpha t))}{\text{rms}(P_0(\alpha t))} = \alpha A_0 \quad (5)$$

Thus, α can be viewed as a scaling factor between the given profile and the default profile variabilities:

$$\alpha = \frac{A}{A_0} \quad (6)$$

The definitions for the forecast and forecast error are introduced next. Fundamentally speaking, while the net load is a continuously varying function in time, the forecast has a specific value resolved with each day ahead market time block (e.g. 1 h). Therefore, the two are inherently different types of quantities. To address this issue, the concept of a “Best Forecast” is introduced as:

Definition 3.2.8 (The Best Forecast (Muzhikyan et al., 2014b)). Given the output $P(t)$ (e.g. the VER generation, the load, the net load), the best forecast \bar{P}_k is equivalent to the average value of that output during the k th market time block of duration T :

$$\bar{P}_k = \frac{1}{T} \int_{kT}^{(k+1)T} P(t) dt \quad (7)$$

Similarly, the forecast error defines the deviation between the actual and best forecasts, which in turn may have various measures such as mean absolute error (MAE) and mean square error (MSE) (Monteiro et al., 2009). Here, the VER forecast error is normalized by the installed capacity.

Definition 3.2.9 (VER Forecast Error (ε) (Muzhikyan et al., 2014b)). The standard deviation of the difference between the best (\bar{P}_k) and actual VER forecasts (\hat{P}_k) is normalized by the installed capacity:

$$\varepsilon = \frac{\sqrt{\frac{1}{n} \sum_{k=0}^n (\bar{P}_k - \hat{P}_k)^2}}{P_V^{\max}} \quad (8)$$

The above definitions are used to simulate different integration scenarios. More specifically, in developing sensitivity cases, the VER model systematically changes five main parameters: penetration level, capacity factor, variability, day-ahead and short-term forecast errors. First, the definitions of VER penetration level and capacity factor in (1) and (2) respectively can be used to define the actual VER output.

$$P_V(t) = \frac{P_V(t) \bar{P}_V(t)}{P_V(t) P_V^{\max}} \cdot \frac{P_V^{\max}}{P_L^{\max}} \cdot P_L^{\text{peak}} = p_V(t) \cdot \gamma \cdot \pi \cdot P_L^{\text{peak}} \quad (9)$$

where $p_V(t)$ is VER power normalized to a unit capacity factor. Eq. (9) shows that if a single $p_V(t)$ is taken as a default profile,

the actual VER output can be systematically adjusted with the values of π and γ . Next, the definition of VER forecast error in Eq. (8) can be used to define the actual VER forecast error. Two types of forecasts (and their errors) are used in the power system simulations, day-ahead and short-term. The day-ahead forecast is used in the SCUC model for day-ahead resource scheduling. It normally has a 1 h resolution and up to 48 h forecast horizon. The short-term forecast is used in the RTUC model for the same-day resource scheduling and the SCED model for real-time balancing operations. It has a ten minute time resolution and up to six hour time horizon (Giebel et al., 2011; Moreno-Munoz et al., 2008). The VER forecast can be expressed as:

$$\hat{P}_V(t) = P_V(t) - E(t) \quad (10)$$

where $\hat{P}_V(t)$ is the forecasted VER profile, and $E(t)$ is the error term. Using the definition of the forecast error in (8), the error term can be written as:

$$E(t) = \frac{E(t)}{\text{std}(E(t))} \cdot \frac{\text{std}(E(t))}{P_V^{\max}} \cdot \frac{P_V^{\max}}{P_L^{\text{peak}}} \cdot P_L^{\text{peak}} = e(t) \cdot \varepsilon \cdot \pi \cdot P_L^{\text{peak}} \quad (11)$$

where $e(t)$ is the error term normalized to the unit standard deviation. Eq. (11) shows that if a single $e(t)$ is taken for each type of market as a default profile, the actual error profile can be systematically adjusted with the values of π and ε . It is important to emphasize that the error term $e(t)$ is different for the day-ahead and short-term applications. They may have different probability distributions and power spectra. Additionally, the forecast error ranges are generally different with the short-term forecast having higher accuracy as compared to the day-ahead forecast. Finally, the actual variability can be similarly adjusted with the value of α . Using Eqs. (9) and (11) and the properties of variability in Eqs. (4) and (6), the VER model can be expressed as follows:

$$P_V(t) = p_V(\alpha t) \cdot \gamma \cdot \pi \cdot P_L^{\text{peak}} \quad (12)$$

$$\hat{P}_V(t) = (\gamma \cdot p_V(\alpha t) - \varepsilon \cdot e(\alpha t)) \cdot \pi \cdot P_L^{\text{peak}} \quad (13)$$

$$\alpha = A/A_0 \quad (14)$$

This set of equations defines the VER model used in this study. As an input, it requires the actual VER profile $p_V(t)$ normalized to unit capacity factor, and the error term profile $e(t)$, normalized to unit standard deviation. The model explicitly includes the five major parameters of VER.

3.3. Fundamental definitions of operating reserves

In addition to the definitions associated with variable energy resources, a number of definitions related to operating reserves are provided. The challenge here is that the taxonomy and definition of operating reserves from one power system geography to the next varies (Holtinen et al., 2012b). Furthermore, this taxonomy and definition is often different from the methodological foundations found in the literature (Holtinen et al., 2012b). There is even significant differences in the definitions found within the literature itself (Holtinen et al., 2012b; Ela et al., 2011; Rebours et al., 2007; CIGRE, 2010). Therefore, this report first introduces the definitions of operating reserves in the EPECS simulator in Section 3.3.1, then introduces the definitions used in ISO New England in Section 3.3.2, and then concludes by reconciling these concepts in Section 3.3.3.

3.3.1. Operating reserves in the EPECS simulator methodology

The EPECS simulator methodology adopts the operating reserves concepts found in Holtinen et al. (2012b), Ela et al. (2010) with minor differences. Fig. 5 shows the taxonomy of the various

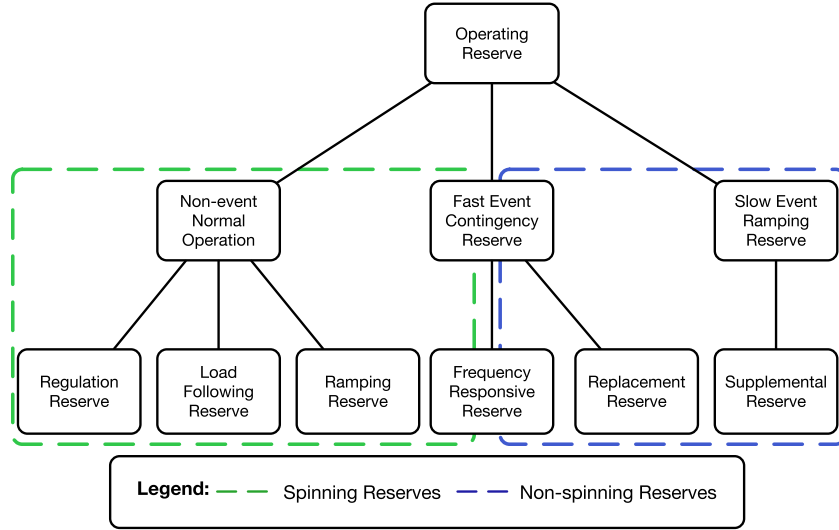


Fig. 5. Operating reserves classification.

Source: Adapted from [Holtinen et al. \(2012b\)](#).

types of operating reserves. The primary distinction is between the operating reserves used to respond to contingency events and those used during normal operation to respond to forecast errors and variability in the net load. Since the outage of any individual wind or solar generation facility has a much smaller impact on the system than the largest thermal plant, solar and wind integration will not increase contingency reserves requirements ([Holtinen et al., 2012b](#)). The exception to this general rule is when a transmission line transports a large amount of power from variable energy resources in a remote area (e.g. off-shore wind). In such a case, the loss of the transmission line could be comparable in size to the loss of a large thermal power plant. In spite of this exception, the focus of most renewable energy integration has primarily been on normal operating reserves. They are further classified as load following, ramping, and regulation reserves depending on the mechanisms by which they are acquired and activated.

Definition 3.3.1 (*Load Following Reserves* ([Ela et al., 2010](#); [Holtinen et al., 2012b](#))). Power capacity available during normal operations for assistance in active power balance to correct the future anticipated imbalances upward or downward. The actual quantity of upward load following reserves is given by:

$$\sum_{k=1}^{N_G} (w_{kt} P_k^{\max} - P_{kt}) \quad (15)$$

where N_G is the number of generators, w_{kt} is the (binary) on-line state of the k th generator at time t , P_k^{\max} is the maximum capacity of the k th generator, and P_{kt} is the value at which it is currently generating. Similarly, the actual quantity of downward load following reserves is given by:

$$\sum_{k=1}^{N_G} (P_{kt} - w_{kt} P_k^{\min}) \quad (16)$$

where P_k^{\min} is the minimum capacity of the k th generator. Within ISO-NE, load following reserves are often called economic surplus reserves.

Example 3.3.1. Consider [Fig. 6](#) as an example. It consists of a single generator generating at 400 MW. It has a maximum

capacity of 500 MW and a minimum capacity of 200 MW. It provides 100 MW of upward load following reserves and 200 MW of downward load following reserves.

Returning back to [Fig. 4](#), load following reserves are acquired during the day-ahead and same-day resource scheduling steps in the EPECS simulator. Furthermore, they are utilized during the real-time balancing operation. Note that this definition of load following reserves is purely a property of the physical system. This is entirely independent of whether some system operators monetize this property in the form of a *reserve product* or not.

Definition 3.3.2 (*Ramping Reserves* ([Ela et al., 2010](#); [Holtinen et al., 2012b](#))). Ramp rate capacity available during normal operations for assistance in active power balance to correct the future anticipated imbalances upward or downward. The actual quantity of upward ramping reserves is given by:

$$\sum_{k=1}^{N_G} \left(w_{kt} R_k^{\max} - \frac{P_{kt} - P_{k,t-1}}{\Delta T} \right) \quad (17)$$

where R_k^{\max} is the maximum upward ramp rate of the k th generator, and ΔT is duration of a time step between the generator levels P_{kt} and $P_{k,t-1}$. Normally, ΔT is equal to one hour. Similarly, the actual quantity of downward ramping reserves is given by:

$$\sum_{k=1}^{N_G} \left(w_{kt} R_k^{\min} - \frac{P_{kt} - P_{k,t-1}}{\Delta T} \right) \quad (18)$$

where R_k^{\min} is the maximum downward ramp rate of the k th generator.

Example 3.3.2. Consider [Fig. 7](#) as an example. It consists of a single generator that is scheduled to ramp from 400 MW to 425 MW within a given period ΔT equal to one hour. It has the ability to ramp up at 50 MW/hr and ramp down at 60 MW/hr. It provides 25 MW/hr of upward ramping reserves and 85 MW/hr of downward ramping reserves.

Returning back to [Fig. 4](#), ramping reserves, much like load following reserves, are acquired during the day-ahead and same-day resource scheduling steps in the EPECS simulator. Furthermore, they are utilized during the real-time balancing operation. Note

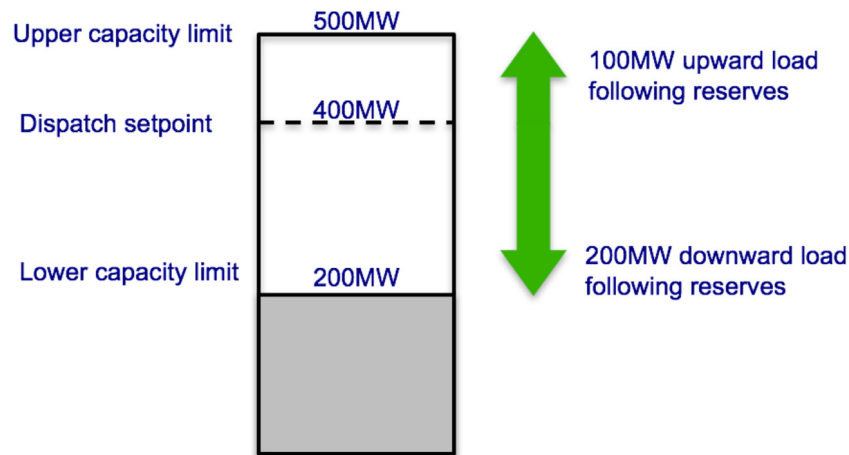


Fig. 6. Load following reserves example.

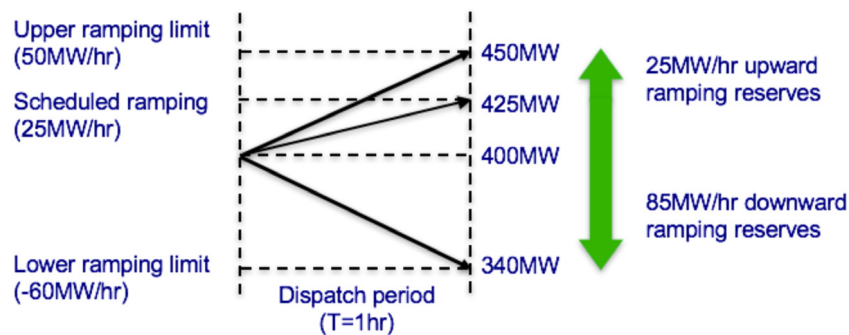


Fig. 7. Ramping reserves example.

that this definition of ramping reserves is purely a property of the physical system. This is entirely independent of whether some system operators monetize this property in the form of a *reserve product* or not.

Definition 3.3.3 (*Regulation Reserves* (Ela et al., 2010; Holttinen et al., 2012b)). Power capacity available during normal conditions for assistance in active power balance to correct the current imbalance that requires a fast, real-time, automatic response. The regulation reserve requirement up or down is given by P_{REG}^{REQ} . The regulation level at a given time t is given by G_t . Its absolute value must remain less than the requirement.

Returning back to Fig. 4, the regulation reserve requirement is taken as an input and is utilized in the automatic generation control (AGC) algorithm of the regulation service (See Section 3.7 for further details). It is a physical property of the saturation limits on the AGC. In most power systems, this quantity is monetized.

Example 3.3.3. Consider Fig. 8 for example. It consists of a single generator that is dispatched to an arbitrary level. Its automatic generation control has saturation limits of 50 MW upward and downward. Consequently, it provides 50 MW of regulation reserves.

Together, these three types of operating reserves are used to respond to forecast errors and variability in the net load during normal operation. In all cases, the actual quantities of these reserves are physical properties of the power system. They exist regardless of whether the system operator places requirements on these physical quantities or whether they incentivize generators to provide these reserve quantities in the form of reserve products.

3.3.2. Operating reserve requirements in ISO New England

In contrast to the above, ISO-NE maintains three types of operating reserve requirements (ISO New England, 2017c).

Definition 3.3.4 (*Ten-Minute Spinning Reserve (TMSR)* (ISO New England, 2017c)). The TMSR is the largest reserve product that is provided by *on-line resources* able to increase their output within ten minutes. It is currently set to the largest contingency on the system.

Definition 3.3.5 (*Ten-Minute Nonspinning Reserve (TMNSR)* (ISO New England, 2017c)). The TMNSR is the second largest reserve quantity that is provided by *off-line units* that can successfully synchronize to the grid and ramp up within ten minutes. It is currently set to one half of the second largest contingency on the system.

Definition 3.3.6 (*Thirty-Minute Operating Reserve (TMOR)* (ISO New England, 2017c)). TMOR is the lowest reserve quantity that is provided by *on-line resources* that can ramp up within 30 min and *off-line units* that synchronize to the grid and ramp up within 30 min. Furthermore, there exist Local TMOR requirements for three reserve zones: Connecticut (CT), Southwest Connecticut (SWCT), and NEMA/Boston (NEMABSTN). Until recently, it was set equal to the sum of the two ten-minute operating reserve requirements. As of October 2013, an additional replacement reserve requirement of 160 MW in the summer and 180 MW in the winter was added to the TMOR (ISO New England, 2017c).

The above definitions imply a taxonomy of operating reserves shown in Fig. 9. Note that all three of the reserve products are defined in an upward direction as result of their focus on

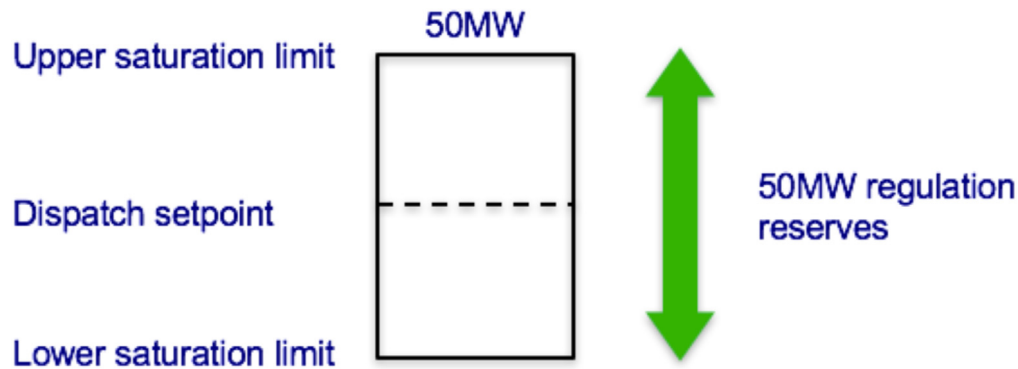


Fig. 8. Regulating reserves example.

contingency events and because historically downward reserves have not been difficult to obtain in day-to-day operations. Furthermore, the ten-minute spinning reserve includes regulation reserves but also serves as a fast-event contingency reserve.

3.3.3. Reconciliation of operating reserve definitions for the SOARES project

In order to apply the EPECS simulator methodology to the ISO New England region, the two taxonomies of operating reserves summarized in Figs. 5 and 9 must be reconciled. First, it is important to recognize that the EPECS operating reserves definitions reflect physical quantities while the ISO-NE operating reserves definitions reflect requirements. Furthermore, it is beyond the scope of this study to define new types of operating reserve requirements. Therefore, this project makes the following reconciliation:

Regulation reserves: For regulation reserves, there appears to be no conceptual discrepancy. The maximum and minimum quantities of regulating reserves are equated to the regulating reserve requirement.

Ten-minute spinning reserves & load following reserves: For the ten-minute spinning reserves, we observe that this requirement is imposed on the quantity of load following reserves. While the system will continue to require a TMSR of at least the largest contingency on the system, a high penetration of variable energy resources might require this quantity to be significantly increased.

Example 3.3.4. Consider a hypothetical scenario in New England on a year where the peak load is 25 GW. A 40% penetration of variable energy resources would equate to 10 GW. If 50% of these VERS were to drop out suddenly (beyond the forecast),² there would be a 5 GW shortfall. This is significantly larger than the largest single-facility contingency in the system. Therefore, there would need to be a load following reserve requirement to address such a situation. In the absence of a new reserve requirement, the TMSR can be increased so as to respond to both single-facility contingencies as well as the variability and forecast error of variable energy resources.

Therefore, this study sets the TMSR requirement equal to the greater of two quantities: (1) the size of the largest contingency (2) the load following reserve requirement. The determination of the latter is part of the central objective of this work. In this context, the TMSR needs to be understood in both an upward as well as a downward direction.

Non-spinning reserves: The two non-spinning reserve requirements will remain unchanged. VER integration is fundamentally a normal operation phenomena. Non-spinning reserves only protect the system in the event of a loss of generation but do not protect the system in the event of an excess of generation. Furthermore, the variability of renewable energy generation means that a system with a negative imbalance can quickly switch to a system with a positive imbalance. Therefore, it is inadvisable to try to protect the power system from VER variability and forecast error with non-spinning reserves.

Ramping reserves: Finally, in the case of ramping reserves, currently there is no requirement in ISO New England that provides an effective equivalent. This study will determine the ramping reserve requirements for the scenarios described in Section 4.1. Such results may motivate the need for the implementation of a ramping reserve requirement.

3.4. Day-ahead resource scheduling at ISO New England

Power system balancing operations start with day-ahead resource scheduling implemented as a security-constrained unit commitment (SCUC). The goal of the SCUC problem is to choose the right set of generation units that are able to meet the real-time demand at minimum cost. In the original formulation, the SCUC problem is formulated as a mixed integer nonlinear optimization program with integrated power flow equations and system security requirements (Frank and Rebennack, 2012). However, the optimization constraints are often linearized, as in Muzhikyan et al. (2015a,b), to avoid potential convergence issues. The SCUC formulation in Muzhikyan et al. (2015a,b) has been further modified to reflect ISO-NE operations. In particular:

1. Constraints reflecting minimum up time, minimum down time and maximum number of daily start-ups of the generators are added, which also take the initial online hours into account.
2. The outages are incorporated into the model.
3. The optimization program models pumped-storage units to reflect operating parameters, including the maximum daily energy constraints, the maximum draw down, and the reservoir limitations.
4. Constraints ensuring procurement of system-wide ten-minute and 30-minute reserve requirements are added to the SCUC model.
5. A zonal network model is implemented.
6. External transactions with proper interface limits are modeled.

The generation cost curves are modeled as quadratic functions of heat rates. The total operation cost is a combination of the

² Note that a 50% forecast error is highly unlikely for a system with 20% penetration rate. The choice of values is purely illustrative in nature.

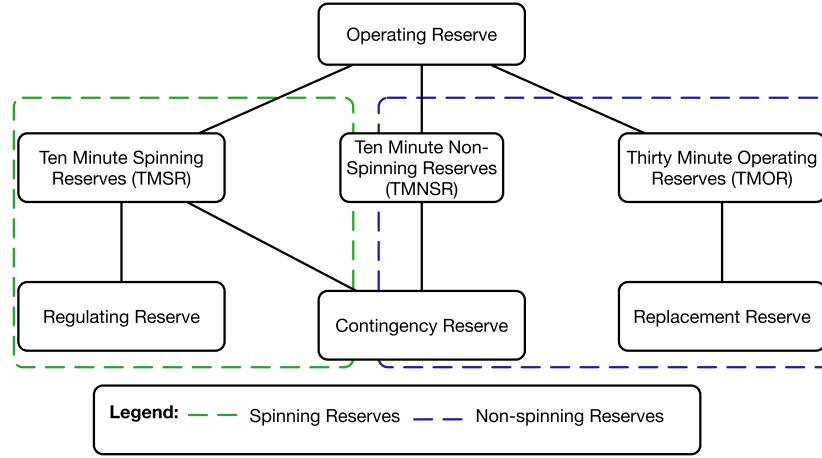


Fig. 9. Operating reserve classification in ISO New England.

generation cost, generator startup and shutdown costs, and the “supergeneration”³ cost:

$$\begin{aligned}
 \min \sum_{t=1}^T & \left(\sum_{k=1}^{N_G} C_{Fkt} (w_{Gkt} H_{Fk} + H_{Lk} P_{kt} + H_{Qk} P_{kt}^2 + u_{Gkt} H_{Uk} + v_{Gkt} H_{Dk}) \right. \\
 & + \sum_{m=1}^{N_D} C_m P_{mt} + \sum_{x=1}^{N_X} C_{Fxt} H_{Lx} (P_{xt} + N_{xt}) + \sum_{\mathcal{L}=1}^{N_{\mathcal{L}}} C_{\mathcal{L}} d_{\mathcal{L}} w_{\mathcal{L}t} \tilde{P}_{\mathcal{L}t} \\
 & + \sum_{\mathcal{W}=1}^{N_{\mathcal{W}}} C_{\mathcal{W}} (1 - d_{\mathcal{W}} w_{\mathcal{W}t}) \tilde{P}_{\mathcal{W}t} + \sum_{\mathcal{V}=1}^{N_{\mathcal{V}}} C_{\mathcal{V}} (1 - d_{\mathcal{V}} w_{\mathcal{V}t}) \tilde{P}_{\mathcal{V}t} \\
 & + \sum_{\mathcal{H}=1}^{N_{\mathcal{H}}} C_{\mathcal{H}} (1 - d_{\mathcal{H}} w_{\mathcal{H}t}) \tilde{P}_{\mathcal{H}t} \\
 & \left. + \sum_{\mathcal{T}=1}^{N_{\mathcal{T}}} C_{\mathcal{T}} (1 - w_{\mathcal{OT}t}) (1 - d_{\mathcal{T}} w_{\mathcal{T}t}) \tilde{P}_{\mathcal{T}t} \right) \quad (19)
 \end{aligned}$$

The optimization program is subject to the following constraints:

$$\begin{aligned}
 & \sum_{k=1}^{N_G} A_{nk} P_{kt} + \sum_{s=1}^{N_S} A_{ns} (P_{st} - S_{st}) + \sum_{x=1}^{N_X} A_{nx} (P_{xt} - N_{xt}) \\
 & + \sum_{m=1}^{N_D} A_{nm} P_{mt} - (1 + \gamma) \sum_{\mathcal{L}=1}^{N_{\mathcal{L}}} A_{n\mathcal{L}} (1 - d_{\mathcal{L}} w_{\mathcal{L}t}) \tilde{P}_{\mathcal{L}t} \\
 & + (1 + \gamma) \sum_{\mathcal{W}=1}^{N_{\mathcal{W}}} A_{n\mathcal{W}} (1 - d_{\mathcal{W}} w_{\mathcal{W}t}) \tilde{P}_{\mathcal{W}t} \\
 & + (1 + \gamma) \sum_{\mathcal{V}=1}^{N_{\mathcal{V}}} A_{n\mathcal{V}} (1 - d_{\mathcal{V}} w_{\mathcal{V}t}) \tilde{P}_{\mathcal{V}t} \\
 & + (1 + \gamma) \sum_{\mathcal{H}=1}^{N_{\mathcal{H}}} A_{n\mathcal{H}} (1 - d_{\mathcal{H}} w_{\mathcal{H}t}) \tilde{P}_{\mathcal{H}t} \\
 & + \sum_{\mathcal{T}=1}^{N_{\mathcal{T}}} A_{n\mathcal{T}} (1 - w_{\mathcal{OT}t}) (1 - d_{\mathcal{T}} w_{\mathcal{T}t}) \tilde{P}_{\mathcal{T}t}
 \end{aligned}$$

³ Mathematically speaking, “super-generators” implement a penalty factor in the objective function so that the hard power balance constraint can be turned into a soft one. This provides a robust solution that protects against infeasible optimization solutions. Physically speaking, negative values of super-generation indicates the need for curtailment of semi-dispatchable resources. Positive values of super-generation indicates a short-fall of dispatchable generation which rarely occurs in operations timescale studies.

$$= \sum_{l=1}^{N_L} B_{nl} F_{lt} \quad n = 1 : N_B; t = 1 : T \quad (20)$$

$$\sum_{l=1}^{N_L} K_{il} F_{lt} \leq I_i^{max} \quad i = 1 : N_I; t = 1 : T \quad (21)$$

$$w_{Gkt} P_k^{min} \leq P_{kt} \leq w_{Gkt} (1 - w_{Okt}) P_k^{max} \quad k = 1 : N_G; t = 1 : T \quad (22)$$

$$P_m^{min} \leq P_{mt} \leq P_m^{max} \quad m = 1 : N_D; t = 1 : T \quad (23)$$

$$w_{Pst} P_s^{min} \leq P_{st} \leq w_{Pst} P_s^{max} \quad s = 1 : N_S; t = 1 : T \quad (24)$$

$$w_{Sst} S_s^{min} \leq S_{st} \leq w_{Sst} S_s^{max} \quad s = 1 : N_S; t = 1 : T \quad (25)$$

$$\begin{aligned}
 R_k^{min} - \frac{P_k^{max}}{T_h} v_{Gkt} & \leq \frac{P_{kt} - P_{k,t-1}}{T_h} \\
 & \leq R_k^{max} + \frac{P_k^{max}}{T_h} u_{Gkt} \quad k = 1 : N_G; t = 1 : T \quad (26)
 \end{aligned}$$

$$E_{st} = E_{s,t-1} + (\eta_s S_{st} - P_{st}) \cdot T_h \quad s = 1 : N_S; t = 1 : T \quad (27)$$

$$E_s^{min} \leq E_{st} \leq E_s^{max} \quad s = 1 : N_S; t = 1 : T \quad (28)$$

$$P_{k0} = \xi_k \quad k = 1 : N_G \quad (29)$$

$$E_{s0} = \varepsilon_s \quad s = 1 : N_S \quad (30)$$

$$w_{Gk,t-1} + u_{Gkt} - v_{Gkt} = w_{Gkt} \quad k = 1 : N_G; t = 1 : T \quad (31)$$

$$u_{Gkt} + v_{Gkt} \leq 1 \quad k = 1 : N_G; t = 1 : T \quad (32)$$

$$w_{Pst} + w_{Sst} \leq 1 \quad s = 1 : N_S; t = 1 : T \quad (33)$$

$$w_{Pst} + w_{Ss,(t-1)} \leq 1 \quad s = 1 : N_S; t = 1 : T \quad (34)$$

$$w_{Ps,(t-1)} + w_{Sst} \leq 1 \quad s = 1 : N_S; t = 1 : T \quad (35)$$

$$w_{Ps0} = \omega_{Ps0} \quad s = 1 : N_S \quad (36)$$

$w_{Ss0} = \omega_{Ss0}$	$s = 1 : N_S$	(37)	K_{il}	incidence matrix of branches to interfaces;
$w_{Gkt} \geq u_{Gk,(t-\tau)}$	$k = 1 : N_G; t = 1 : T,$		T_h, T	SCUC time step and horizon;
	$\tau = 1 : T_u - 1$	(38)	$H_{Fk}, H_{Lk}, H_{Qk}, H_{Uk}, H_{Dk}$	fixed, linear, quadratic, startup and shutdown heat rates for generator k ;
$1 - w_{Gkt} \geq v_{Gk,(t-\tau)}$	$k = 1 : N_G; t = 1 : T,$			fuel cost of generator k at time t ;
	$\tau = 1 : T_d - 1$	(39)	C_{Fkt}	linear cost of active DR unit m ;
$\sum_{t=1}^T u_{Gkt} \leq u_{Gk}^{max}$	$k = 1 : N_G$	(40)	C_m	load, wind, solar, hydro and tie line curtailment threshold prices respectively;
$C_{1t} \geq A_{nk} w_{Gkt} P_k^{max}$	$t = 1 : T$	(41)	$C_{\mathcal{L}}, C_{\mathcal{W}}, C_{\mathcal{V}}, C_{\mathcal{H}}, C_{\mathcal{T}}$	minimum/maximum power outputs of generator k ;
$C_{1t} \geq A_{n\mathcal{T}}(1 - w_{O\mathcal{T}t})(1 - d_{\mathcal{T}} w_{\mathcal{T}t}) \tilde{P}_{\mathcal{T}t}$	$t = 1 : T$	(42)		maximum/minimum ramping rate of generator k ;
$P_{Gkt}^{TMSR} \leq w_{Gkt} P_k^{max} - P_{kt}$	$k = 1 : N_G; t = 1 : T$	(43)	P_k^{max}, P_k^{min}	minimum/maximum power outputs of storage s ;
$P_{Gkt}^{TMSR} \leq R_k^{max} \cdot T_{10}$	$k = 1 : N_G; t = 1 : T$	(44)	R_k^{max}, R_k^{min}	minimum/maximum pumping rate of storage s ;
$P_{nt}^{TMSR} = \sum_{k=1}^{N_G} A_{nk} P_{Gkt}^{TMSR}$	$n = 1 : N_B; t = 1 : T$	(45)	P_s^{max}, P_s^{min}	minimum/maximum energy capacity of storage s ;
$P_{nt}^{TMSR} \geq \alpha_n^{TMSR} \cdot \alpha_{sys}^{TMR} \cdot C_{1t}$	$n = 1 : N_B; t = 1 : T$	(46)	S_s^{max}, S_s^{min}	minimum up time, minimum down time and maximum startups in a day for generator k ;
$\sum_{n=1}^{N_B} P_{nt}^{TMSR} \geq \alpha_{sys}^{TMSR} \cdot \alpha_{sys}^{TMR} \cdot C_{1t}$	$t = 1 : T$	(47)	E_s^{max}, E_s^{min}	curtailable fractions of load, wind, solar, hydro and tie line respectively;
$P_{Gkt}^{TMOR} \leq (1 - w_{Gkt}) P_k^{max}$	$k = 1 : N_G; t = 1 : T$	(48)	T_u, T_d, u_{Gk}^{max}	ON/OFF, startup and shutdown statuses of generator k at time t ;
$P_{Gkt}^{TMOR} \leq R_k^{max} \cdot T_{30}$	$k = 1 : N_G; t = 1 : T$	(49)	$d_{\mathcal{L}}, d_{\mathcal{W}}, d_{\mathcal{V}}, d_{\mathcal{H}}, d_{\mathcal{T}}$	fractions of curtailable load, wind, solar, hydro and tie line curtailed at time t ;
$P_{nt}^{TMOR} = \sum_{k=1}^{N_G} A_{nk} P_{Gkt}^{TMOR}$	$n = 1 : N_B; t = 1 : T$	(50)	$w_{Gkt}, u_{Gkt}, v_{Gkt}$	fractions of generator k and tie-line \mathcal{T} under outage at time t ;
$P_{nt}^{TMSR} + P_{nt}^{TMOR} \geq \alpha_n^{TMOR} \cdot \alpha_{sys}^{TMR} \cdot C_{1t}$	$n = 1 : N_B; t = 1 : T$	(51)	$w_{\mathcal{L}t}, w_{\mathcal{W}t}, w_{\mathcal{V}t}, w_{\mathcal{H}t}, w_{\mathcal{T}t}$	generation and pumping mode indicators of storage s at time t ;
$\sum_{n=1}^{N_B} (P_{nt}^{TMSR} + P_{nt}^{TMOR}) \geq \alpha_{sys}^{TMOR} \cdot \alpha_{sys}^{TMR} \cdot C_{1t}$	$t = 1 : T$	(52)	$w_{Okt}, w_{O\mathcal{T}t}$	power output of generator k at time $t \geq 1$ and $t = 0$;
where the following notations are used:				generation and pumping rates of storage s at time t ;
k, m, x, s, n, l, i, t	generator, active DR, supergenerator, storage, bubble, branch, interface and time indices respectively;			reservoir level of storage s at time $t \geq 1$ and $t = 0$;
$N_G, N_D, N_X, N_S, N_B, N_L, N_I$	number of generators, active DR's, supergenerators, storages, bubbles, branches and interfaces respectively;			positive and negative components of supergenerator x output at time t ;
$\mathcal{L}, \mathcal{W}, \mathcal{V}, \mathcal{H}, \mathcal{T}$	load, wind, solar, hydro, tie line indices respectively;			power flow through branch l at time t ;
$N_{\mathcal{L}}, N_{\mathcal{W}}, N_{\mathcal{V}}, N_{\mathcal{H}}, N_{\mathcal{T}}$	number of loads, winds, solars, hydros, tie lines respectively;			load, wind, solar, hydro and tie line forecasts at time t ;
$A_{n,(k,s,x,\mathcal{L},\mathcal{W},\mathcal{V},\mathcal{H},\mathcal{T})}$	incidence matrix of (generators, storages, supergenerators, loads, winds, solars, hydros, tie lines) to bubbles;			transmission losses as a percentage of the total demand;
B_{nl}	incidence matrix of branches to bubbles;			

C_{1t}	largest contingency at time t ;
$P_{Gkt}^{TMSR}, P_{Gkt}^{TMOR}$	amount of TMSR and TMOR
	obtained from generator k at time t ;
$P_{nt}^{TMSR}, P_{nt}^{TMOR}$	amount of TMSR and TMOR
	available at bubble n at time t ;
$\alpha_n^{TMSR}, \alpha_n^{TMR}, \alpha_n^{TMOR}$	TMSR, TMR and TMOR requirements
	at bubble n as percentages of the
	largest contingency;
$\alpha_{sys}^{TMSR}, \alpha_{sys}^{TMR}, \alpha_{sys}^{TMOR}$	system-wide TMSR, TMR and TMOR
	requirements as percentages of the
	largest contingency.

Constraint (20) is the DC power flow equation with incorporated loss term. Constraint (21) sets the interface limits. Constraints (22)–(25) set generator, active demand response and storage power output maximum and minimum limits. Constraint (26) places limits on the generator up and down ramping rates. Constraints (27)–(28) set storage energy limits. Constraints (31)–(37) logically bind the status binary variables of generators and storage units. Constraints (38) and (39) set the generator minimum up and minimum down times respectively. Constraint (40) limits the maximum number of generator startups in a day. Constraints (41)–(42) calculate the largest generator and tie line contingencies respectively. Constraints (43)–(47) procure ten-minute spinning reserves (TMSR) from online units. Similarly, constraints (48)–(52) procure thirty-minute operating reserves (TMOR) from offline fast-start units.

3.5. Same-day resource scheduling at ISO-NE

The same-day resource scheduling uses an optimization program similar to that of the SCUC. The optimization program, called real-time unit commitment (RTUC), is modified in the following ways to reflect ISO-NE operations:

1. The optimization considers 16 15-minute time intervals, spanning a 4-hour period.
2. This optimization program is run once every hour rather than once a day (in the case of the day-ahead resource scheduling).
3. The process only commits and de-commits fast-start units.
4. The commitment is based upon short-term load and VER forecasts (a couple of hours look-ahead).
5. This optimization model enforces system reserve requirements.

The formulation of the RTUC is similar to the SCUC. The objective function is written as:

$$\begin{aligned} \min \sum_{t=1}^T & \left(\sum_{k=1}^{N_G} C_{Fkt} (w_{Gkt} H_{Fk} + H_{Lk} P_{kt} + H_{Qk} P_{kt}^2 + u_{Gkt} H_{Uk} + v_{Gkt} H_{Dk}) \right. \\ & + \sum_{m=1}^{N_D} C_m P_{mt} + \sum_{x=1}^{N_X} C_{Fxt} H_{Lx} (P_{xt} + N_{xt}) + \sum_{\mathcal{L}=1}^{N_{\mathcal{L}}} C_{\mathcal{L}} d_{\mathcal{L}} w_{\mathcal{L}t} \tilde{P}_{\mathcal{L}t} \\ & + \sum_{\mathcal{W}=1}^{N_{\mathcal{W}}} C_{\mathcal{W}} (1 - d_{\mathcal{W}} w_{\mathcal{W}t}) \tilde{P}_{\mathcal{W}t} + \sum_{\mathcal{V}=1}^{N_{\mathcal{V}}} C_{\mathcal{V}} (1 - d_{\mathcal{V}} w_{\mathcal{V}t}) \tilde{P}_{\mathcal{V}t} \\ & + \sum_{\mathcal{H}=1}^{N_{\mathcal{H}}} C_{\mathcal{H}} (1 - d_{\mathcal{H}} w_{\mathcal{H}t}) \tilde{P}_{\mathcal{H}t} \\ & \left. + \sum_{\mathcal{T}=1}^{N_{\mathcal{T}}} C_{\mathcal{T}} (1 - w_{\mathcal{OT}t}) (1 - d_{\mathcal{T}} w_{\mathcal{T}t}) \tilde{P}_{\mathcal{T}t} \right) \end{aligned} \quad (53)$$

The optimization program is subject to the following constraints:

$$\begin{aligned} & \sum_{k=1}^{N_G} A_{nk} P_{kt} + \sum_{s=1}^{N_S} A_{ns} (\mathcal{P}_{st} - \mathcal{S}_{st}) + \sum_{x=1}^{N_X} A_{nx} (P_{xt} - N_{xt}) \\ & + \sum_{m=1}^{N_D} A_{nm} P_{mt} - (1 + \gamma) \sum_{\mathcal{L}=1}^{N_{\mathcal{L}}} A_{n\mathcal{L}} (1 - d_{\mathcal{L}} w_{\mathcal{L}t}) \tilde{P}_{\mathcal{L}t} \\ & + (1 + \gamma) \sum_{\mathcal{W}=1}^{N_{\mathcal{W}}} A_{n\mathcal{W}} (1 - d_{\mathcal{W}} w_{\mathcal{W}t}) \tilde{P}_{\mathcal{W}t} \\ & + (1 + \gamma) \sum_{\mathcal{V}=1}^{N_{\mathcal{V}}} A_{n\mathcal{V}} (1 - d_{\mathcal{V}} w_{\mathcal{V}t}) \tilde{P}_{\mathcal{V}t} \\ & + (1 + \gamma) \sum_{\mathcal{H}=1}^{N_{\mathcal{H}}} A_{n\mathcal{H}} (1 - d_{\mathcal{H}} w_{\mathcal{H}t}) \tilde{P}_{\mathcal{H}t} \\ & + \sum_{\mathcal{T}=1}^{N_{\mathcal{T}}} A_{n\mathcal{T}} (1 - w_{\mathcal{OT}t}) (1 - d_{\mathcal{T}} w_{\mathcal{T}t}) \tilde{P}_{\mathcal{T}t} \\ & = \sum_{l=1}^{N_L} B_{nl} F_{lt} \quad n = 1 : N_B; t = 1 : T \end{aligned} \quad (54)$$

$$\sum_{l=1}^{N_L} K_{il} F_{lt} \leq I_i^{\max} \quad i = 1 : N_I; t = 1 : T \quad (55)$$

$$w_{Gkt} P_k^{\min} \leq P_{kt} \leq w_{Gkt} (1 - w_{Okt}) P_k^{\max} \quad k = 1 : N_G; t = 1 : T \quad (56)$$

$$P_m^{\min} \leq P_{mt} \leq P_m^{\max} \quad m = 1 : N_D; t = 1 : T \quad (57)$$

$$\begin{aligned} R_k^{\min} - \frac{P_k^{\max}}{T_r} v_{Gkt} & \leq \frac{P_{kt} - P_{k,t-1}}{T_r} \\ & \leq P_k^{\max} + \frac{P_k^{\max}}{T_r} u_{Gkt} \quad k = 1 : N_G; t = 1 : T \end{aligned} \quad (58)$$

$$P_{k0} = \xi_k \quad k = 1 : N_G \quad (59)$$

$$w_{Gk,t-1} + u_{Gkt} - v_{Gkt} = w_{Gkt} \quad k = 1 : N_G; t = 1 : T \quad (60)$$

$$w_{Gkt} = \omega_{Gkt} \quad \kappa = 1 : N_{\mathcal{G}}; t = 1 : T \quad (61)$$

$$u_{Gkt} + v_{Gkt} \leq 1 \quad k = 1 : N_G; t = 1 : T \quad (62)$$

$$w_{Gkt} \geq u_{Gk,(t-\tau)} \quad k = 1 : N_G; t = 1 : T, \quad \tau = 1 : T_u - 1 \quad (63)$$

$$1 - w_{Gkt} \geq v_{Gk,(t-\tau)} \quad k = 1 : N_G; t = 1 : T, \quad \tau = 1 : T_d - 1 \quad (64)$$

$$n_{Gk} + \sum_{t=1}^T u_{Gkt} + m_{Gk} \leq u_{Gk}^{\max} \quad k = 1 : N_G \quad (65)$$

$$C_{1t} \geq A_{nk} w_{Gkt} P_k^{\max} \quad t = 1 : T \quad (66)$$

$$C_{1t} \geq A_{n\mathcal{T}} (1 - w_{\mathcal{OT}t}) (1 - d_{\mathcal{T}} w_{\mathcal{T}t}) \tilde{P}_{\mathcal{T}t} \quad t = 1 : T \quad (67)$$

$$P_{Gkt}^{TMSR} \leq w_{Gkt} P_k^{\max} - P_{kt} \quad k = 1 : N_G; t = 1 : T \quad (68)$$

$$P_{Gkt}^{TMSR} \leq R_k^{\max} \cdot T_{10} \quad k = 1 : N_G; t = 1 : T \quad (69)$$

$$P_{nt}^{TMSR} = \sum_{k=1}^{N_G} A_{nk} P_{Gkt}^{TMSR} \quad n = 1 : N_B; t = 1 : T \quad (70)$$

$$P_{nt}^{TMSR} \geq \alpha_n^{TMSR} \cdot \alpha_{sys}^{TMR} \cdot C_{1t} \quad n = 1 : N_B; t = 1 : T \quad (71)$$

$$\sum_{n=1}^{N_B} P_{nt}^{TMSR} \geq \alpha_{sys}^{TMSR} \cdot \alpha_{sys}^{TMR} \cdot C_{1t} \quad t = 1 : T \quad (72)$$

$$P_{Gkt}^{TMR} \leq (1 - w_{Gkt}) P_k^{max} \quad k = 1 : N_G; t = 1 : T \quad (73)$$

$$P_{Gkt}^{TMR} \leq R_k^{max} \cdot T_{30} \quad k = 1 : N_G; t = 1 : T \quad (74)$$

$$P_{nt}^{TMR} = \sum_{k=1}^{N_G} A_{nk} P_{Gkt}^{TMR} \quad n = 1 : N_B; t = 1 : T \quad (75)$$

$$P_{nt}^{TMSR} + P_{nt}^{TMR} \geq \alpha_n^{TMR} \cdot \alpha_{sys}^{TMR} \cdot C_{1t} \quad n = 1 : N_B; t = 1 : T \quad (76)$$

$$\sum_{n=1}^{N_B} (P_{nt}^{TMSR} + P_{nt}^{TMR}) \geq \alpha_{sys}^{TMR} \cdot \alpha_{sys}^{TMR} \cdot C_{1t} \quad t = 1 : T \quad (77)$$

where the following notations are used in addition to the ones introduced in the previous section:

κ	indices not-fast-start generators;
N_G	number not-fast-start generators;
T_r, T	RTUC time step and horizon;
n_{Gk}, m_{Gk}	number of startups during the day before and after the current RTUC time block respectively;
ω_{Gkt}	the commitment schedules of not-fast-start units obtained from SCUC
P_{st}, S_{st}	storage generation and pumping schedules obtained from the SCUC.

3.6. Real-time balancing operations at ISO-NE

The real-time balancing operations move available generator outputs to new setpoints (dispatch) in the most cost-efficient way. In its original formulation, generation dispatch is implemented as a non-linear optimization model, called AC optimal power flow (ACOPF) (Carpentier, 1962). Due to problems with convergence and computational complexity (Frank and Rebenack, 2012), most of the U.S. independent system operators (ISO) moved from ACOPF to linear optimization models. The most commonly used model is called security-constrained economic dispatch (SCED) (Stott et al., 2009). This SCED formulation has been further modified to reflect ISO-NE operations. In particular:

1. The modified SCED adopts a 10-min look-ahead window, and considers the initial state of a unit (UCM code) and its start-up and shut-down instruction from the RTUC.
2. Area interchanges are honored.

The objective function is written as:

$$\min \left(\sum_{k=1}^{N_G} C_{Fk} (H_{Lk} P_k + H_{Qk} P_k^2) + \sum_{m=1}^{N_D} C_m P_m + \sum_{x=1}^{N_X} C_{Fx} H_{Lx} (P_x + N_x) \right)$$

$$\begin{aligned} & + \sum_{\mathcal{L}=1}^{N_{\mathcal{L}}} C_{\mathcal{L}} d_{\mathcal{L}} w_{\mathcal{L}} \tilde{P}_{\mathcal{L}} + \sum_{\mathcal{W}=1}^{N_{\mathcal{W}}} C_{\mathcal{W}} (1 - d_{\mathcal{W}} w_{\mathcal{W}}) \tilde{P}_{\mathcal{W}} \\ & + \sum_{\mathcal{V}=1}^{N_{\mathcal{V}}} C_{\mathcal{V}} (1 - d_{\mathcal{V}} w_{\mathcal{V}}) \tilde{P}_{\mathcal{V}} \\ & + \sum_{\mathcal{H}=1}^{N_{\mathcal{H}}} C_{\mathcal{H}} (1 - d_{\mathcal{H}} w_{\mathcal{H}}) \tilde{P}_{\mathcal{H}} + \sum_{\mathcal{T}=1}^{N_{\mathcal{T}}} C_{\mathcal{T}} (1 - w_{O\mathcal{T}}) (1 - d_{\mathcal{T}} w_{\mathcal{T}}) \tilde{P}_{\mathcal{T}} \end{aligned} \quad (78)$$

The optimization program is subject to the following constraints:

$$\begin{aligned} & \sum_{k=1}^{N_G} A_{nk} P_k + \sum_{s=1}^{N_S} A_{ns} (P_s - S_s) + \sum_{x=1}^{N_X} A_{nx} (P_x - N_x) \\ & + \sum_{k=1}^{N_G} A_{nm} P_m - (1 + \gamma) \sum_{\mathcal{L}=1}^{N_{\mathcal{L}}} A_{n\mathcal{L}} (1 - d_{\mathcal{L}} w_{\mathcal{L}}) \tilde{P}_{\mathcal{L}} \\ & + (1 + \gamma) \sum_{\mathcal{W}=1}^{N_{\mathcal{W}}} A_{n\mathcal{W}} (1 - d_{\mathcal{W}} w_{\mathcal{W}}) \tilde{P}_{\mathcal{W}} \\ & + (1 + \gamma) \sum_{\mathcal{V}=1}^{N_{\mathcal{V}}} A_{n\mathcal{V}} (1 - d_{\mathcal{V}} w_{\mathcal{V}}) \tilde{P}_{\mathcal{V}} \\ & + (1 + \gamma) \sum_{\mathcal{H}=1}^{N_{\mathcal{H}}} A_{n\mathcal{H}} (1 - d_{\mathcal{H}} w_{\mathcal{H}}) \tilde{P}_{\mathcal{H}} \\ & + \sum_{\mathcal{T}=1}^{N_{\mathcal{T}}} A_{n\mathcal{T}} (1 - w_{O\mathcal{T}}) (1 - d_{\mathcal{T}} w_{\mathcal{T}}) \tilde{P}_{\mathcal{T}} \\ & = \sum_{l=1}^{N_l} B_{nl} F_l \quad n = 1 : N_B \end{aligned} \quad (79)$$

$$\sum_{l=1}^{N_l} K_{il} F_l \leq I_i^{max} \quad i = 1 : N_l \quad (80)$$

$$\omega_{Gk} P_k^{min} \leq P_k \leq \omega_{Gk} (1 - w_{Ok}) P_k^{max} \quad k = 1 : N_G \quad (81)$$

$$P_m^{min} \leq P_m \leq P_m^{max} \quad m = 1 : N_D \quad (82)$$

$$P_k^{min} - \frac{P_k^{max} - P_k^0}{T_m} v_{Gk} \leq \frac{P_k - P_k^0}{T_m} \leq R_k^{max} + \frac{P_k^{max} - P_k^0}{T_m} u_{Gk} \quad k = 1 : N_G \quad (83)$$

where the following notations are used in addition to the ones introduced in previous sections:

T_m	real-time balancing time step;
$\omega_{Gk}, u_{Gk}, v_{Gk}$	generator state, startup and shutdown indicators for the given time step obtained from the RTUC;
P_k^0	current power output of generator k ;

Constraint (79) is the DC power flow equation with incorporated loss term. Constraint (80) sets the interface limits. Constraints (81) and (82) set generator and active demand response power output limits respectively. Constraint (83) places limits on the generator up and down ramping rates.

3.7. Regulation service model

The regulation service is provided by generation units that are fully or partially controlled by the dynamic AGC model described in Fig. 10. This study uses one minute increments as its finest time scale resolution. In the meantime, the cycle time of slow transient stability phenomena is approximately ten seconds. Given the 6x

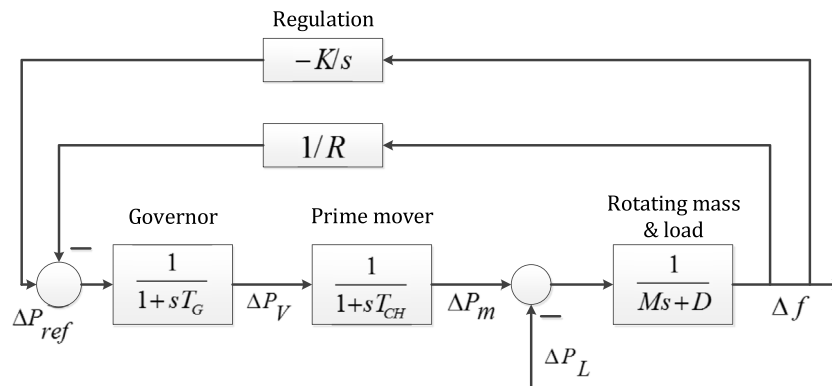


Fig. 10. Power system automatic generation control (Wood and Wollenberg, 2014).

difference, the transfer function shown in Fig. 10 can be replaced with the steady-state equivalent of a gain with saturation limits. Furthermore, this work allows for the regulation service to be rate limited so as to have an “automatic-response-rate”. In this work, the automatic response rate is set to 10% of the regulation service saturation limits. These, in turn, are defined by the percentage of the capacity in the corresponding generation unit controlled by AGC. In implementation, the regulation service responds to the imbalances by moving the regulation units in the opposite direction according to their predefined participation factors. The regulation units change their outputs until imbalances are mitigated or regulation service reaches saturation.

3.8. Physical power grid model

The pseudo-steady-state approximation of the regulation service model ties directly to a power flow analysis model of the physical power grid. Normally, the imbalances at the output of the regulation service model would be represented in frequency changes. However, for steady-state simulations, the concept of frequency is not applicable. Instead, a designated *virtual* swing bus consumes the mismatch of generation and consumption to make the steady-state power flow equations solvable. Therefore, for steady state simulations, the power system imbalance is measured at the slack generator output (Gomez-Exposito et al., 2008).

In the SOARES study, the full AC topology of ISO-NE is replaced by the zonal network (i.e. pipe and bubble) model shown in Fig. 11. It consists of 13 bubbles, their interfaces and external tie-lines with neighboring ISOs. This model is represented by a DC power flow analysis with each zone-bubble represented as a bus and each zone-interface is represented as a line. In order to recognize that ISO New England is part of the Eastern Interconnect, the swing bus is added to represent power imbalances exchanged with New York ISO. This swing bus is connected to the Vermont, Western Massachusetts, Connecticut, and Norwalk bubbles but is distinct from the tie-lines to these bubbles. In such a way, the power flows to and from this New York swing bus also represent the deviations away from scheduled tie-line flows.

In the normal operating mode, the regulation service and the real-time balancing operations are able to keep the system balanced. However, a sudden line or generator outage can create a large imbalance that the real-time market and regulation service are unable to mitigate. The EPECS simulator is able to address forced outage events by switching from a normal operations to an emergency operations mode. In the event of a forced outage, the ISO-NE contingency operations are assumed to run a RTUC in the same time step. The simulator then continues to run the regulation and SCED models until a time that is evenly divisible by 15 min at which point the RTUC is called as in normal operations.

4. Data: Characteristics of the ISO New England case study

This section describes the six scenarios analyzed for this study and the ISO New England data used for each scenario.

4.1. Study scenarios

A total of 12 scenarios are studied for the years 2025 and 2030; six scenarios for each year. Each scenario is described by different characteristics of load profiles, renewable energy integration and the generation base as shown in Table 1. These scenarios are described in more detail in ISO New England (2017b).

4.1.1. Scenario 1 – “RPSs + Gas”

Scenario 1 uses the generation base expected for 2019/2020. The gross demand, the solar PV and the energy efficiency values are based on the ISO New England 2016 report on capacity, energy, load, and transmission (2016 CELT report) (ISO New England, 2016a). The amounts of renewable energy sources in the system, such as wind, are chosen according to ISO New England 2016 Renewable Portfolio Standards (RPS) (ISO New England, 2016b). Half of the oldest oil and coal generation units are planned to retire by 2025, while the other half by 2030. The retired units are replaced by natural gas combined-cycle (NGCC) units at the same locations. The amount of new NGCC generation is planned to meet the net Installed Capacity Requirement (NICR). The historical profiles are used for imports from Hydro-Quebec (HQ) and New Brunswick (NB).

4.1.2. Scenario 2 – “ISO Queue”

Scenario 2 is identical to Scenario 1 in terms of generation base, planned retirements, gross demand and energy imports from HQ and NB being based on forecasts in 2016 CELT report. However, for Scenario 2, the retired oil and coal units are replaced by renewable energy sources instead of NGCC. Similar to Scenario 1, the addition of renewable energy sources meets the assumed NICR. The locations of the renewable energy sources are according to ISO Interconnection Queue (Anon, 2017).

4.1.3. Scenario 3 – “Renewables plus”

Scenario 3 uses additional renewable energy sources, such as behind-the-meter (BTM) and utility-scale solar PV and wind units, to replace the retiring units and meet or exceed the existing RPSs. In addition to the new renewable energy source, Scenario 3 adds battery energy systems, energy efficiency and plug-in hybrid electric vehicles (PHEV) to the system. Moreover, two new tie lines are added to increase the hydroelectric imports. The added resources exceed the assumed NICR.

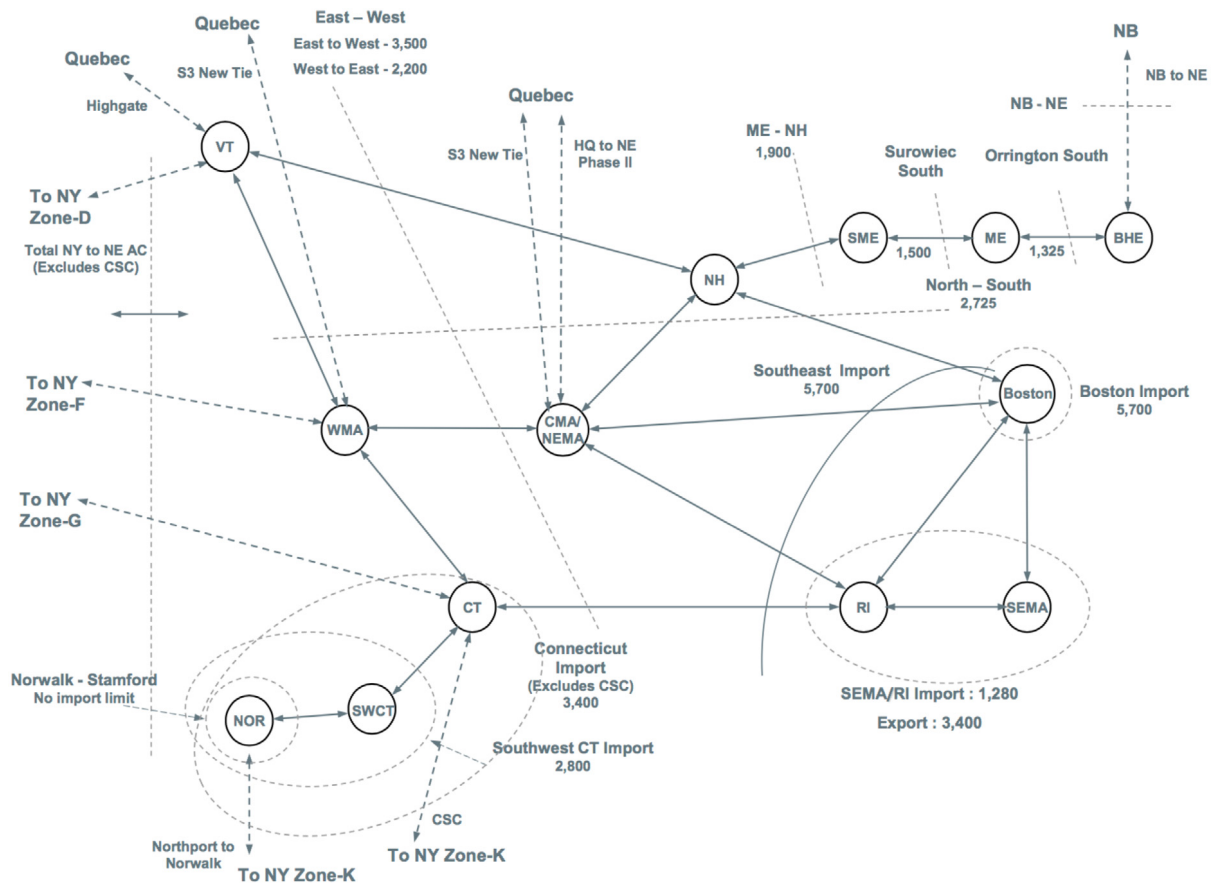


Fig. 11. Topology of the ISO-NE zonal network model (Coste, 2016).

4.1.4. Scenario 4 – “No Retirements beyond FCA #10”

Scenario 4 uses the same data as Scenario 1 in terms of gross demand, energy efficiency and solar PV integration being based on the 2016 CELT report. The historical imports data is also used similar to Scenario 1. However, the renewable energy integration is done according to “1.3.9” approval to meet the RPSs (Anon, 2017). Additionally, in contrast to other scenarios, no generation units are retired beyond known FCA resources which are replaced by NGCC located at the Hub to meet the NICR.

4.1.5. Scenario 5 – “acps + gas”

Scenario 5 uses the same data as Scenario 4 in terms of gross demand, energy efficiency and renewable energy integration being based on the 2016 CELT report. The historical imports data is also used similar to Scenario 4. However, half of the oldest oil and coal generation units are planned to retire by 2025, while the other half by 2030 which are replaced by new NGCC units to meet the NICR.

4.1.6. Scenario 6 – “RPSs + Geodiverse Renewables”

Scenario 6 is identical to Scenario 2 in terms of gross demand, energy efficiency, generation base and retirement schedules being based on 2016 CELT report. The HQ and NB imports are also based on historical data. Also, the addition of renewable energy sources are used to meet the RPSs and the NICR. However, the renewable energy sources are split into three equal groups: the first group consists of solar PV units located mainly in Southern New England area, the second group is the onshore wind power located in Maine, and the third group is the offshore wind located connected to southeastern Massachusetts/Newport, Rhode Island, and Rhode Island bordering Massachusetts (SEMA/RI) and Connecticut. Thus,

the solar PV and offshore wind units are located closer to the main load centers while the onshore wind in Maine is in a remote area.

4.2. Load profiles

This section describes the statistical characteristics of the system load for each of 12 scenarios. As shown in Table 1, all scenarios use the gross demand based on 2016 CELT forecast. Therefore, the gross demand profiles for the scenarios from the same year are identical. However, the combined value of gross demand, energy efficiency and electric vehicles charging loads are studied here as a better representation of the actual load in the system than needs to be served. This introduces some differences between load profiles for different scenarios as discussed below.

Load data can be represented as time profiles, duration curves and histograms, where each representation carries different information about its statistical characteristics. The aggregated load data for Scenario 2025-4 is shown in Fig. 12 as an example. The choice of this scenario is due to the fact that it follows the established evolution pattern of the ISO New England generation base as described in Section 4.1.4, and is often referred to as “business-as-usual” case. The graphs in Fig. 12 show that the aggregated system load varies in a wide range during the year, reaching the summer peak value of 27,950 MW and dropping to the lowest 7142 MW value during spring months. The average load during the year is 14,483 MW with a standard deviation of 3587 MW.

While the ability to serve the system peak load is one of the most important components of power system reliable operations, within the scope of this study the periods of the year with lowest

Table 1

The six scenarios of the ISO New England SOARES project.

Scenario	Retirements	Gross Demand	PV	Energy Efficiency	Wind	New NG Units	HQ and NB External Ties & Transfer Limits
1	1/2 in 2025 1/2 in 2030	Based on 2016 CELT forecast	Based on 2016 CELT forecast	Based on 2016 CELT forecast	As needed to meet RPSs	NGCC	Based on historical profiles
2	1/2 in 2025 1/2 in 2030	Based on 2016 CELT forecast	BTM Based on 2016 CELT forecast; non-BTM same as wind	Based on 2016 CELT forecast	Used to satisfy net ICR	None	Based on historical profiles
3	1/2 in 2025 1/2 in 2030	Based on 2016 CELT forecast	8,000MW (2025) 12,000MW (2030) BTM PV 4,000MW (2025) 6,000MW (2030) Utility PV 4,000MW (2025) 6,000MW (2030)	4,844MW (2025) 7,009MW (2030)	5,733MW (2025) 7,283MW (2030)	None	Based on historical profiles plus additional imports
4	No retirements beyond FCA #10	Based on 2016 CELT forecast	Based on 2016 CELT forecast	Based on 2016 CELT forecast	Existing plus those with I.3.9 approval	NGCC	Based on historical profiles
5	1/2 in 2025 1/2 in 2030	Based on 2016 CELT forecast	Based on 2016 CELT forecast	Based on 2016 CELT forecast	Existing plus those with I.3.9 approval	NGCC	Based on historical profiles
6	1/2 in 2025 1/2 in 2030	Based on 2016 CELT forecast	381MW (2025) 1,611MW (2030)	Based on 2016 CELT forecast	Onshore wind: 381MW (2025) 1,611MW (2030) Offshore wind: 381MW (2025) 1,611MW (2030)	None	Based on historical profiles

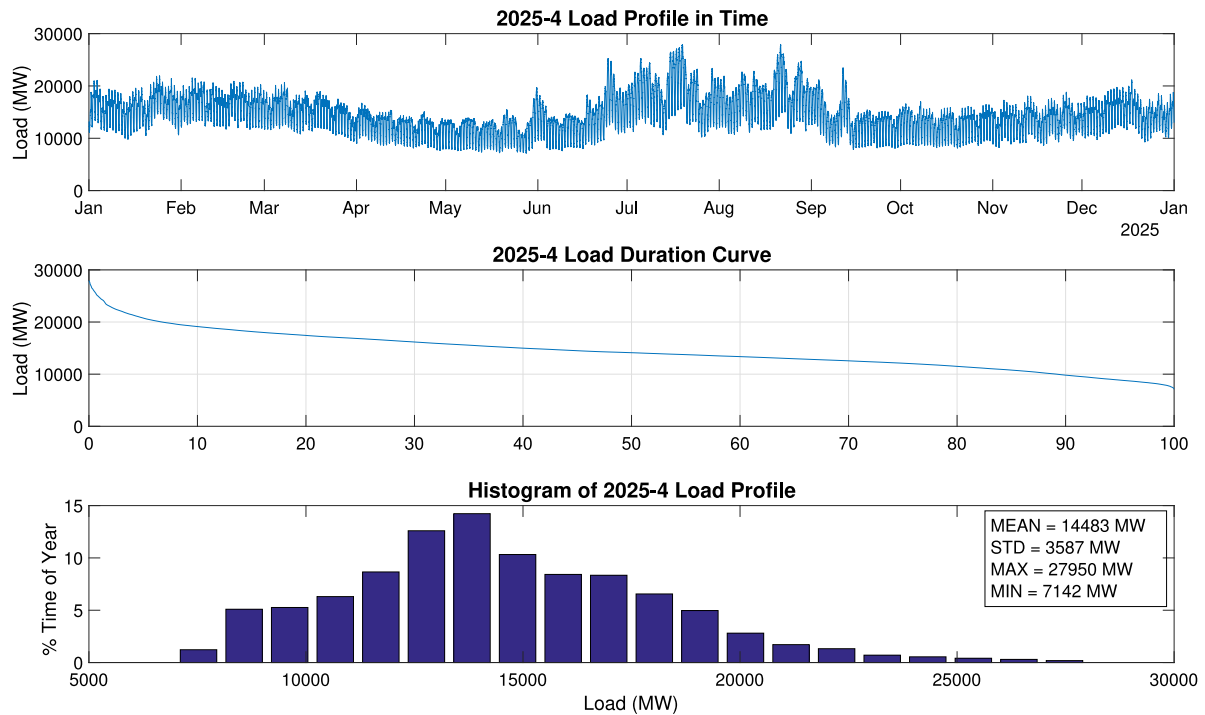
**Fig. 12.** The aggregated load profile for Scenario 2025-4.

Table 2
Load profile statistics for 2025 scenarios.

	2025-1	2025-2	2025-3	2025-4	2025-5	2025-6
Max (MW)	27,950	27,950	26,950	27,950	27,950	27,950
Min (MW)	7,142	7,142	6,302	7,142	7,142	7,142
Energy (TWh)	127	127	122	127	127	127
Mean (MW)	14,483	14,483	13,927	14,483	14,483	14,483
STD (MW)	3,587	3,587	3,302	3,587	3,587	3,587

Table 3
Load profile statistics for 2030 scenarios.

	2030-1	2030-2	2030-3	2030-4	2030-5	2030-6
Max (MW)	28,604	28,604	26,335	28,604	28,604	28,604
Min (MW)	7,840	7,840	5,189	7,840	7,840	7,840
Energy (TWh)	133	133	118	133	133	133
Mean (MW)	15,180	15,180	13,465	15,180	15,180	15,180
STD (MW)	3,583	3,583	3,378	3,583	3,583	3,583

aggregated system load represent a bigger interest due to the following two main factors. First, some of the scenarios described in Table 1 assume integration of large amount of solar and wind resources into the system. This may lead to significantly low, or even negative, net load that the system generation needs to serve. Second, a significant portion of the system generation base are nuclear units and they are assumed to operate in a “must-run” mode. This further increases the possibility of having excess generation in the system and the need of curtailment of renewables.

The histograms of load profiles for the year 2025 are presented in Fig. 13. The load distributions exhibit the same statistical characteristics, except for Scenario 3 due to the addition of energy efficiency and electric vehicle charging loads mentioned above. As a result, Scenario 3 has slightly lower peak load and minimum load levels. Table 2 summarizes the statistical characteristics of the load data for the six scenarios of the year 2025.

Next, the load profiles for 2030 scenarios are studied. Similar to the 2025 case, the profiles for all scenarios have identical distributions except for Scenario 3 due to incorporation of energy efficiency and electric vehicle charging loads as shown in Fig. 14. The statistical characteristics of the load profiles for 2030 scenarios are presented in Table 3. A pattern similar to 2025 scenarios is observed here too when Scenario 3 has slightly lower power and energy indicators. The following observation should be made that while the overall consumption, the peak load, the minimum load experience slight increase for all scenarios compared to 2025, Scenario 3 shows the opposite trend. This is explained by increased amounts of energy efficiency and electric vehicle penetration compared to 2025 as shown in Table 1.

4.3. Net load profiles

Net load is the difference between the aggregated system load and the total generation produced by the renewable energy sources. The shape of the net load profile is more relevant when studying the ability of the system to maintain balance as it represents the actual amount of MW that needs to be supplied by dispatchable resources, such as generators, pumped storage units and demand response. The comparison of the system load and the corresponding net load for Scenario 2025-4 is presented in Fig. 15. The graphs show that the incorporation of renewable energy alters the power demand pattern significantly. The overall system demand decreases, and the shape of the histogram shifts to the left. This indicates that the system may need less generation capacity to meet the demand. On the other hand, it is uncertain whether the system is prepared to effectively harvest the power

Table 4
Net load profile statistics for 2025 scenarios.

	2025-1	2025-2	2025-3	2025-4	2025-5	2025-6
Max (MW)	22,673	22,157	20,097	23,077	23,077	22,182
Min (MW)	943	−577	−5,959	2,395	2,395	−464
Energy (TWh)	78	72	58	85	85	74
Mean (MW)	8,927	8,180	6,639	9,742	9,742	8,420
STD (MW)	3,539	3,707	3,805	3,348	3,348	3,536
% Time Excess Gen.	3.12	8.33	20.13	0.27	0.27	5.09
% Time Neg Net Load	0.00	0.05	3.68	0.00	0.00	0.03

generated by renewable energy units given the limitations of the associated generation fleet.

The relevance of this question is particularly emphasized for Scenario 2025-3 where the net load drops below zero at different instances throughout the year as shown in Fig. 16. Negative net load is an indication of excess renewable energy generation in the system which supports the statement above that the system will necessarily be unable to harvest it all. This is a challenge for a system with a large presence of “must-run” nuclear units. The matter is further complicated when considering that most renewable energy generation is located in remote areas of Maine, relatively far from major consumption areas, such as Massachusetts.

Net load distributions for the six scenarios of 2025 are presented in Fig. 17. Unlike the load data studied above, net load distributions differ from each other due to differences in renewable energy quantities present in each scenario. The graphs show that three out of six scenarios reach negative net load at some point during the year with Scenario 3 being the most severe example; its net load drops to the minimum of −5959 MW due to the heavy presence of renewable energy shown in Table 4. Moreover, when the presence of “must-run” nuclear units is taken into account, it becomes obvious that all six scenarios of 2025 have excess generation in the system.

The challenges described above are exacerbated for the year 2030 as shown in Fig. 18. Significant parts of net load distributions are now below zero. Moreover, Table 5 shows that net load values for three scenarios drop below −10,000 MW. For a system with less than 30,000 MW peak load this is a significant challenge. In order to maintain reliable operations under such conditions, the power system needs to make a comprehensive use of its demand response resources, renewable energy curtailment and pumped storage units. Some scenarios with heavy curtailment of renewables may reveal their infeasibility under the current system configuration, implying the need for more critical changes in the system, such as the construction of new transmission lines or availability of more storage or demand response capabilities.

4.4. Net load ramping characteristics

In addition to the net load variations, another important characteristic that defines the dynamics of the system is the rate at which the consumption profile changes (i.e. the system ramping rate). It is shown in Fig. 19 for Scenario 2025-4. Considering ramping dynamics is particularly important when the study deals with a significant integration of highly volatile renewable energy sources. A system with a significant presence of nuclear power (especially when assumed to must-run at full capacity) may lack the flexibility to follow such a net load profile; creating another challenge for the full utilization of available renewable generation by the system. However, emergence of more flexible natural gas units may compensate for their lack of flexibility.

Ramping rates for four different time resolutions are defined and studied here, namely 1-minute, 10-minute, 1-hour and 4-hour, to capture net load dynamics at various layers of control, such as real-time, SCED, RTUC and SCUC. They indicate whether

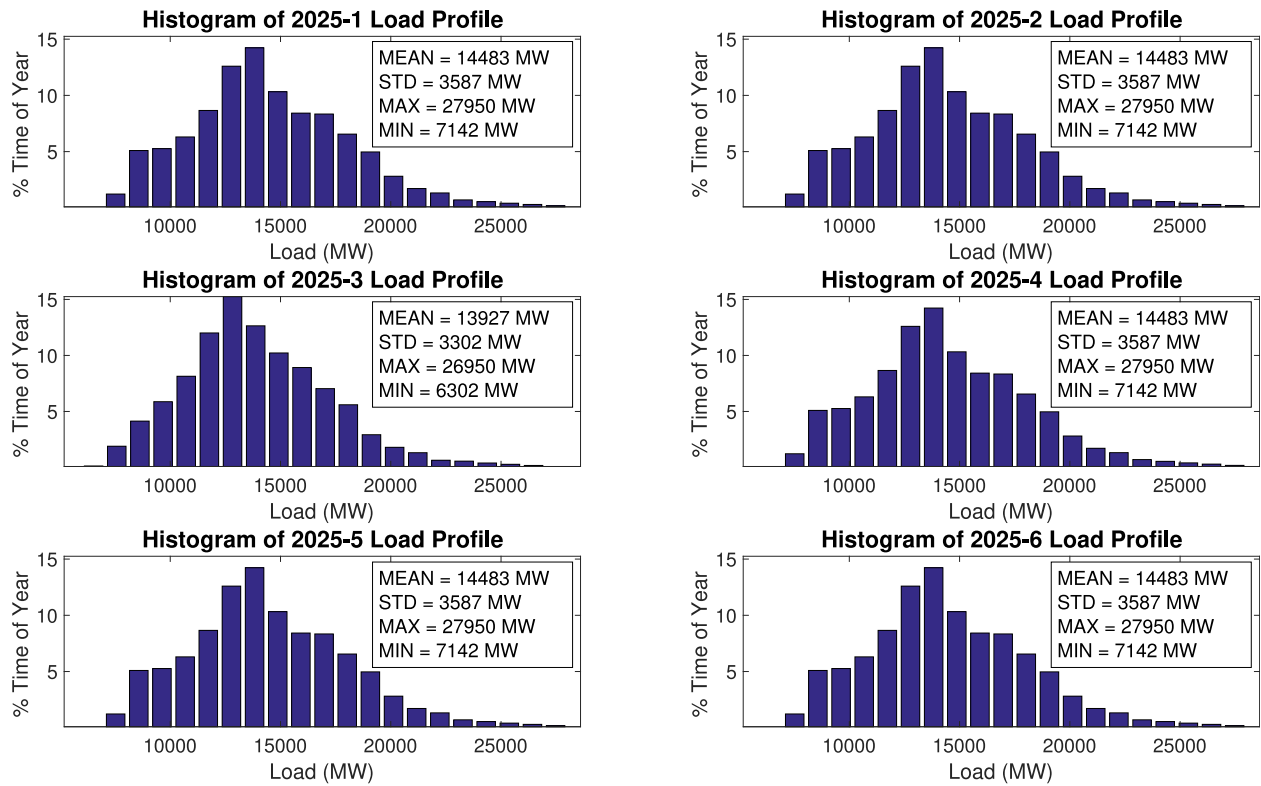


Fig. 13. Load profile histograms for 2025 scenarios.

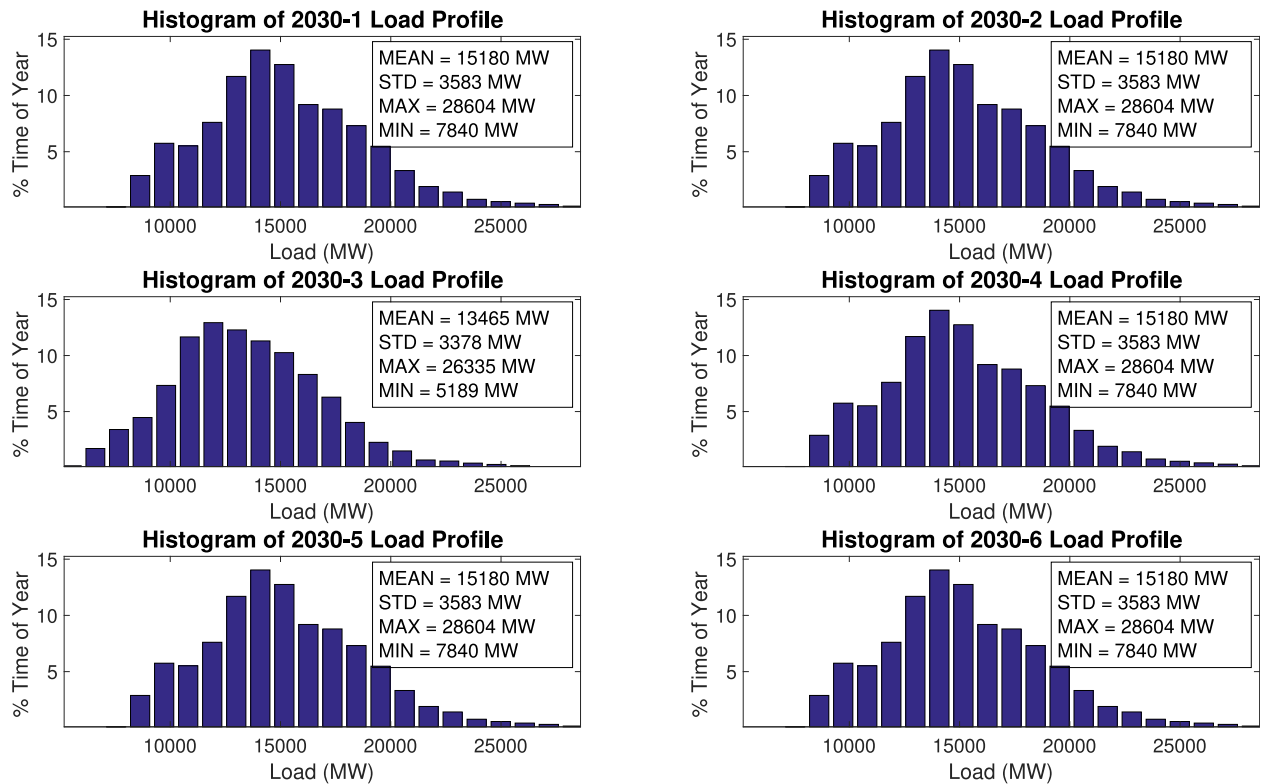


Fig. 14. Load profile histograms for 2030 scenarios.

the system will be able to schedule the necessary generation, dispatch them and supply the demand in the real-time. The definitions of these ramping rates with different time resolutions are defined below.

Definition 4.4.1 (Inter-1-Minute Ramping Rate). The difference between consecutive points on the net load profile with one minute resolution.

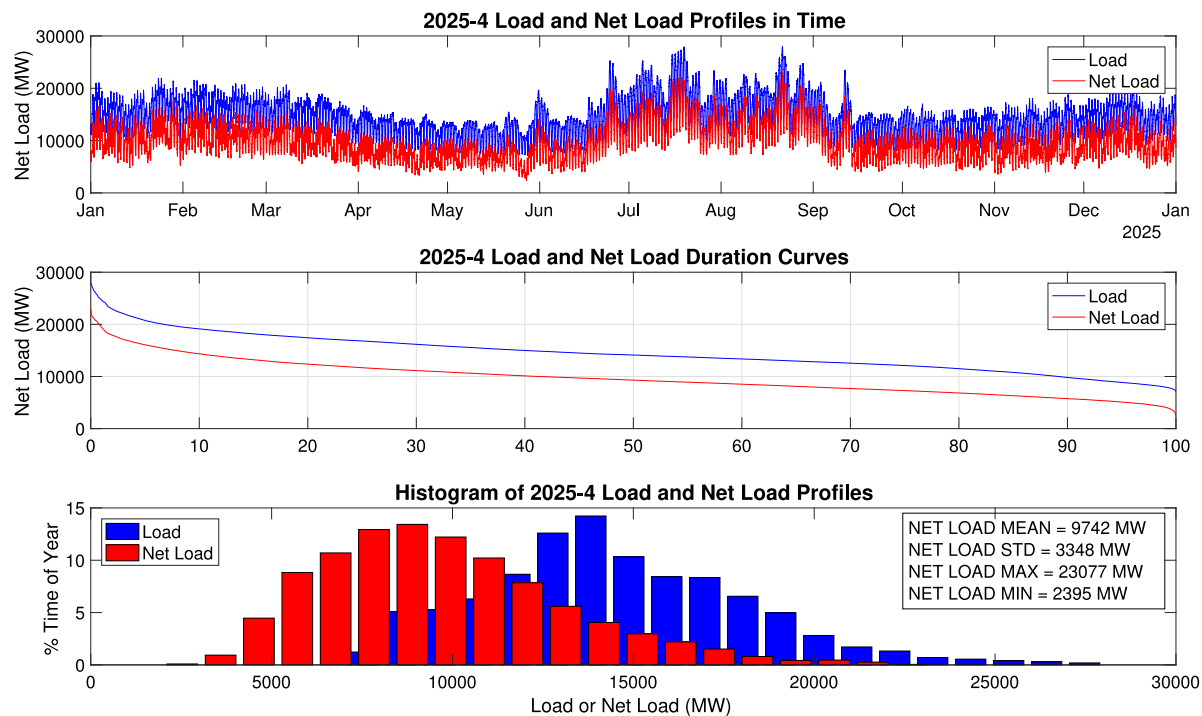


Fig. 15. Comparison of load and net load for Scenario 2025-4.

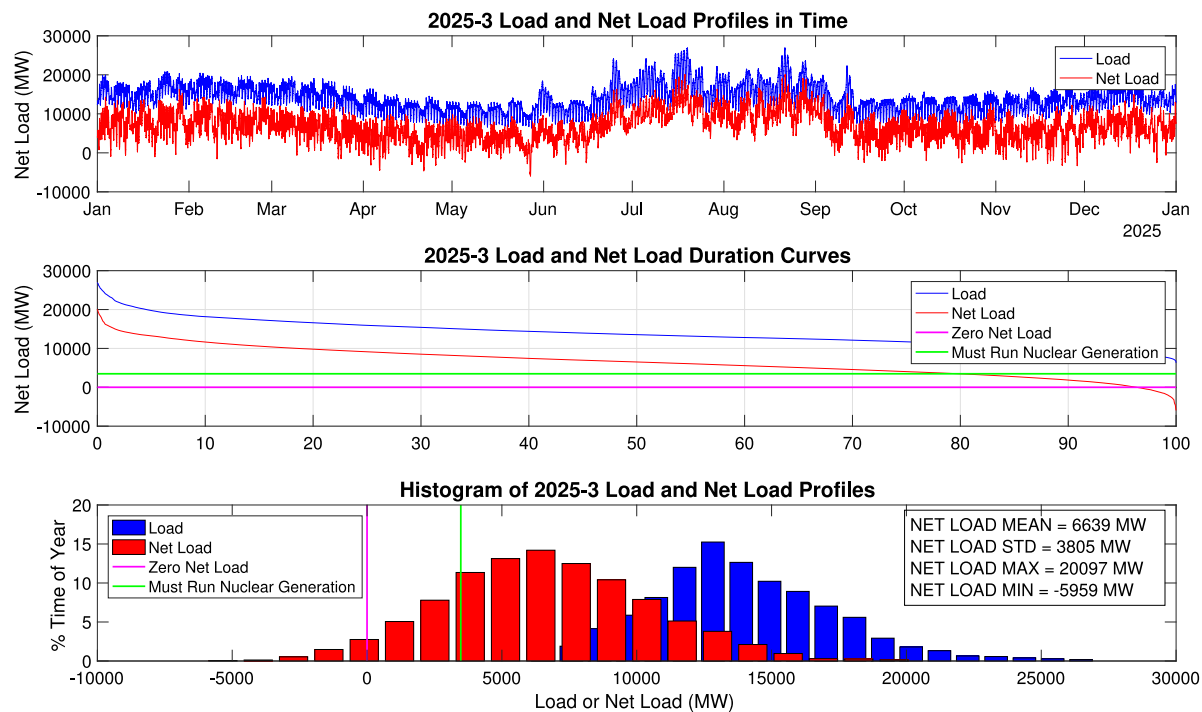


Fig. 16. Comparison of load and net load for Scenario 2025-3.

Table 5
 Net load profile statistics for 2030 scenarios.

	2030-1	2030-2	2030-3	2030-4	2030-5	2030-6
Max (MW)	22,938	21,291	19,251	23,523	23,523	20,871
Min (MW)	597	−10,705	−11,851	2,465	2,465	−10,575
Energy (TWh)	80	32	41	90	90	36
Mean (MW)	9,158	3,675	4,720	10,310	10,310	4,094
STD (MW)	3,621	5,629	4,688	3,337	3,337	5,022
% Time Excess Gen.	2.91	48.11	37.02	0.09	0.09	45.74
% Time Neg. Net Load	0.00	27.49	15.79	0.00	0.00	21.38

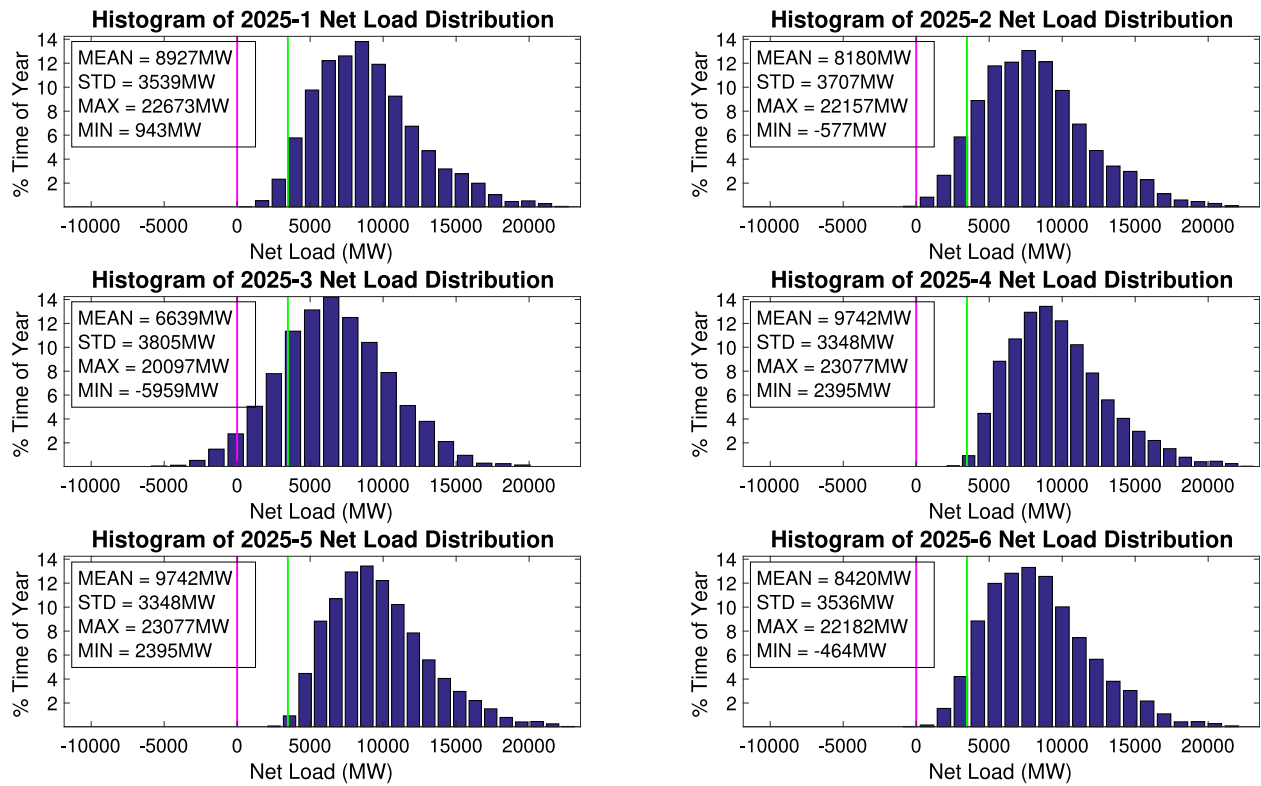


Fig. 17. Net load profile histograms for 2025 scenarios.

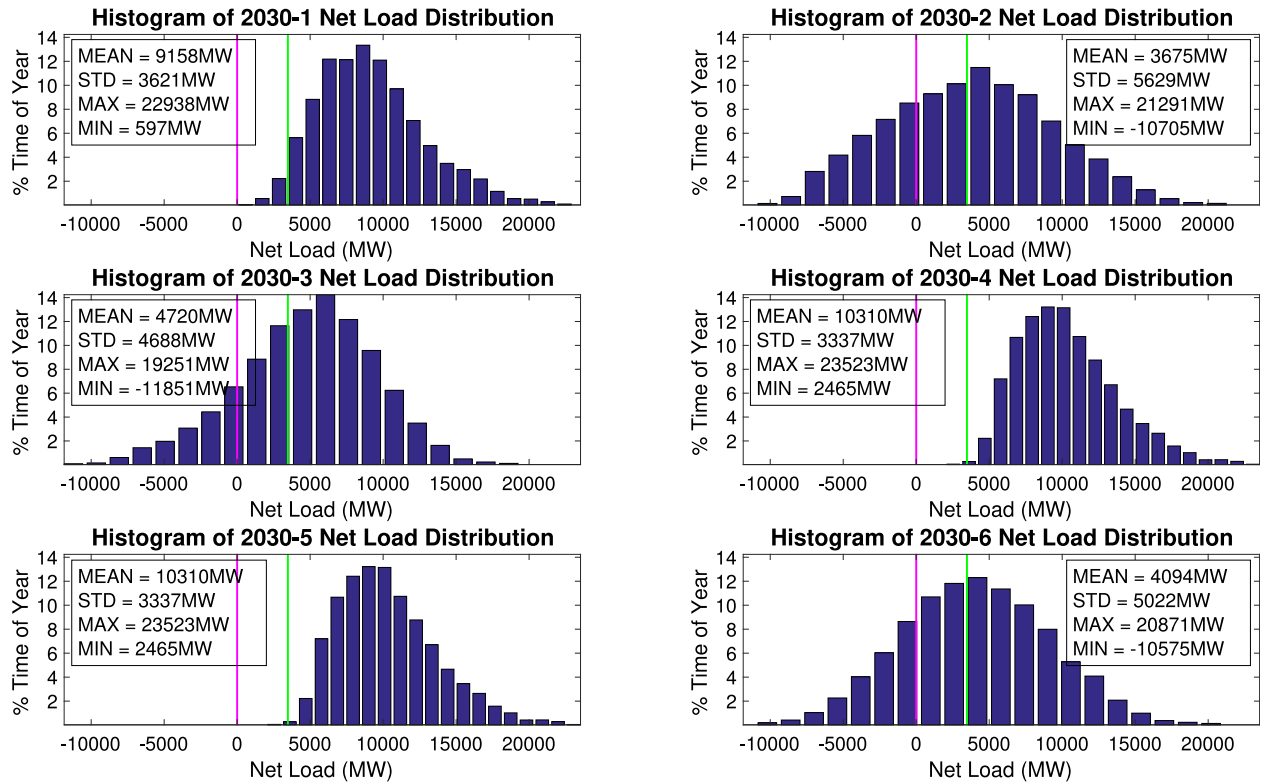


Fig. 18. Net load profile histograms for 2030 scenarios.

Definition 4.4.2 (*Inter-10-Minute Ramping Rate*). The difference between consecutive points on the net load profile after it has been averaged into 10 min time blocks.

Definition 4.4.3 (*Inter-1-Hour Ramping Rate*). The difference between consecutive points on the net load profile after it has been averaged into one hour time blocks.

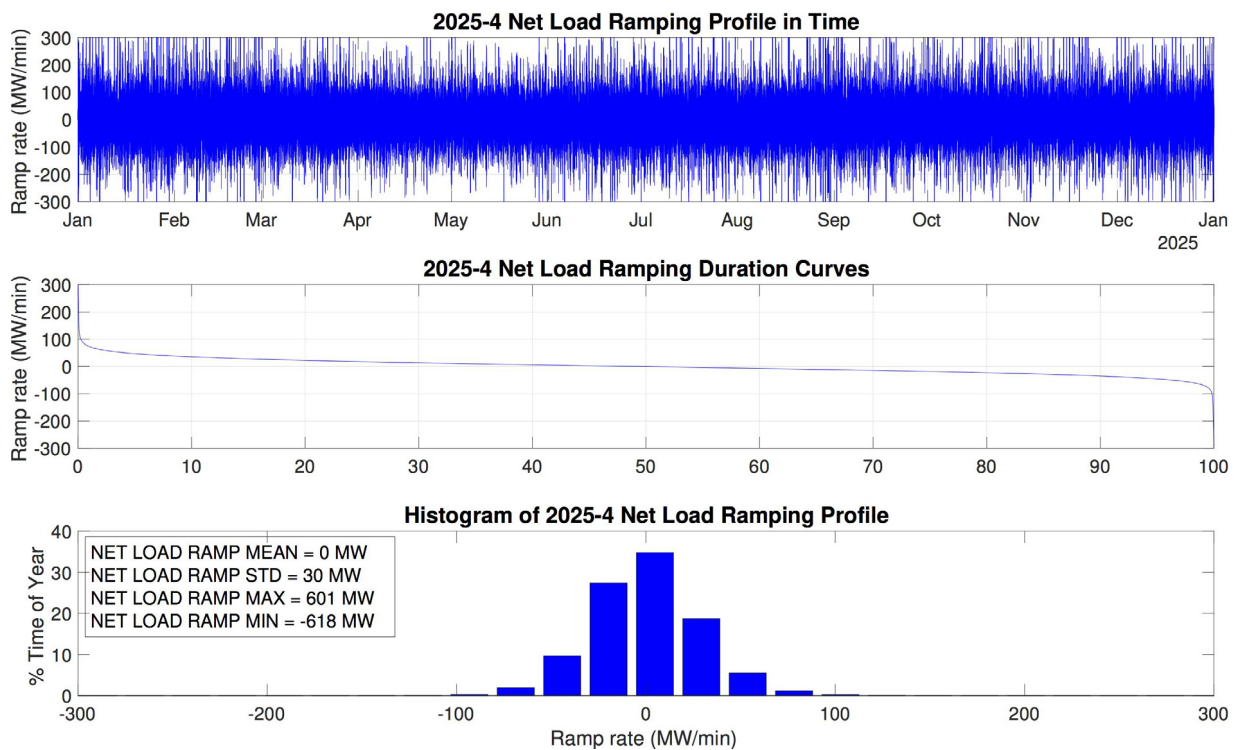


Fig. 19. Net load ramping profile for Scenarios 2025-4.

Definition 4.4.4 (*Inter-4-Hour Ramping Rate*). The average sustained ramp within a four hour window that covers the minimum and maximum net load values of that time period.

Comparison of 1-minute ramping rate distributions for different scenarios of 2025 in Fig. 20 shows that they have comparably similar ramping characteristics. Table 6 summarizes net load ramping characteristics for the six scenarios of 2025. The data in Table 6 shows that ramping rates are the highest when calculated with 1-minute resolution and generally decreases with a coarser resolution. This is due to the fact that ramping rates calculated with coarser time resolution are equivalent to averaging ramping rates with finer resolution which narrows the range of their maximum and minimum values. This is a key observation, since it indicates that generation scheduling programs with coarser time steps always underestimate the need for ramping capabilities. This issue becomes more relevant as more renewable energy is integrated into the system, and, therefore, present an argument in favor of the procurement of ramping reserves.

Table 6 also shows that scenarios 2025-2 and 2025-3 exhibit the greatest net load ramp up at 1-minute, 10 min and 4 h resolution. Also, the maximum 1 min down ramp and the maximum 10 min down ramp are similar for all 2025 scenarios. Scenario 2025-3 exhibits the greatest net load ramp up and down at the 1-hour resolution. Scenarios 2025-3 and 2025-6 exhibit the largest intra 4-hour ramp in an upward direction.

Similarly, the ramping rate distributions for the year 2030 are plotted in Fig. 21. The statistical characteristics in Table 7 show that scenarios 2030-2, 2030-3 and 2030-6 exhibit the greatest net load ramp up at 1-minute, 10 min, 1 h and 4 h resolutions. Also, the maximum 1 min down ramp is similar for all 2030 scenarios except for 2030-3. The maximum 10 min ramps down are similar for all 2030 scenarios. Scenarios 2030-2, 2030-3, and 2030-6 exhibit the greatest net load ramp down at the 1-hour and 4-hour resolutions.

4.5. Load, solar, & wind forecast errors in the net load

The forecast errors for each type of resource used in this study are defined in Table 8. The SCUC, RTUC and SCED optimization programs uses different forecasts of the net load and, thus, have different forecast errors respectively. The trend shows that the smaller the time horizon of the optimization program is, the more accurate the forecast becomes because it is easier to forecast closer time intervals.

Also, there is a clear distinction between forecast errors for load and renewable energy sources such as wind and solar. Load forecast technologies have been developed and refined during long decades of power system operations, starting from its inception. In contrast, wind and solar powers are comparably recent phenomena for power system operations and their forecasts are not as accurate. This also has to do with different technologies used to predict the system load and renewable energy generation. This fact demonstrates another challenge associated with renewable energy integration; significantly increased uncertainty in system resource scheduling and procurement.

5. Case study results

This section presents the case study results in terms of key performance characteristics of the power system including: load following and ramping reserves, curtailment of renewables, interface & tie-line performances, regulation reserves and the system balancing performance. Each of these metrics are analyzed in the following subsections.

5.1. Load following reserves

Upward and downward load following reserves are procured during the day-ahead resource scheduling and are dispatched in the real-time balancing in response to net load variations. Traditionally, the procurement of sufficient upward load following

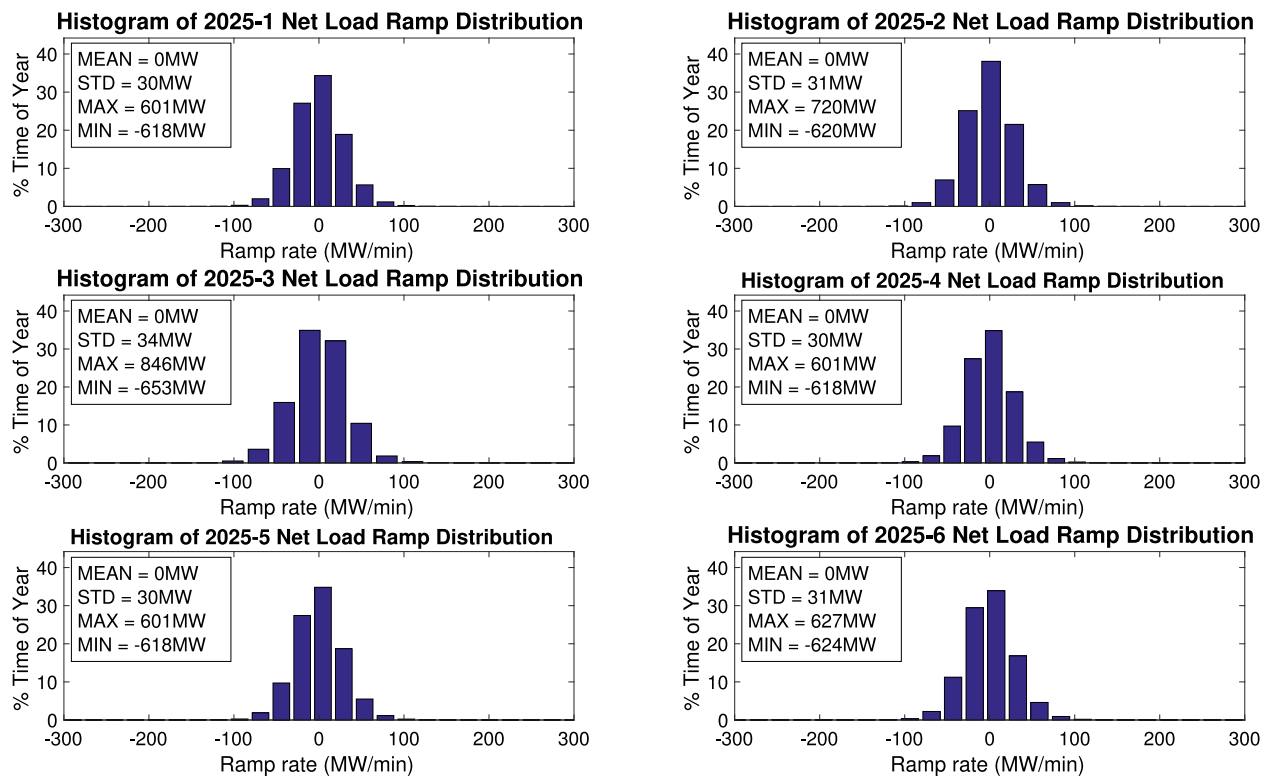


Fig. 20. Net load ramping histograms for 2025 scenarios.

Table 6

Net load ramping statistics for 2025 scenarios.

	2025-1	2025-2	2025-3	2025-4	2025-5	2025-6
Max 1-Min-Up ^a (MW/min)	601	720	846	601	601	627
Max 1-Min-Down ^a (MW/min)	618	620	653	618	618	624
Max 10-Min-Up ^b (MW/min)	184	251	312	126	126	220
Max 10-Min-Down ^b (MW/min)	81	84	78	73	73	78
Max 1 h-Up ^b (MW/min)	49	52	73	49	49	57
Max 1 h-Down ^b (MW/min)	46	45	60	40	40	44
Max 4 h-Up ^c (MW/min)	30	33	49	29	29	37
Max 4 h-Down ^c (MW/min)	38	40	42	36	36	38

^aInter 1-minute ramps are calculated as the difference between consecutive points on the net load profile with 1-minute resolution.^bInter 10 min and Inter 1 h ramps are calculated as the difference between consecutive points on the net load profile after it has been averaged into 10 min or 1 h blocks respectively.^cIntra 4 h ramps are calculated as the average *sustained* ramp within a four hour window that covers the minimum and maximum net load values of that time period.

Table 7

Net load ramping statistics for 2030 scenarios.

	2030-1	2030-2	2030-3	2030-4	2030-5	2030-6
Max 1-Min-Up ^a (MW/min)	660	1034	1008	611	611	899
Max 1-Min-Down ^a (MW/min)	879	878	677	879	879	879
Max 10-Min-Up ^b (MW/min)	228	748	383	126	126	672
Max 10-Min-Down ^b (MW/min)	109	108	115	109	109	161
Max 1 h-Up ^b (MW/min)	53	103	95	52	52	99
Max 1 h-Down ^b (MW/min)	45	76	94	40	40	67
Max 4 h-Up ^c (MW/min)	33	61	67	32	32	69
Max 4 h-Down ^c (MW/min)	39	49	63	36	36	51

^aInter 1-minute ramps are calculated as the difference between consecutive points on the net load profile with 1-minute resolution.^bInter 10 min and Inter 1 h ramps are calculated as the difference between consecutive points on the net load profile after it has been averaged into 10 min or 1 h blocks respectively.^cIntra 4 h ramps are calculated as the average *sustained* ramp within a four hour window that covers the minimum and maximum net load values of that time period.

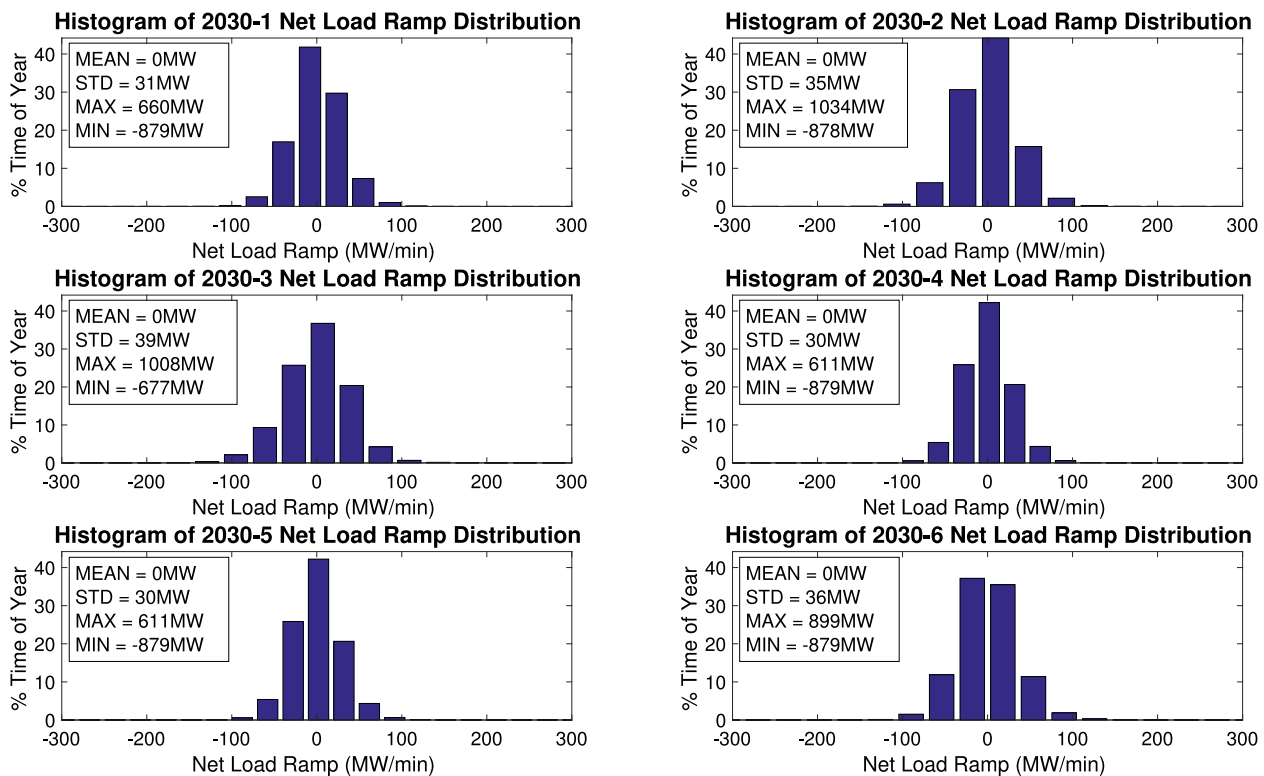


Fig. 21. Net load ramping histograms for 2030 scenarios.

reserves has been of the primary concern, while the ability of the system to provide downward load following service by reducing the generation output was assumed generally unconstrained. However, for the power system configuration scenarios considered in this study, both upward and downward load following reserves are equally important, as demonstrated by the results below.

As an example, the performance of load following reserves for Scenario 2025-4 is shown in Fig. 22. The amounts of upward and downward load following reserves fluctuate over time but are never completely exhausted (approach the zero black line). The closest the system gets to exhausting its downward load following reserves is during low-load spring and fall periods. Thus, when the system adheres to Scenario 2025-4, it is able to operate reliably without the need for more load following reserves.

In contrast to Scenario 2025-4, the results for Scenario 2025-3 in Fig. 23 tell a different story. Both upward and downward load following reserves are often exhausted or nearly so. The system is often unable to respond to the net load fluctuations. The integration of massive amounts of renewable energy for this scenario reduces the system net load significantly. This, coupled with the “must-run” nuclear units, fosters situations with nearly no downward load following reserves and an excess of upward load following reserves. In the meantime, as the system net load rises, upward load following reserves can become constrained before additional units can be committed. Fig. 23 shows that in the Spring and the Fall, the ability to track such low net load conditions is particularly constrained.

Fig. 24 shows the upward and downward load following reserve performances for all scenarios of 2025. The key performance statistics for each scenario are extracted into Table 9. Here, the 95th percentile indicates that the system has more than this quantity of upward/downward load following reserves for 95% of the time. The results show that for most of the scenarios the system exhibit sufficient downward load following reserves

Table 8

Forecast error statistics.

	Load	Wind	Solar
SCUC	1.65%	12%	7%
RTUC	1.5%	3%	3%
SCED	0.15%	3%	3%

throughout the year. The lowest level of the downward load following reserves is only 97 MW for Scenario 2025-3. However, judging by the corresponding 95th percentile value, such low-value occurrences are rare. On the other hand, Scenario 2025-3 completely exhausts its upward load following reserves at least 5% of the time, which represents a bigger issue. Thus, it can be concluded that despite the addition of significant renewable energy sources for Scenario 2025-3, the system is able to maintain adequate amount of downward load following reserves. However, such an increase of renewables energy capacity may require more upward load following reserves (in the form of newly committed units) to maintain the system’s ability to follow upward net load trends as renewable energy generation diminishes.

Such a result is consonant with the often discussed “duck curve” shown in Fig. 25 and first discussed by California ISO in the context of its solar integration planning studies. The duck curve presents three important operational challenges. During the midday hours, solar generation causes low net load conditions that will test a power system’s ability to track downward using downward load following reserves. Hours later, as solar generation wanes, net load conditions rise to their daily peak testing the power system’s ability to track upward with upward load following reserves. Finally, in the meantime, and as discussed in the next section, the transition hours between trough and peak conditions exhibits a sharp system ramp.

Similar to Fig. 24, Fig. 26 shows upward and downward load following reserve performances for all 2030 scenarios, and the

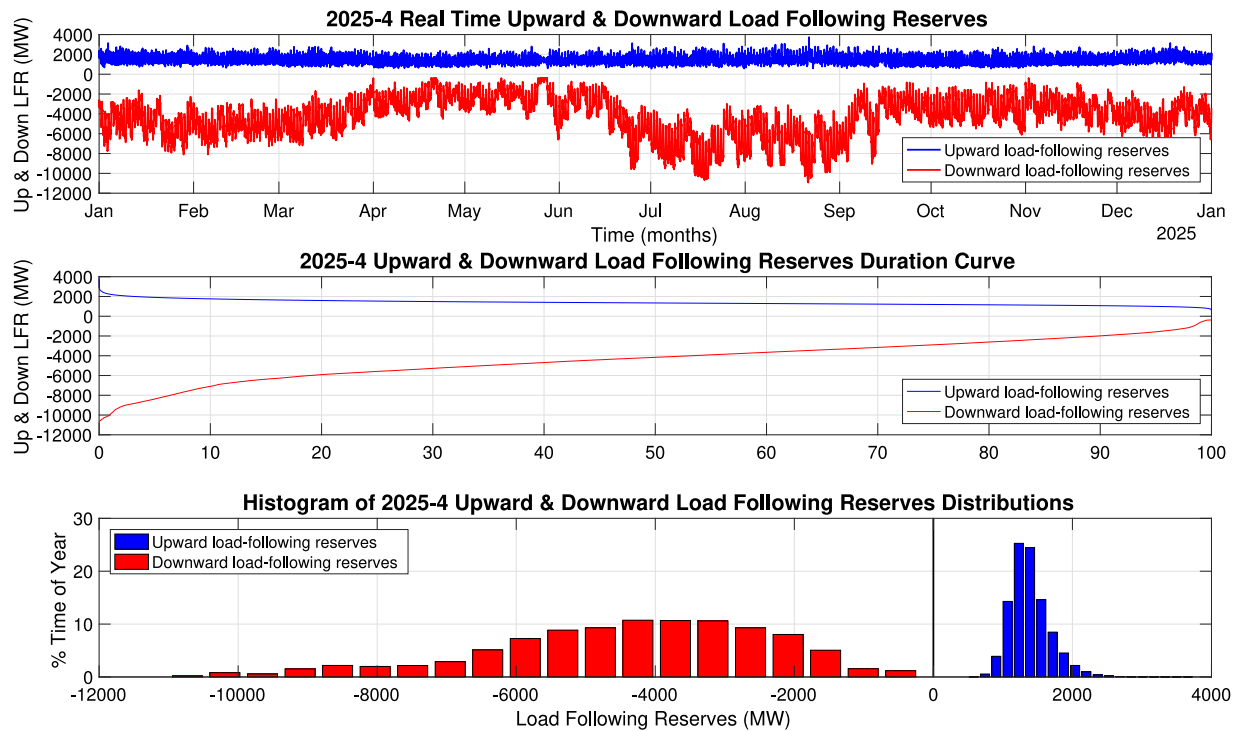


Fig. 22. Load following reserve profiles for Scenario 2025-4.

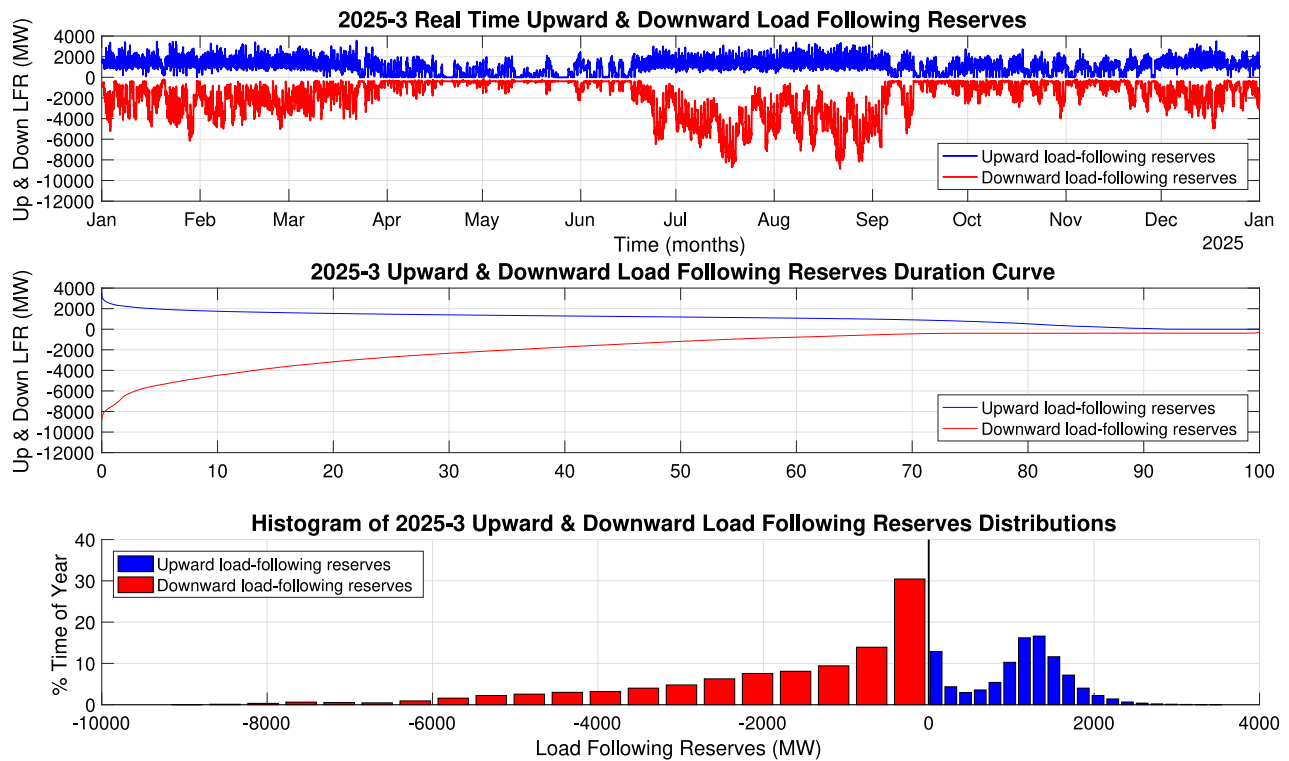


Fig. 23. Load following reserve profiles for Scenario 2025-3.

key performance statistics for each scenario are extracted into Table 10. The results here are significantly different from 2025 scenarios and reveal several important aspects of systems overloaded with renewable energy sources. All scenarios, except for Scenario 2030-4, completely exhaust their upward load following reserves during some periods of the year. While such events occur in less than 5% of time for all scenarios, except Scenario

2030-3, this is an overall negative trend compared to the system performance for 2025. Scenario 2030-3 experiences upward load following reserve shortages more often and requires an increase of such resources to maintain the balance of the system. The statistics in Table 10 show that Scenarios 2030-3 and 2030-6 entirely exhaust their downward load following reserves; albeit for a fairly short part of the year. Despite such rare occurrences,

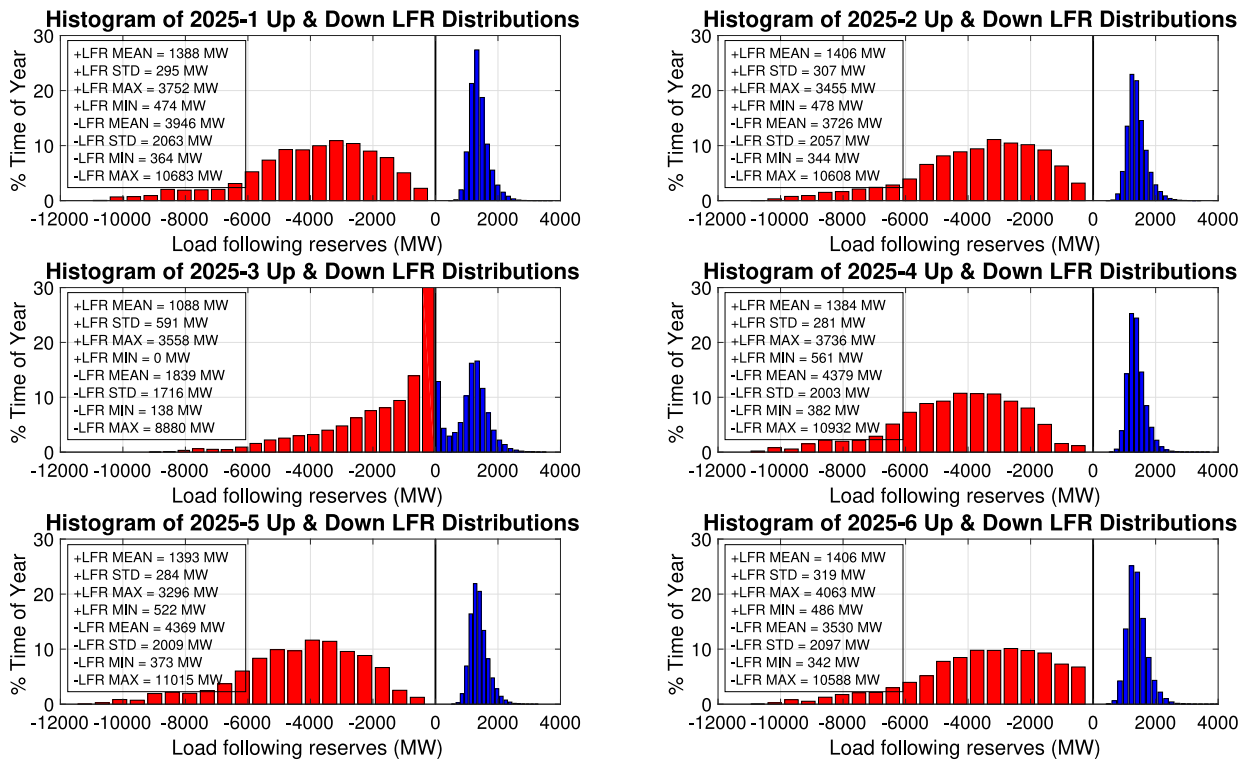


Fig. 24. Load following reserve distributions for 2025.

Table 9

Upward and downward load following reserve statistics for 2025 scenarios.

	2025-1	2025-2	2025-3	2025-4	2025-5	2025-6
Up LFR Mean (MW)	1,376	1,385	1,160	1,377	1,380	1,392
Up LFR STD (MW)	302	307	558	286	285	321
Up LFR Min (MW)	10	28	0	277	142	81
Up LFR 95 percentile (MW)	958	957	1	977	976	937
Down LFR Mean (MW)	4,096	3,850	1,937	4,498	4,501	3,729
Down LFR STD (MW)	1,860	1,848	1,656	1,798	1,816	1,936
Down LFR Min (MW)	339	342	97	383	382	340
Down LFR 95 percentile (MW)	1,318	1,180	342	1,784	1,788	786

the depletion of a resource that was assumed to be adequately available in the system for following the net load fluctuations shows the need for procurement of both upward and downward load following reserves in the day-ahead unit commitment. That said, the commitment of dispatchable resources and their associated quantities of commitment of load following and ramping reserves has a complex, difficult to predict, non-linear dependence on the amount of variable resources and the load profile statistics. Here, despite the similarities between Scenario 2030-4 and 2030-5, their associated quantities of load following reserves is quite different as a result of the differences in the resource characteristics between the two scenarios.

While the primary purpose of load following reserves is to mitigate the system imbalances induced by the net load variability and day-ahead forecast errors, increasing the quantity of load following reserves in the system is not always a comprehensive solution for imbalance mitigation. Certain portions of imbalances may be due to inadequate ramping capabilities of the resources or topological limitations of the system. To demonstrate this phenomenon, Fig. 27 shows the relationship between load following reserves and the imbalances for Scenario 2025-4. In the gray regions, upward and downward load following reserves do not serve to mitigate positive and negative imbalances respectively. In the white regions, upward and downward load following reserves serve to mitigate positive and negative imbalances respectively. In the magenta regions, a 1 MW increase of

load following reserves leads to a 1 MW reduction of imbalances. This region represents when there are insufficient amounts of load following reserves to serve the system imbalance. In Scenario 2025-4, imbalances do not coincide with low load following reserves; suggesting that imbalance mitigation requires use of another means.

Fig. 28 shows the relationship between load following reserves and the imbalances for the 2025 scenarios. These results confirm the conclusion reached above that all of the 2025 scenarios have sufficient downward load following reserves and, of the 2025 scenarios, only Scenario 2025-3 would benefit from additional upward load following reserves. Similarly, Fig. 29 shows the relationship between load following reserve requirements and the imbalances for the 2030 scenarios. Here, Scenarios 2030-3 and 2030-6 show the coincidence of downward load following reserves and positive imbalances; suggesting a need for more of this type of reserve. Also, all 2030 scenarios, except for Scenarios 2030-4, would benefit from additional upward load following reserves. To summarize, most scenarios require varying degrees of additional load following reserves.

5.2. Ramping reserves

Upward and downward ramping reserves are procured during the day-ahead resource scheduling to enhance the ramping

Spring/Autumn Load Profile with Increasing Behind-the-Meter Solar Power

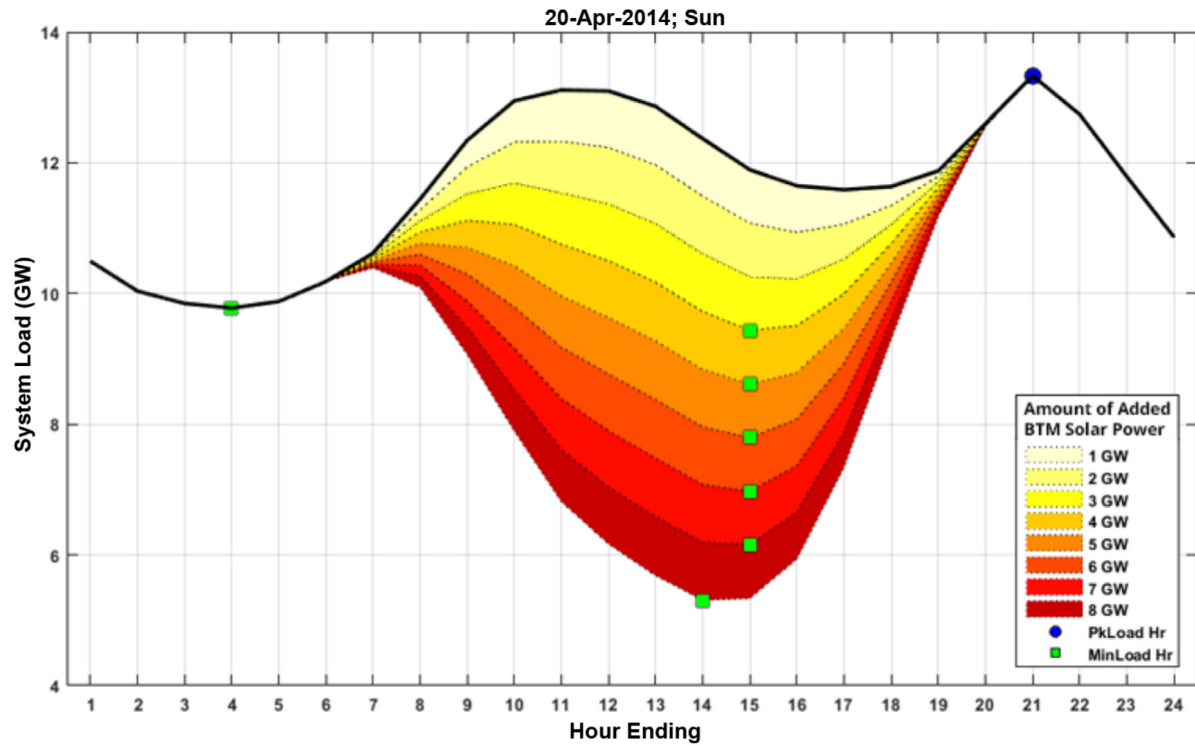


Fig. 25. The “Duck Curve” in ISO NEWSWIRE (2018).

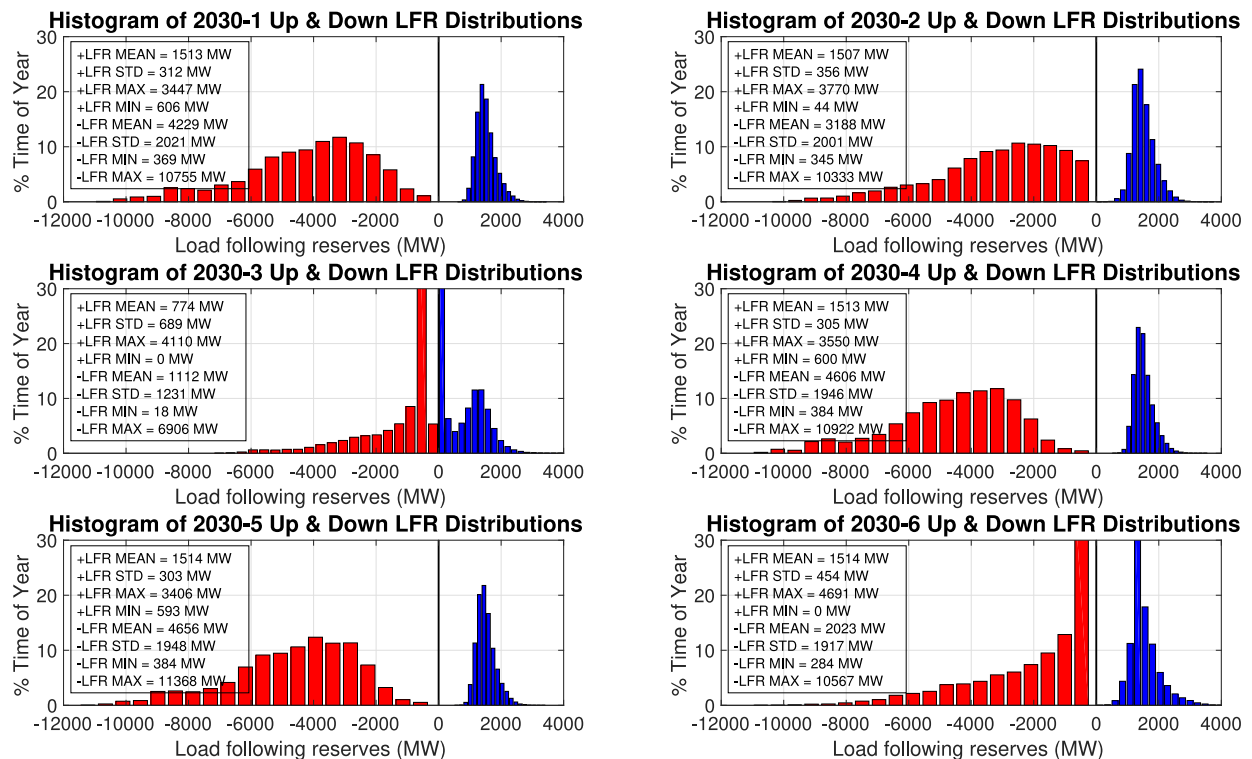


Fig. 26. Load following reserve distributions for 2030.

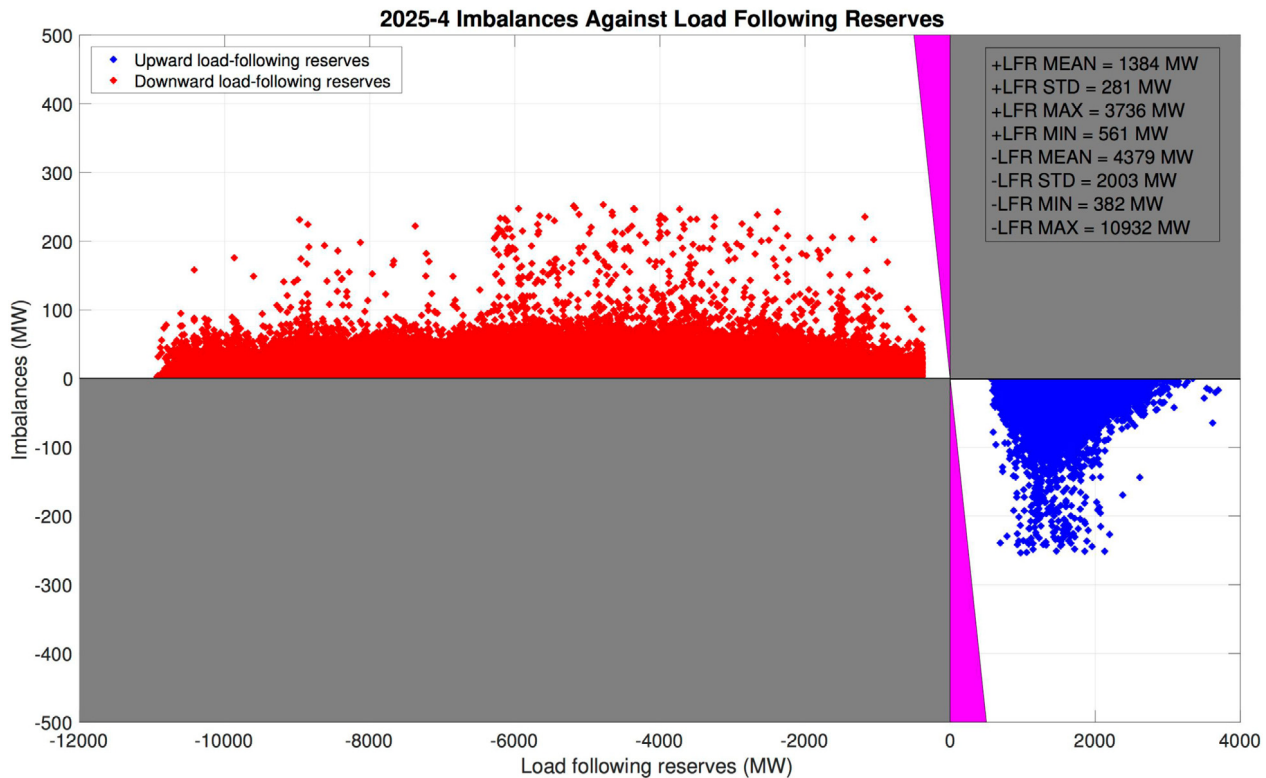
capabilities of generation units when responding to net load variations in real-time. Traditionally, procurement of sufficient load following reserves has been of the primary concern, while the generator ramping constraints in the day-ahead scheduling

were assumed to provide sufficient ramping capabilities to the system. However, for the power system configuration scenarios considered in this study, both load following and ramping

Table 10

Upward and downward load following reserve statistics for 2030 scenarios.

	2030-1	2030-2	2030-3	2030-4	2030-5	2030-6
Up LFR Mean (MW)	1,507	1,506	818	1,512	1,496	1,525
Up LFR STD (MW)	324	355	683	304	314	478
Up LFR Min (MW)	0	0	0	356	0	0
Up LFR 95 percentile (MW)	1,072	1,022	0	1,104	1,067	935
Down LFR Mean (MW)	4,374	3,333	1,145	4,730	4,805	2,125
Down LFR STD (MW)	1,805	1,827	1,212	1,738	1,714	1,865
Down LFR Min (MW)	351	340	0	425	389	0
Down LFR 95 percentile (MW)	1,728	714	335	2,167	2,285	342

**Fig. 27.** Imbalances against load following reserves for Scenario 2025-4.

reserves are equally important, as demonstrated by the results below.

As an example, the performance of ramping reserves for Scenario 2025-4 is shown in Fig. 30. The amount of upward ramping reserves fluctuate over time but is never completely exhausted (approach the zero black line). Downward ramping reserves hit the zero line for a few brief instances only. Similar to load following reserves, ramping reserves get the closest to depletion during low-load spring and fall periods. Thus, when the system follows the Scenario 2025-4, it is generally able to operate reliably without the need for more ramping capabilities.

Fig. 31 shows the upward and downward ramping reserve performances for all scenarios of 2025, and the key performance statistics for each scenario are extracted into Table 11. Here, the 95th percentile indicates that the system has more than this quantity of upward/downward ramping reserves for 95% of the time. The results show that downward ramping reserves for all scenarios hit the zero value at some point during the year. However, except for Scenario 2025-3, such occurrences are brief. For Scenario 2025-3, on the other hand, both upward and downward ramping reserves have zero values far more often. Furthermore, their distributions are shifted closer to the zero black line, which also explains the low 95th percentile values. Thus, it can be concluded that the addition of significant renewable

energy sources for Scenario 2025-3 requires more upward and downward ramping reserves to maintain the system's ability to follow the net load fluctuations.

Similarly, Fig. 32 shows upward and downward ramping reserve performances for all scenarios of 2030, and the key performance statistics for each scenario are extracted into Table 12. The results here are similar to those for 2025 scenarios. Downward ramping reserves for all scenarios hit the zero value at some point during the year. However, except for Scenario 2030-3, such occurrences are brief. Despite that, the depletion of a resource that was assumed to be adequately available in the system shows the need for the procurement of both upward and downward ramping reserves in the day-ahead unit commitment. For Scenario 2030-3, on the other hand, both upward and downward ramping reserves have zero values far more often. Furthermore, their distributions are shifted closer to the zero black line, which also explains the low 95th percentile values. Thus, it can be concluded that the addition of significant renewable energy sources for Scenarios 2025-3 and 2030-3 requires more upward and downward ramping reserves to maintain the system's ability to follow the net load fluctuations. These results are consonant with the "duck curve" discussion found in the previous section on load following reserves.

Along with load following reserves, the primary purpose of ramping reserves is to mitigate the system imbalances induced

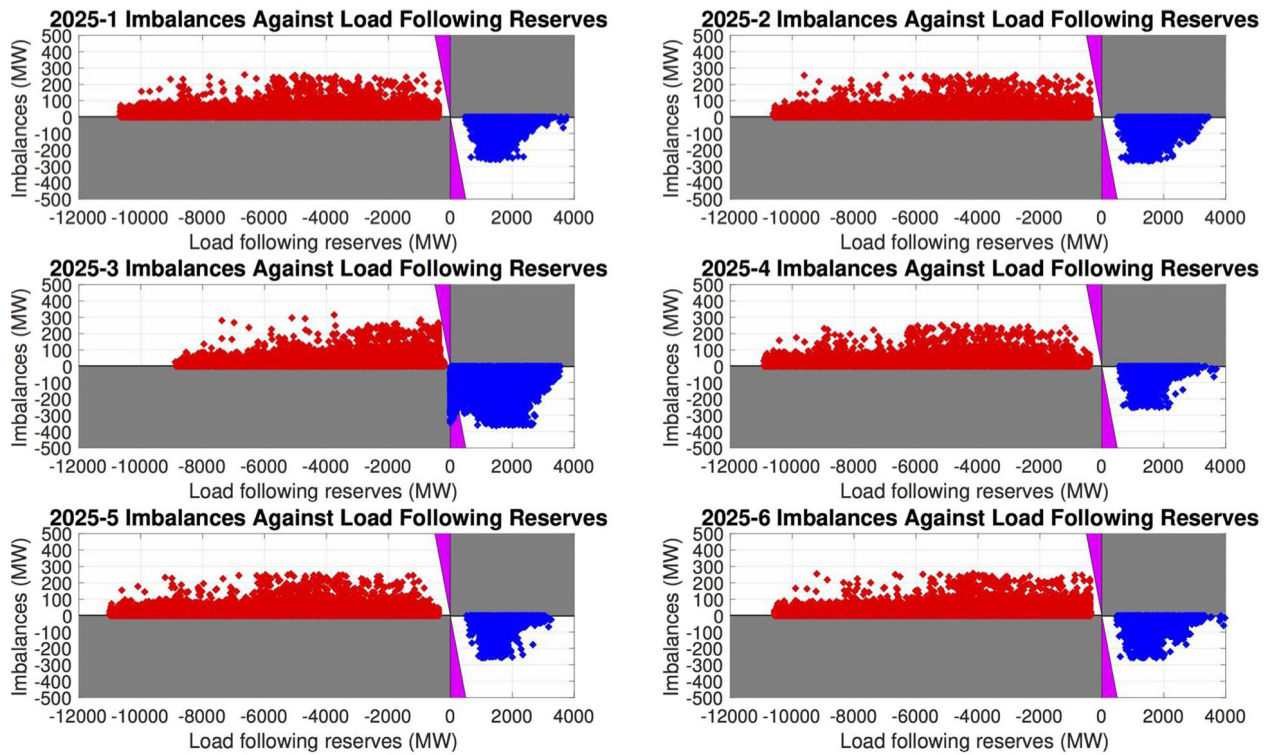


Fig. 28. Imbalances against load following reserves for 2025 scenarios.

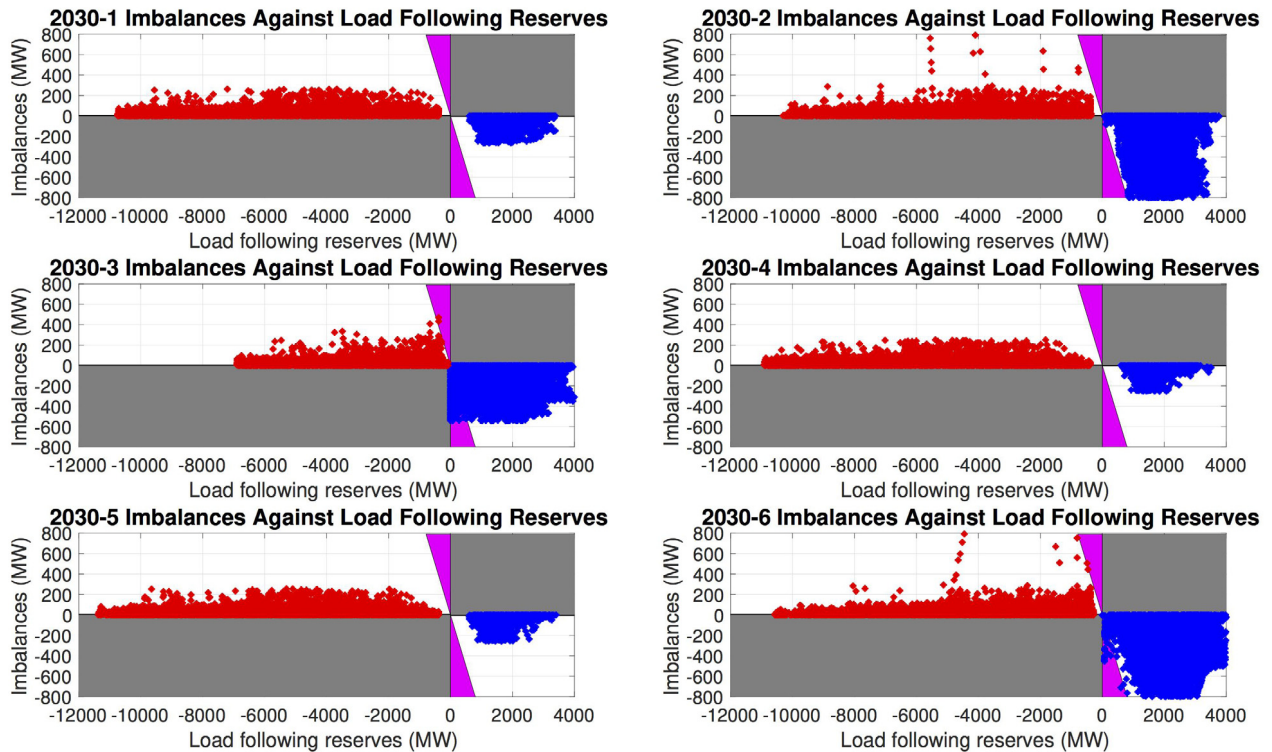


Fig. 29. Imbalances against load following reserves for 2030 scenarios.

by the net load variability and day-ahead forecast errors. Figs. 33 and 34 show the relationship between ramping reserves and the imbalances for 2025 and 2030 scenarios respectively. In the gray regions, upward and downward ramping reserves do not serve to mitigate positive and negative imbalances respectively. In the white regions, upward and downward ramping reserves serve

to mitigate positive and negative imbalances respectively. In the magenta regions, a 1 MW/min increase of ramping reserves leads to a 1 MW reduction of imbalances. This region represents when there are insufficient amounts of ramping reserves to serve the system imbalance. The results in Figs. 33 and 34 confirm the conclusions reached above that while for Scenarios 2025-3 and

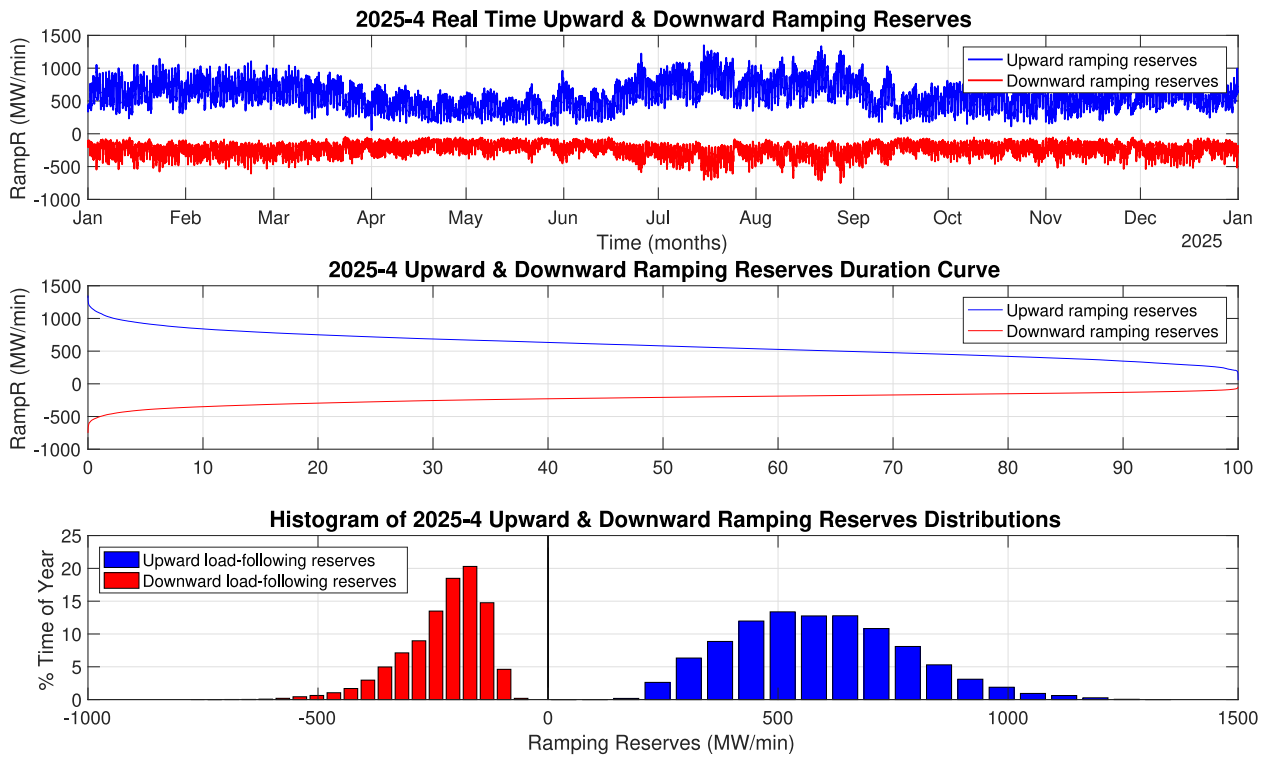


Fig. 30. Ramping reserves profile for Scenario 2025-4.

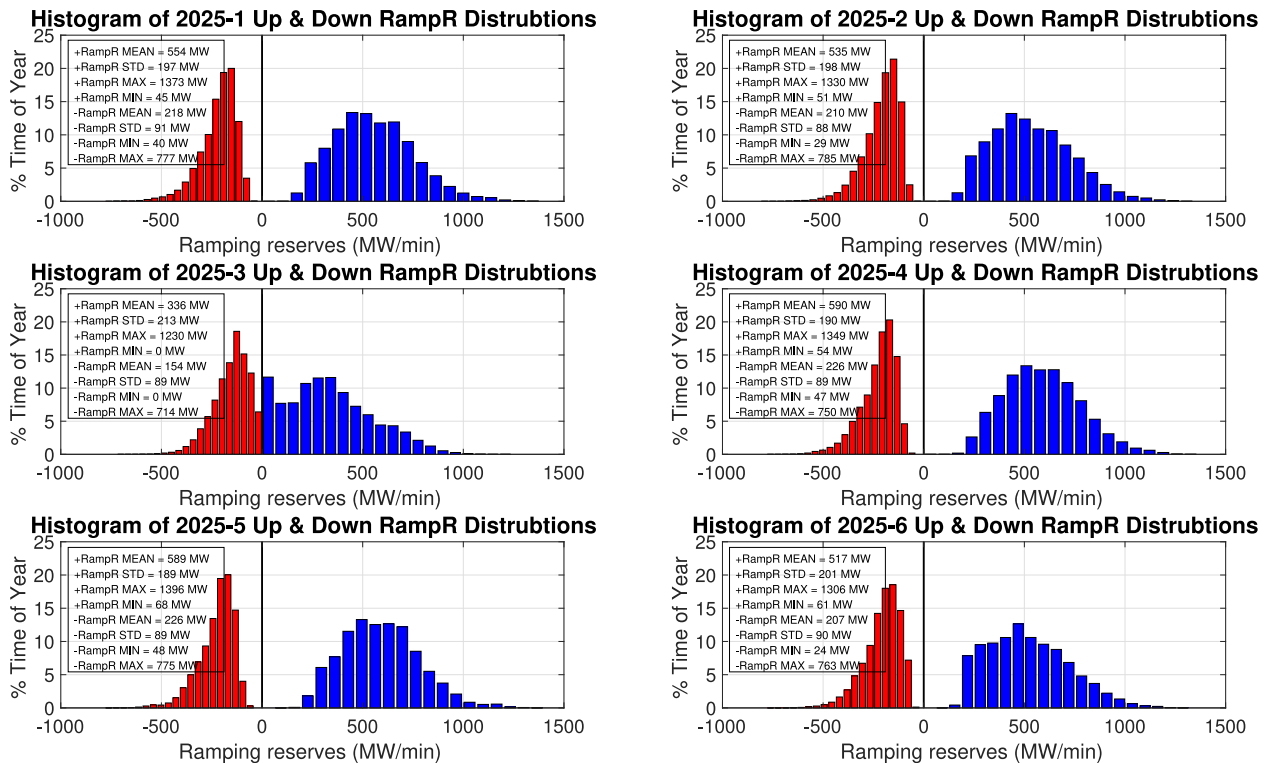


Fig. 31. Ramping reserves distributions for 2025 scenarios.

2030-3 both shortages of upward and downward ramping reserves experience far more often, all scenarios would benefit from varying degrees of additional upward and downward ramping reserves.

5.3. Curtailment of semi-dispatchable resources

In the absence of adequate load following and ramping reserves, the curtailment of production from renewable energy

Table 11

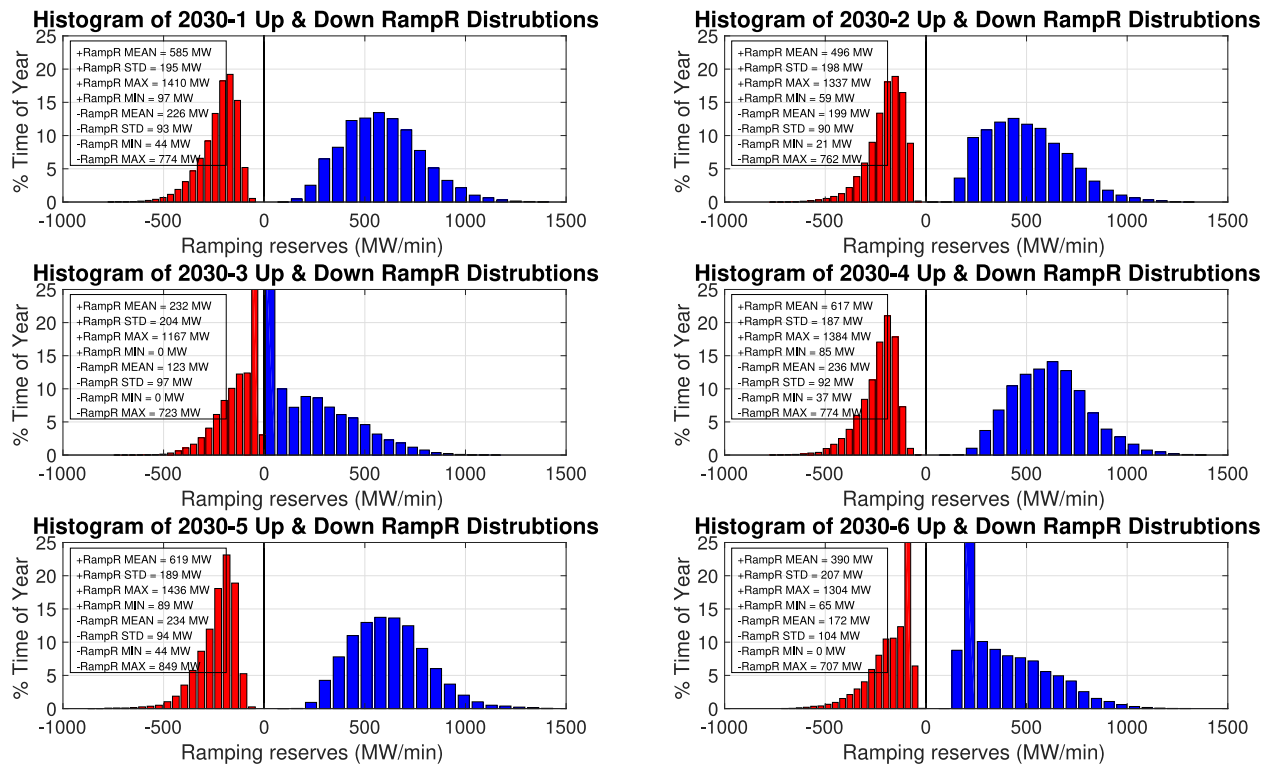
Upward and downward ramping reserves statistics for 2025 scenarios.

	2025-1	2025-2	2025-3	2025-4	2025-5	2025-6
Up RampR Mean (MW/min)	591	571	367	621	623	554
Up RampR STD (MW/min)	204	204	218	194	197	210
Up RampR Max (MW/min)	1,412	1,390	1,291	1,420	1,433	1,362
Up RampR Min (MW/min)	78	85	0	69	38	95
Up RampR 95 percentile (MW/min)	285	267	38	329	326	243
Down RampR Mean (MW/min)	235	226	167	238	243	220
Down RampR STD (MW/min)	102	100	94	98	100	100
Down RampR Min (MW/min)	0	0	0	0	0	0
Down RampR Max (MW/min)	805	782	766	802	819	780
Down RampR 95 percentile (MW/min)	112	105	36	120	123	93

Table 12

Upward and downward ramping reserves statistics for 2030 scenarios.

	2030-1	2030-2	2030-3	2030-4	2030-5	2030-6
Up RampR Mean (MW/min)	623	531	254	656	659	414
Up RampR STD (MW/min)	206	209	216	190	200	220
Up RampR Max (MW/min)	1,458	1,420	1,239	1,424	1,459	1,388
Up RampR Min (MW/min)	87	59	0	95	86	52
Up RampR 95 percentile (MW/min)	316	228	33	370	362	177
Down RampR Mean (MW/min)	242	213	134	251	250	182
Down RampR STD (MW/min)	109	101	105	102	112	111
Down RampR Min (MW/min)	0	0	0	0	0	0
Down RampR Max (MW/min)	850	801	771	845	836	791
Down RampR 95 percentile (MW/min)	118	91	31	129	123	70

**Fig. 32.** Ramping reserves distributions for 2030 scenarios.

sources, serves a vital balancing function. To emphasize the ability to reduce their power outputs, this study also refers to renewable energy sources as “semi-dispatchable resources”. While curtailment of semi-dispatchable resources wastes generally cheaper and greener energy and, therefore, is a less desirable balancing method, it allows more flexibility and can help overcome topological limitations of the system where load following and ramping reserves might be ineffective. It is also important to emphasize that some of these topological limitations are due to the integration of semi-dispatchable resources in remote areas

that replace the traditional generation units located close to the main consumption centers. Thus, semi-dispatchable resources might have a self-limiting feature which also defines the ability of the system to accommodate them. As an example, Fig. 35 shows the curtailment profile for Scenario 2025-3. The graph shows that some form of curtailment occurs for all but 0.1% of the year. Also, the largest curtailments occur during spring and fall when the system load is at its lowest.

Curtailment duration curves in Fig. 36 show that curtailment becomes an integral part of balancing operations for all 2025

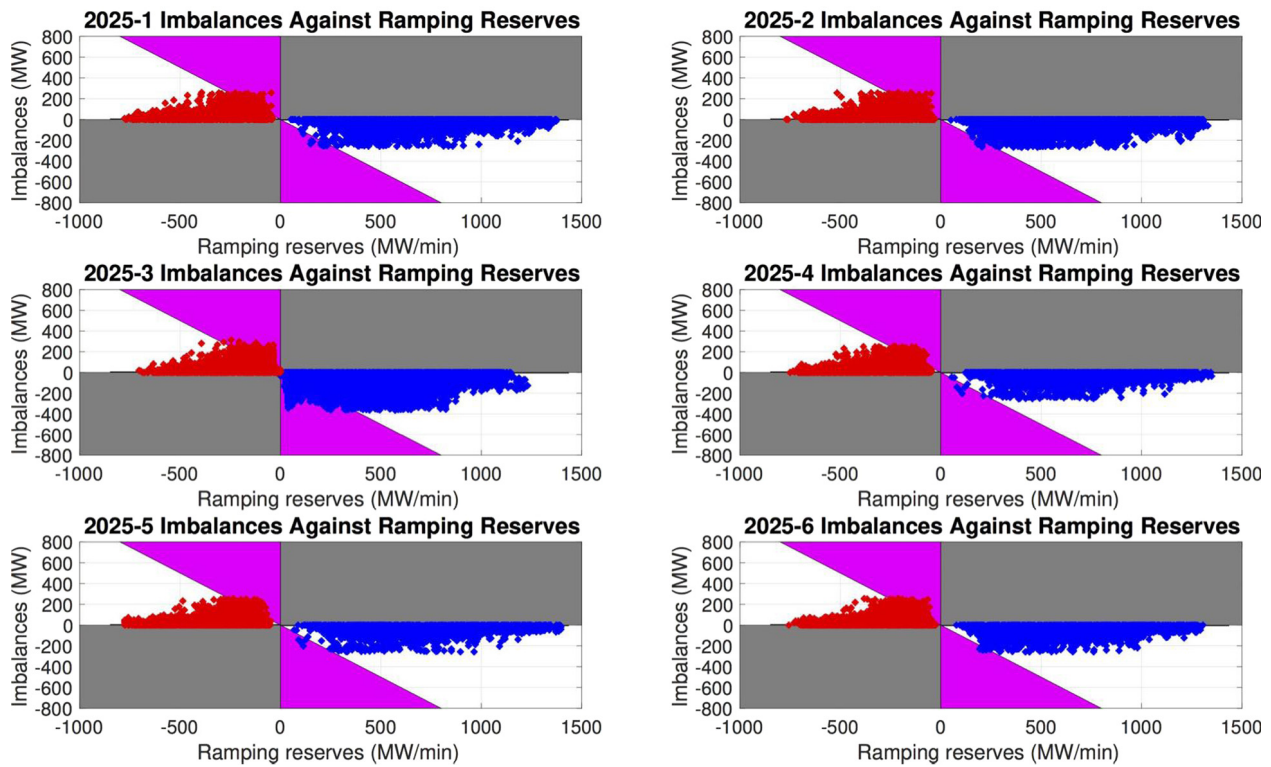


Fig. 33. Imbalances against ramping reserves for 2025 scenarios.

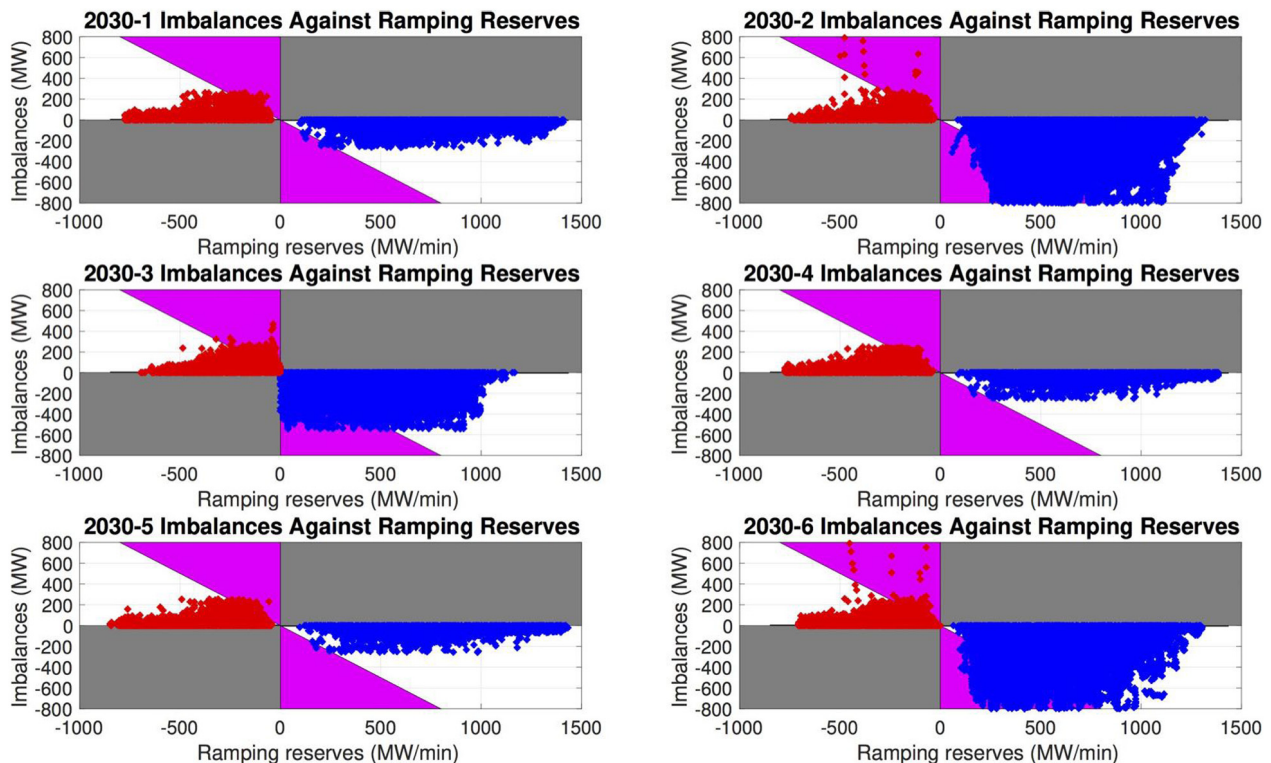


Fig. 34. Imbalances against ramping reserves for 2030 scenarios.

Scenarios except 2025-4 and 2025-5. The results show that the largest curtailments occur for Scenarios 2025-2 and 2025-3. This is explained by the fact that Scenario 2025-3 is defined by the integration of large amounts of semi-dispatchable resources, and in Scenario 2025-2 the retired oil and coal units are replaced

by semi-dispatchable resources instead of NGCC. This supports the statement above that the curtailment of semi-dispatchable resources is often times a way to mitigate topological limitations of the system amplified by the integration of the same semi-dispatchable resources. The curtailment statistics for 2025

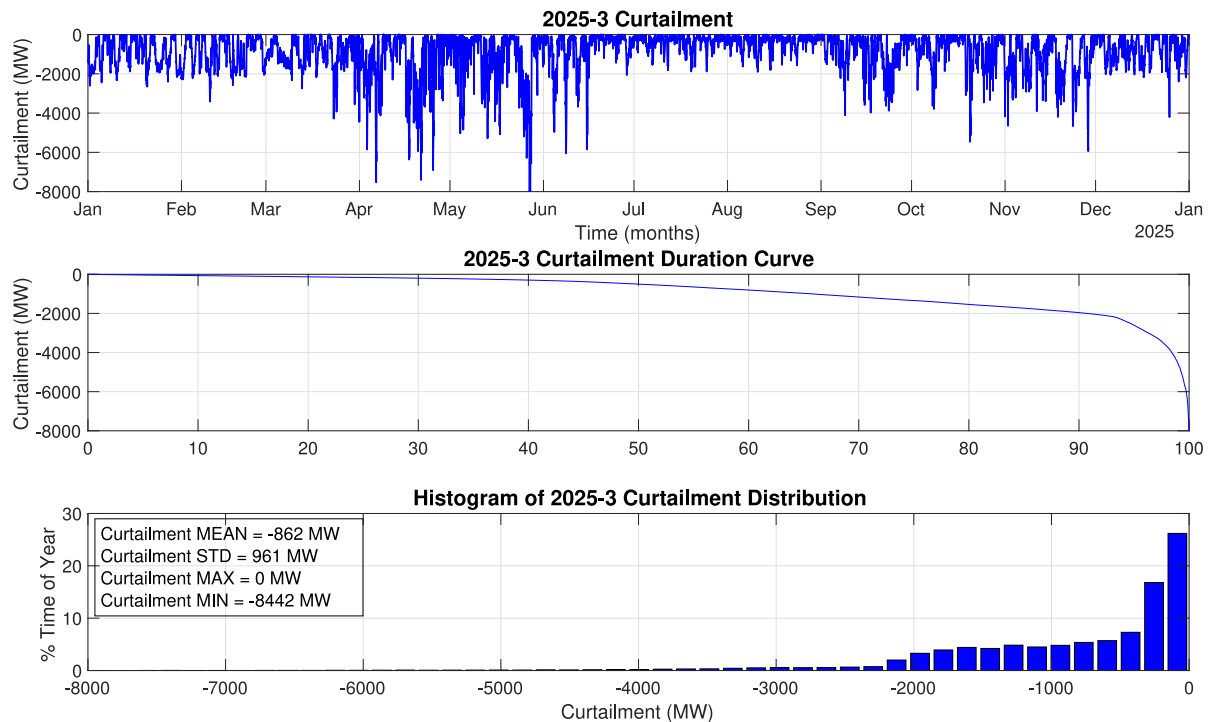


Fig. 35. Curtailments for Scenario 2025-3.

scenarios in Table 13 show that they are used almost for the whole duration of the year for all scenarios. However, their magnitudes vary significantly for different scenarios, reaching the maximum of 8,442 MW for Scenario 2025-3.

Curtailment duration curves for 2030 scenarios are shown in Fig. 37. Here too, curtailment plays an integral part of balancing operations for all Scenarios except 2030-4 and 2030-5. The results show that the largest curtailments occur for Scenarios 2030-2, 2030-3 and 2030-6. The emergence of Scenario 2030-6 as the case with the second largest curtailment is due to integration of large amounts of offshore wind units in 2030. Again, it can be observed that the curtailment of semi-dispatchable resources is often times a way to mitigate topological limitations of the system amplified by the integration of the same semi-dispatchable resources. The curtailment statistics for 2030 scenarios in Table 14 show that they are used almost for the whole duration of the year for all scenarios. However, their magnitudes vary significantly for different scenarios, reaching the maximum of 14,534 MW for Scenario 2030-2.

5.4. Interface and tie-line performances

As mentioned in the previous section, one of the main reasons for curtailment of semi-dispatchable resources are topological limitations of the system. These limitations are primarily due to the enforcement of several interface flow limits depicted in Fig. 11, which may cause congestion in the system and require curtailment. The performance of the following four key interfaces are discussed here:

- Orrington-South
- Surowiec-South
- North-South
- SEMA-RI Import

The other interfaces and tie-lines in their respective scenarios exhibit negligible or no congestion.

Fig. 38 shows the duration curve for flows across the Orrington South interface. It shows that the system experiences significant

congestion on the Orrington-South interface for Scenarios 2025-1, 2025-2, 2025-3, and 2025-6 compared to Scenarios 2025-4 and 2025-5 that have no congestions at all. A similar pattern, but to a lesser degree, is observed on the Surowiec-South interface shown in Fig. 39. The important observation here is that these scenarios are defined by a significant increase of renewable energy resources in the system. The power generated by these resources needs to flow down from remote areas of Maine towards the main consumption centers, such as Massachusetts, which causes the congestion on these two interfaces. On the other hand, the North-South interface shown in Fig. 40 exhibits congestion only in rare cases. This is due to the fact that the North-South interface has a much higher interface limit of 2,725 MW, and is able to pass the additional renewable energy generation coming through the Orrington-South and the Surowiec-South interfaces without being congested. Finally, the SEMA-RI import interface in Fig. 41 exhibits some congestion for all 2025 scenarios. The interface congestion statistics for 2025 are summarized in Table 15.

The results for 2030 are fairly similar to those for 2025. Fig. 42 shows that the system experiences significant congestions on the Orrington-South interface for Scenarios 2030-1, 2030-2, 2030-3, and 2030-6 compared to Scenarios 2030-4 and 2030-5 that have no congestions at all. A similar pattern, but to a lesser degree, is observed on the Surowiec-South interface shown in Fig. 43. On the other hand, the North-South interface shown in Fig. 44 exhibits congestion only in rare cases. This is due to the fact that the North-South interface has much higher interface limit of 2,725 MW, and is able to pass the additional renewable energy generation coming through the Orrington-South and the Surowiec-South interfaces without being congested. Finally, the SEMA-RI import interface in Fig. 45 exhibits some congestion for all 2030 scenarios. The SEMA area has high penetrations of PV. During the midday, dispatchable units are turned off. As the sun sets, dispatchable units cannot be turned on and ramped fast enough to meet the demand and consequently the imported power exceeds the import limit. The interface congestion statistics for 2030 are summarized in Table 16.

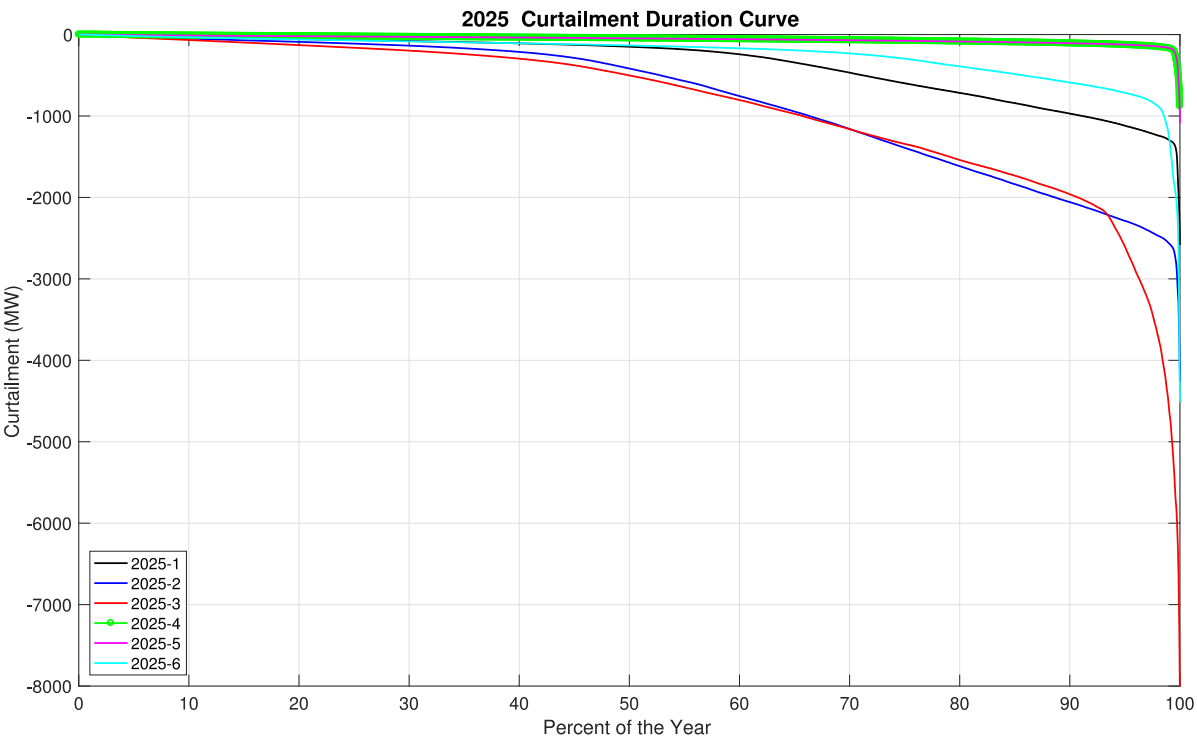


Fig. 36. Curtailment duration curves for 2025 scenarios.

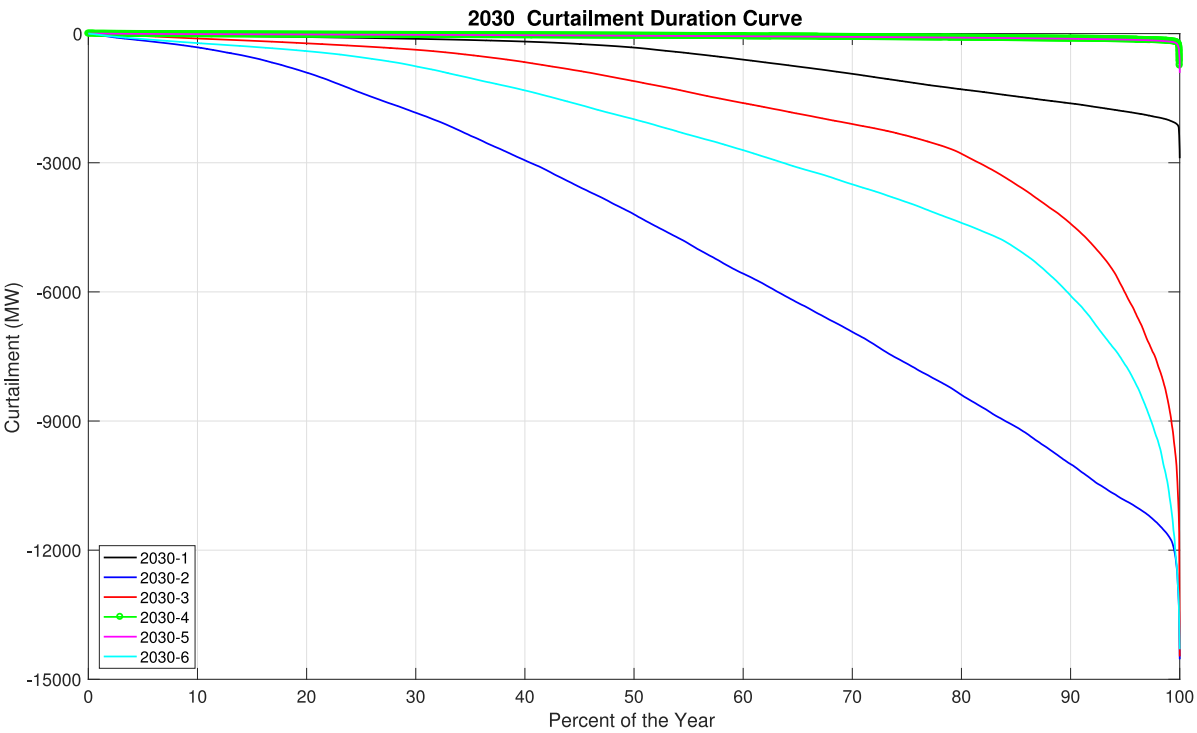


Fig. 37. Curtailment duration curves for 2030 scenarios.

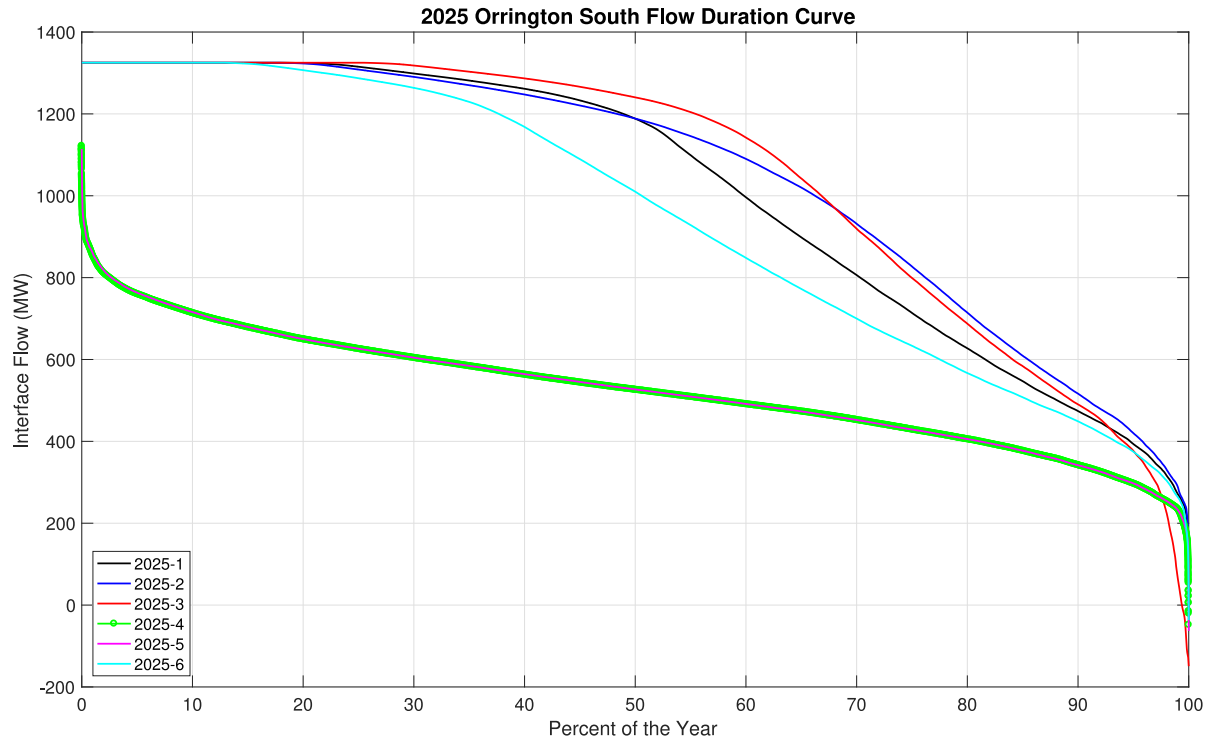
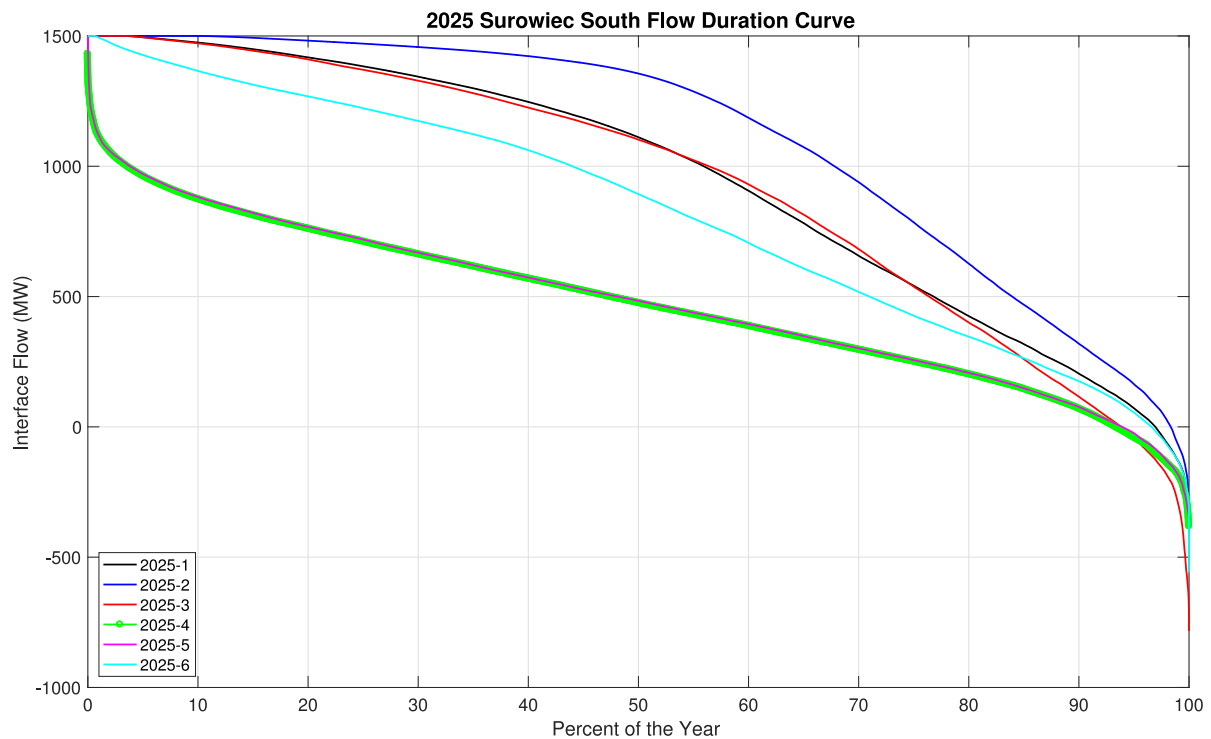
Table 13
Curtailment statistics for 2025 scenarios.

	2025-1	2025-2	2025-3	2025-4	2025-5	2025-6
Tot. Semi-Disp. Res. (GWh)	48,674	55,215	63,850	41,532	41,532	53,118
Tot. Curtailed Semi-Disp. Energy (GWh)	3,604	7,333	7,600	1,130	1,123	2,585
% Semi-Disp. Energy Curtailed	7.41	13.28	11.90	2.72	2.70	4.87
% Time Curtailed	99.61	99.79	99.90	98.89	98.83	99.63
Max Curtailment Level (MW)	2,880	4,115	8,442	1,605	1,701	4,748

Table 14

Curtailment statistics for 2030 scenarios.

	2030-1	2030-2	2030-3	2030-4	2030-5	2030-6
Tot. Semi-Disp. Res. (GWh)	52,748	100,786	76,606	42,662	42,662	97,115
Tot. Curtailed Semi-Disp. Energy (GWh)	5,993	41,517	14,495	1,149	1,162	22,531
% Semi-Disp. Energy Curtailed	11.36	41.19	18.92	2.69	2.72	23.20
% Time Curtailed	99.85	99.95	99.88	98.84	98.91	99.95
Max Curtailment Level (MW)	3,378	14,534	14,468	1,640	1,637	14,234

**Fig. 38.** Orrington-South flow duration curves for 2025 scenarios.**Fig. 39.** Surowiec-South flow duration curves for 2025 scenarios.

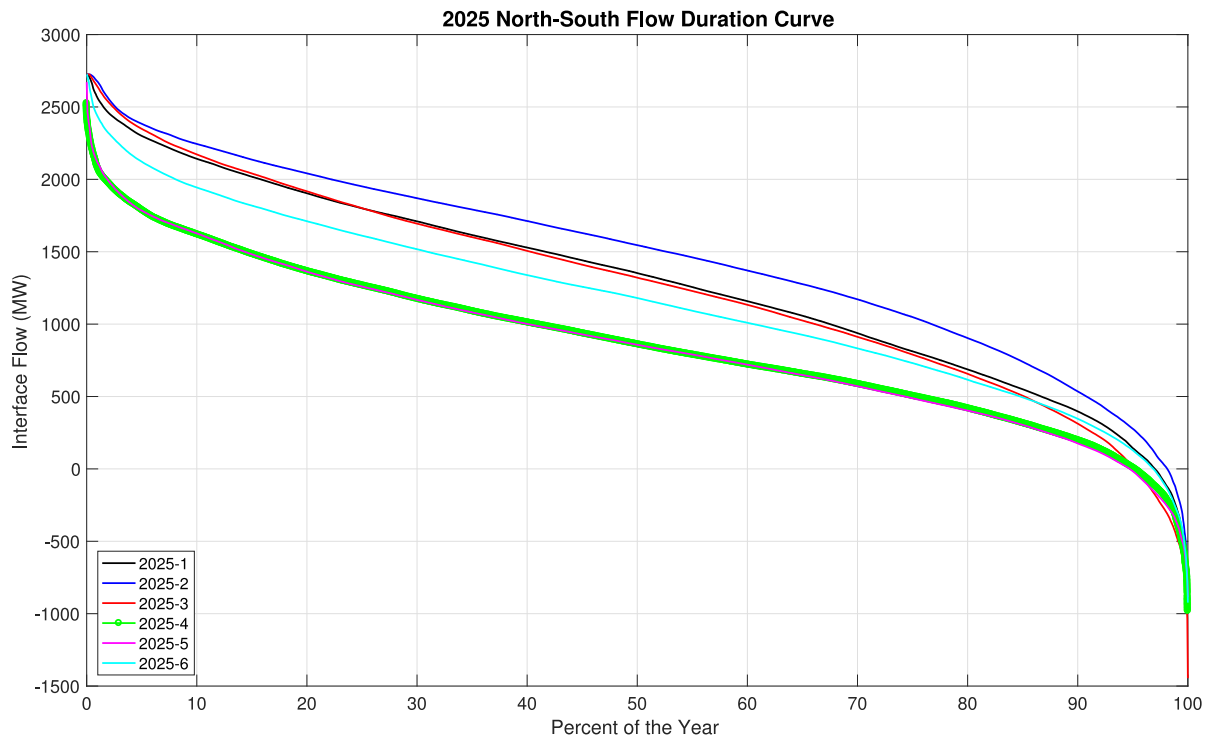


Fig. 40. North-South flow duration curves for 2025 scenarios.

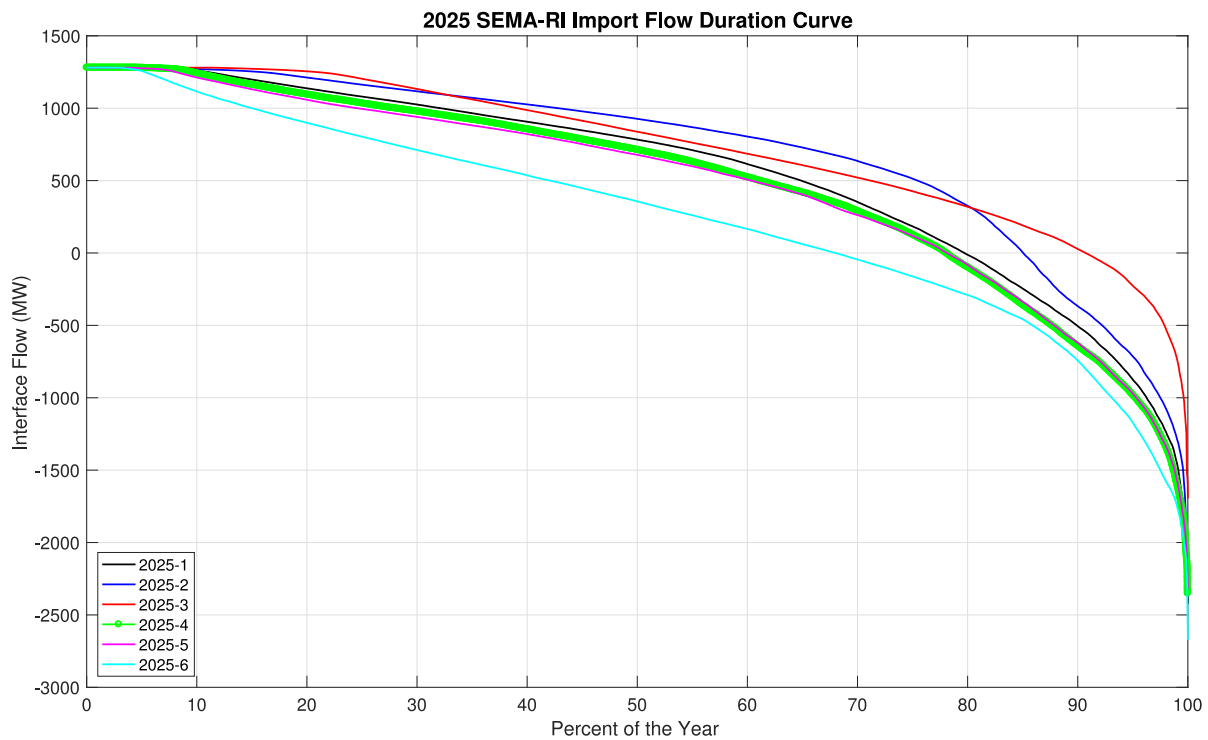


Fig. 41. SEMA-RI Import flow duration curves for 2025 scenarios.

Table 15

Interface congestion statistics for 2025 scenarios.

	2025-1	2025-2	2025-3	2025-4	2025-5	2025-6
Orrington South % Time Congested	20.49	19.05	27.06	0.00	0.00	13.91
Surowiec South % Time Congested	4.39	11.82	4.41	0.00	0.00	0.90
North-South % Time Congested	0.15	0.38	0.51	0.00	0.00	0.04
SEMA-RI Import % Time Congested	3.09	3.61	9.88	3.22	3.07	2.00

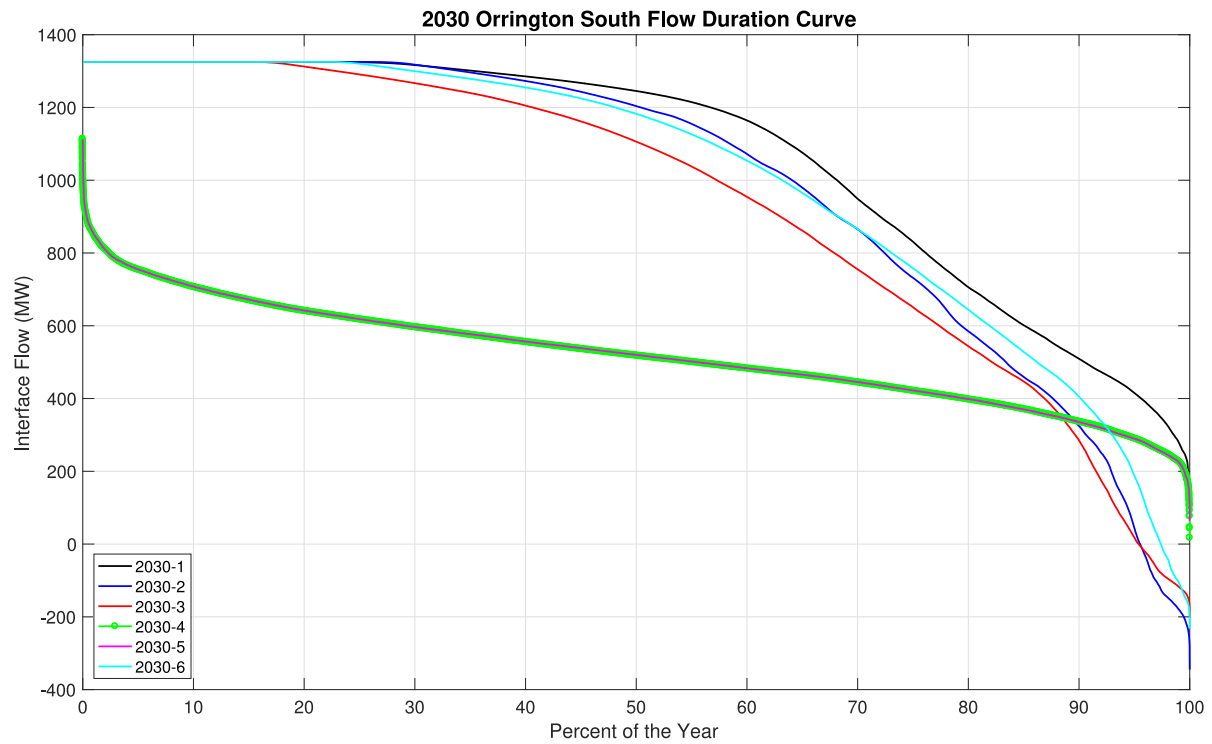


Fig. 42. Orrington-South flow duration curves for 2030 scenarios.

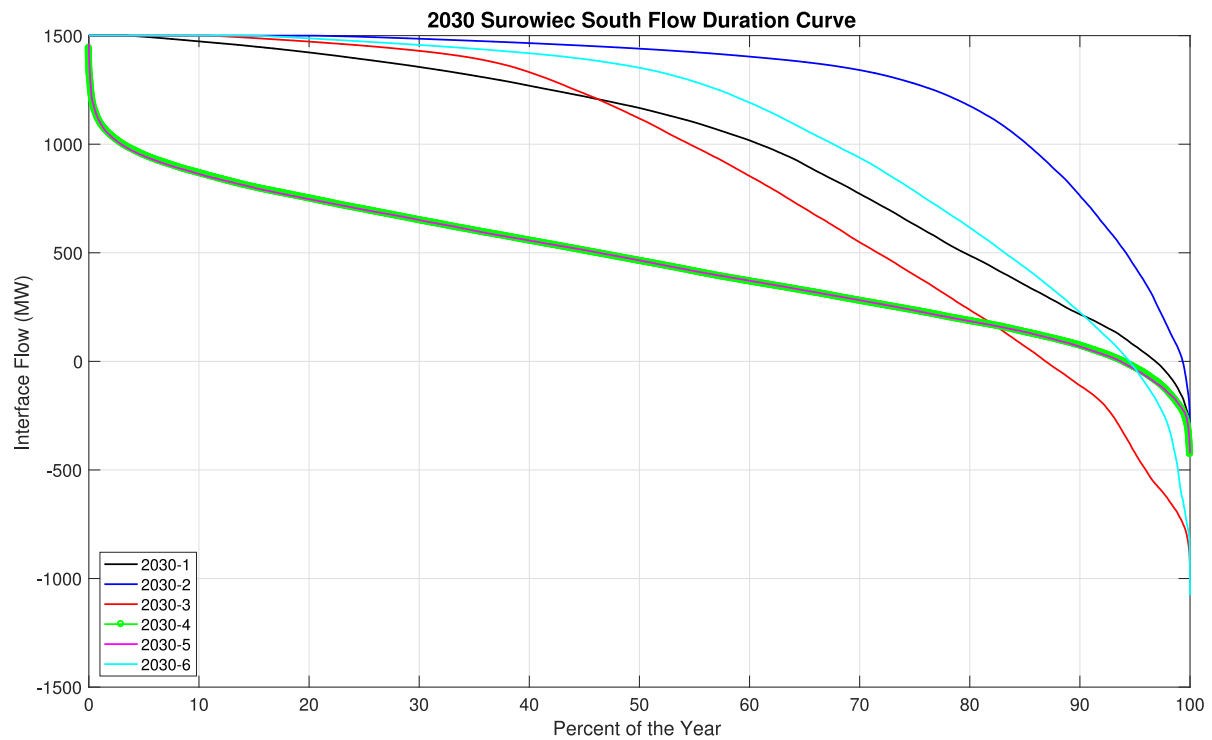


Fig. 43. Surowiec-South flow duration curves for 2030 scenarios.

Table 16

Interface congestion statistics for 2030 scenarios.

	2030-1	2030-2	2030-3	2030-4	2030-5	2030-6
Orrington South % Time Congested	25.80	27.84	17.14	0.00	0.00	24.05
Surowiec South % Time Congested	4.17	21.83	12.00	0.00	0.00	16.30
North-South % Time Congested	0.15	1.13	0.48	0.00	0.00	0.54
SEMA-RI Import % Time Congested	3.45	2.92	9.91	2.65	3.07	1.63

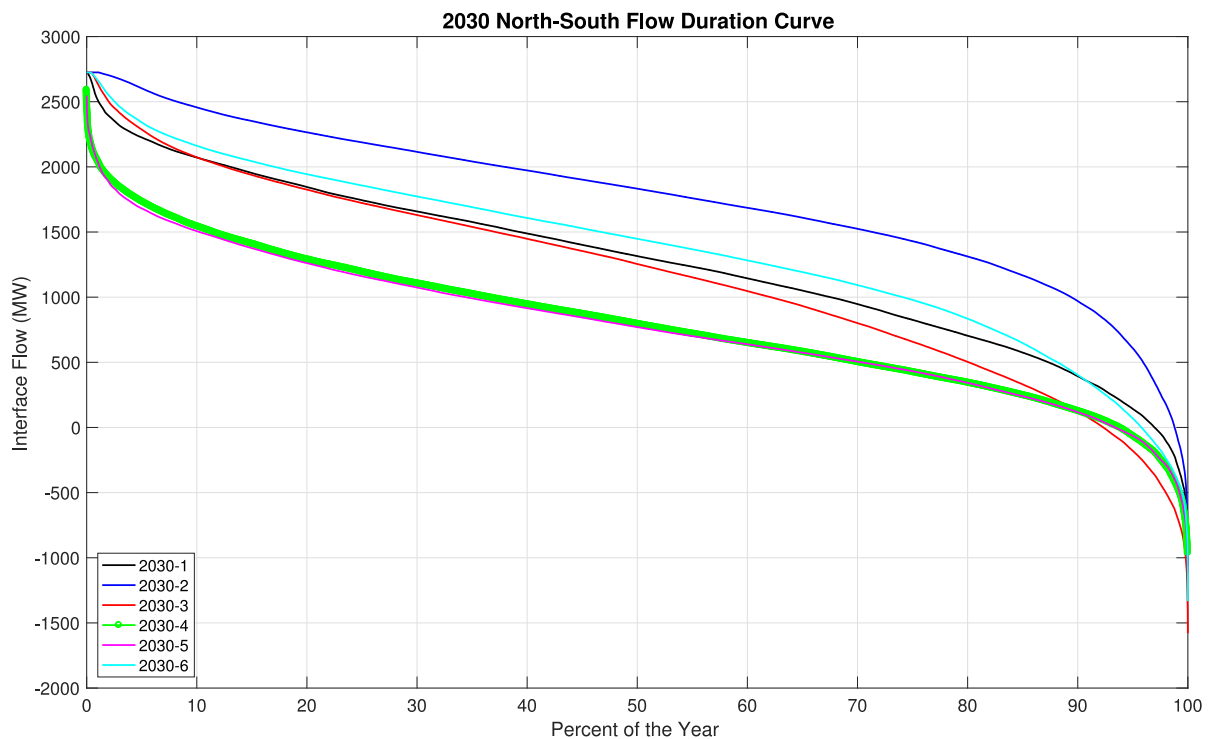


Fig. 44. North–South flow duration curves for 2030 scenarios.

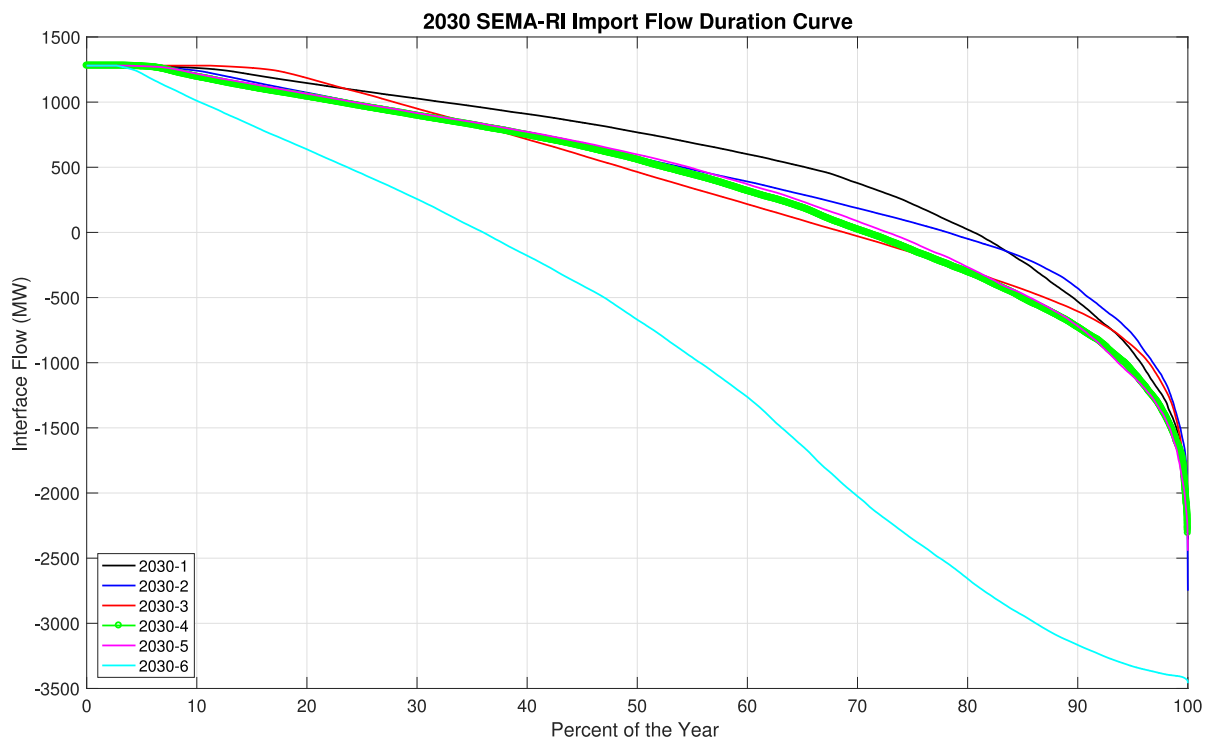


Fig. 45. SEMA-RI Import flow duration curves for 2025 scenarios.

Matching the congestion results of this section to the curtailment results in the previous section, the following conclusion can be drawn; the integration of significant renewable energy resources increases the potential of congestion on several key

interfaces, such as Orrington-South and the Surowiec-South, and, therefore, require heavy curtailments of these resources. Thus, the ability of the system to accommodate more renewables is

limited by its topology, particularly, some of the key interfaces discussed here.

5.5. Regulation reserves

Regulation service is the fastest resource that responds to the residual imbalances after the deployment of load following and ramping reserves and performing the necessary curtailment of semi-dispatchable resources. Therefore, sufficient regulation reserves are instrumental for effective mitigation of imbalances. Fig. 46 shows the regulation reserve performance for Scenario 2025-4. None of three graphs indicate saturation, and, therefore, the system has sufficient regulation reserves. The distribution has a smooth bell-like shape which indicates an efficient use of these resources. Similarly, the associated duration curve does not indicate any clipping at either end of the regulation range.

Fig. 47 shows regulation reserve performances for all 2025 scenarios. Scenarios 2025-1, 2025-2, 2025-3, 2025-6 show heavy saturation of regulation reserves, in contrast to Scenarios 2025-4 and 2025-5. It should be noted that these scenarios are defined by a significant increase of renewable energy resources in the system. Thus, the increased renewable energy sources in the system will also require additional regulation reserves to effectively respond to the residual imbalances. Regulation reserve performances for 2030 scenarios in Fig. 48 show a similar effect. However, regulation reserve saturation occurs more often compared to 2025 since 2030 has more renewable energy sources in the system. The regulation reserve performance statistics are summarized in Table 17.

5.6. Balancing performance

The balancing performance of the system can be assessed from the residual imbalances after the regulation service was deployed. As shown in the previous section, all scenarios exhibit regulation service saturation to varying degrees. For that reason, all scenarios are expected to have residual imbalances. Fig. 49 shows that the imbalances for Scenario 2025-4 are well-controlled with zero mean and moderate variability on the order of 75 MW for the overwhelming majority of the year. Such a low value indicates that the system is well-equipped to mitigate the imbalances effectively.

Figs. 50 and 51 show the imbalance ranges and standard deviations for all scenarios respectively. Scenarios 2030-2 and 2030-6 and to a lesser extent Scenario 2030-3 have a wider range between the maximum and minimum imbalance values, which can be described as a measure of the intensity of improbable or extreme events. The use of imbalance range as a statistic emphasizes single points in time in which brief imbalance excursions can occur. Upon further investigation, these three scenarios also demonstrate significantly higher values of the standard deviation of imbalances as a measure of the continual balancing “stress” on the enterprise control of the power system. From these two complementary results, one can conclude that the 2030-2, 2030-3, and 2030-6 scenarios have a balancing performance that is significantly degraded relative to the other scenarios and a complementary set of measures would be required to achieve the performance of the other scenarios. That said, it would be premature to conclude that these scenarios would result in degraded overall system reliability in real life because it is not clear at which (absolute) imbalance levels disruptive events might occur. Imbalance excursions of several hundred megawatts are found within the historical data and do not immediately correspond to a disruptive reliability event. Finally, all scenarios except these three maintain imbalance variability of less than 50 MW, despite the saturation of regulations reserves observed in the previous section.

6. Conclusion & final insights

6.1. Summary

This report describes the methodology and the key findings of the 2017 ISO New England System Operational Analysis and Renewable Energy Integration Study (SOARES). It argues that with respect to operations, the integration of variable energy resources should not be considered as “business-as-usual”, and instead a more holistic approach is required. It lays out the requirements for such a rigorous assessment. That discussion contextualizes a review of the methodological adequacy of existing renewable energy integration studies.

The heart of the project’s methodology is a novel, but now extensively published, holistic assessment approach called the Electric Power Enterprise Control System (EPECS) simulator. Most fundamentally, the EPECS methodology is *integrated* and *techno-economic*. It characterizes a power system in terms of the physical power grid and its multiple layers of control including commitment decisions, economic dispatch, and regulation services. Consequently, it has the ability to provide clear trade-offs for any changes to the physical power systems and its associated layers of control.

The report begins with a rationale for EPECS simulator. It argues that with respect to operations the integration of variable energy resources should not be considered as “business-as-usual”, and instead a more holistic approach is required. It lays out the requirements for such a rigorous assessment. That discussion contextualizes a review of the methodological adequacy of existing renewable energy integration studies. It highlights several key conclusions found as a consensus across the literature. Combined unit-commitment and economic dispatch (UCED) models are used to assess changes in operating costs. Statistical methods are used to assess the need for greater quantities of operating reserves. The exact degree to which these changes occur ultimately depend on individual power system properties such as generation mix and fuel cost. They also depend on the choice of several significant but not necessarily validated methodological assumptions used in the study. Next, the report describes the EPECS simulator in detail. It provides precise definitions of how variable energy resources and operating reserves are modeled. It also includes detailed models of day-ahead resource scheduling, same-day resource scheduling, real-time balancing operations and regulation service. The report also includes the zonal-network (i.e. pipe & bubble) model of the physical power grid.

6.2. Key findings

The key findings of this study can be summarized in the following points:

1. The commitment of dispatchable resources and their associated quantities of committed load following and ramping reserves has a complex, difficult to predict, non-linear dependence on the amount of VERs and the load profile statistics. High and low levels of VERs do not necessarily correspond to high or low quantities of operating reserves respectively. For example, during the midday hours, solar generation causes low net load conditions that will test a power system’s ability to track downward using downward load following reserves. Hours later, as solar generation wanes, net load conditions rise to their daily peak testing the power system’s ability to track upward with upward load following reserves. In the meantime, the transition hours between trough and peak conditions exhibits a sharp system ramp.

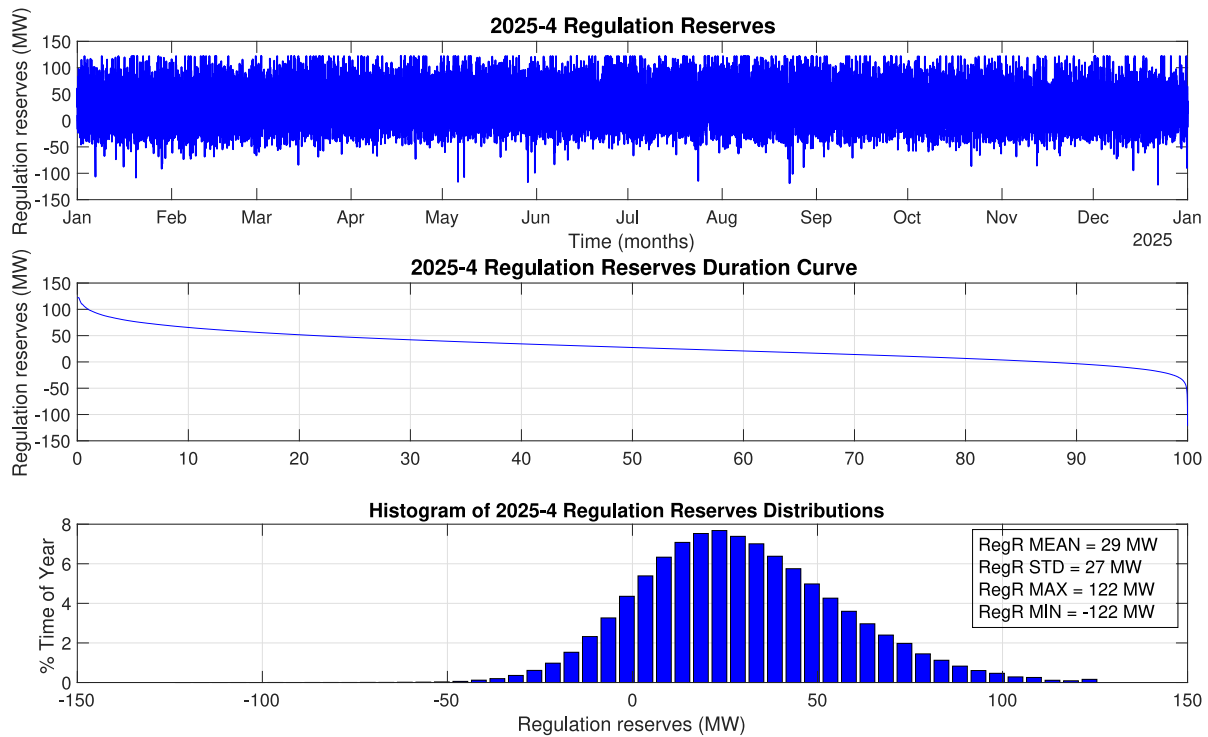


Fig. 46. Regulation reserve performance for Scenario 2025-4.

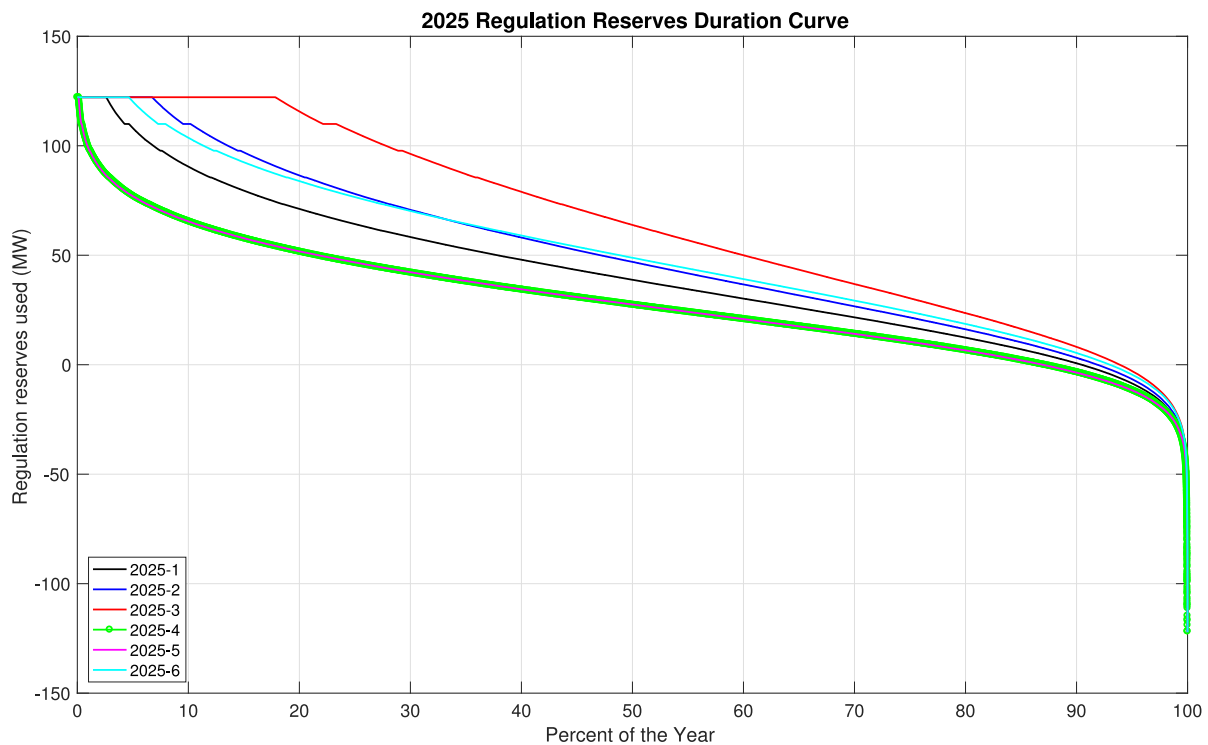


Fig. 47. Regulation reserve performances for 2025 scenarios.

2. For the scenarios with significant presence of VERs (2025-3, 2030-3 and 2030-6), the system may require additional amounts of upward load following reserves to effectively mitigate imbalances and maintain its reliable operations.

Furthermore, these scenarios entirely exhaust their downward load following reserves; albeit for a fairly short part of the year. Despite such occurrences being rare, the depletion of a resource that was assumed to be adequately available in the system for following the net load fluctuations

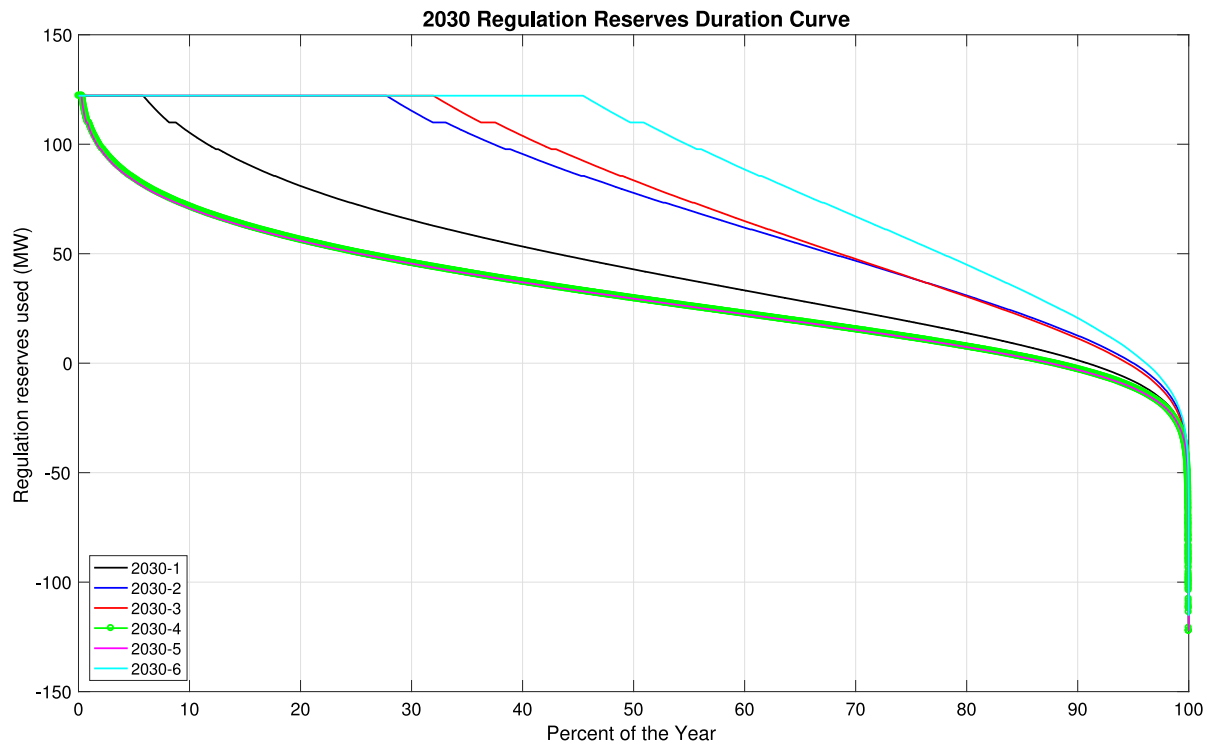


Fig. 48. Regulation reserve performances for 2030 scenarios.

Table 17
Regulation reserve statistics.

	2025-1	2025-2	2025-3	2025-4	2025-5	2025-6
% Time Reg. Res Exhausted	2.74	6.98	18.32	0.17	0.14	4.87
Reg. Res. Mileage (GWh)	389.53	461.72	582.15	283.49	283.73	462.53
	2030-1	2030-2	2030-3	2030-4	2030-5	2030-6
% Time Reg. Res Exhausted	6.07	28.15	33.03	0.37	0.43	46.20
Reg. Res. Mileage (GWh)	433.23	659.09	684.21	307.50	305.54	778.99

shows the need for the procurement of both upward and downward load following reserves in the day-ahead unit commitment.

- For the scenarios with significant presence of VERs (2025-3, 2030-3 and 2030-6), the system entirely exhausts its upward and downward ramping capabilities. Such moments coincide with power system imbalances. These results indicate that the assumption that the generator ramping constraints in the day-ahead scheduling provide sufficient ramping capabilities to the system is inadequate. Therefore, both load following and ramping reserves should be procured in the day-ahead unit commitment.
- Along with the load following and ramping reserves provided by dispatchable resources, the curtailment of semi-dispatchable resources becomes an integral part of balancing performance; in part to complement operating reserves and in part to mitigate the topological limitations of the system. Every scenario uses curtailment in some way at least 98.6% of the time. The maximum level of curtailment for all scenarios ranges from 1605 MW (in Scenario 2025-4) to 14,534 MW (in Scenario 2030-2). In all, these curtailments correspond to a loss of between 2.72% (in Scenario 2030-4) and 41.19% (in Scenario 2030-2) of the total semi-dispatchable energy available. It is also important to emphasize that some of the associated topological limitations only start affecting the system performance after the integration of VERs in remote areas that replace

the traditional generation units located close to the main consumption centers. Thus, VERs might have a self-limiting feature which also defines the ability of the system to accommodate them.

- The integration of significant amounts of VERs increases the potential of congestion on several key interfaces (Orrington-South and Surowiec-South), and, therefore, requires heavy curtailments of these resources. Thus, the ability of the system to accommodate more renewables is limited by its topology. A longer-term solution to accommodating large amounts of VERs while avoiding such congestions would be the construction of new transmission lines from remote areas of VER installation to the main consumption centers.
- For the scenarios with significant presence of VERs (Scenarios 2025-3, 2030-2, 2030-3, and 2030-6), the system experiences heavy saturations of regulation reserves and, therefore, requires additional regulation reserves to effectively respond to the residual imbalances. Scenarios 2025-1, 2025-2, 2025-6, 2030-1 also experience moderate saturations of regulation reserves indicating the need for their increase in 8 out of the 12 scenarios studied.
- The scenarios with significant presence of VERs (Scenarios 2030-2, 2030-3 and 2030-6) have significantly degraded balancing performance relative to the other scenarios studied and a complementary set of new measures would be required to achieve similar performance. It would be premature to conclude that these scenarios would result in

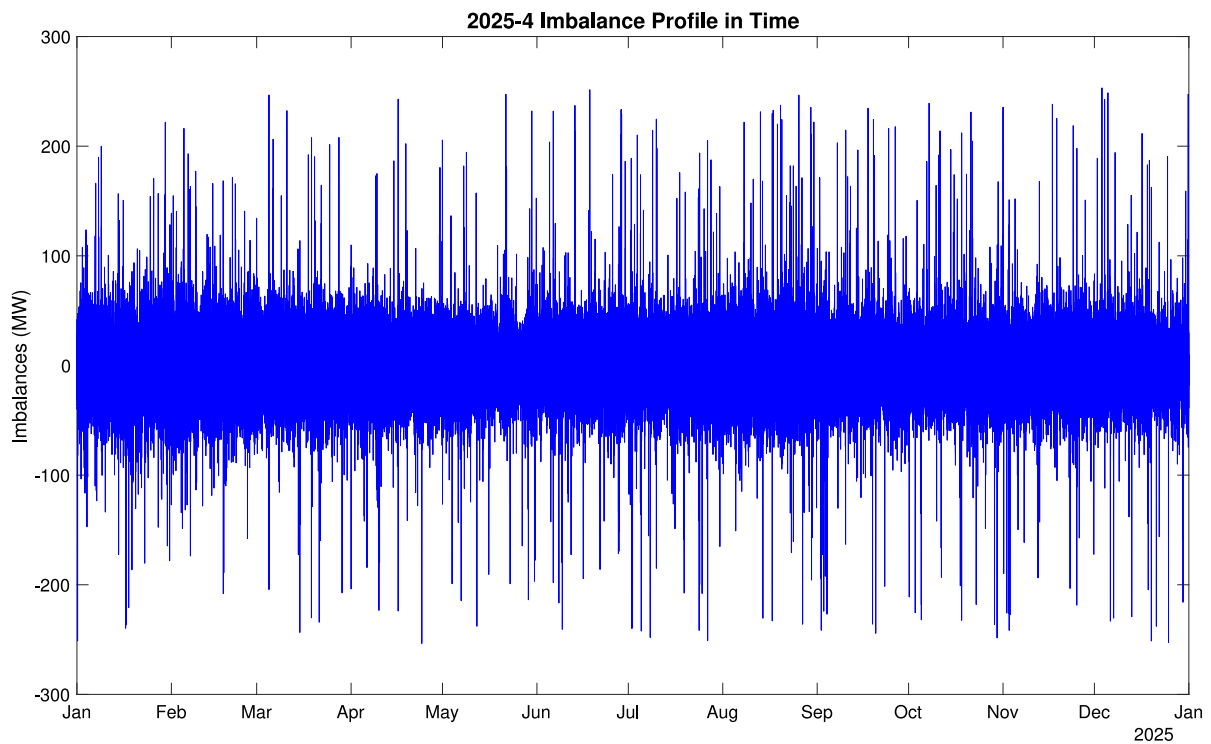


Fig. 49. Imbalance profile for Scenario 2025-4.

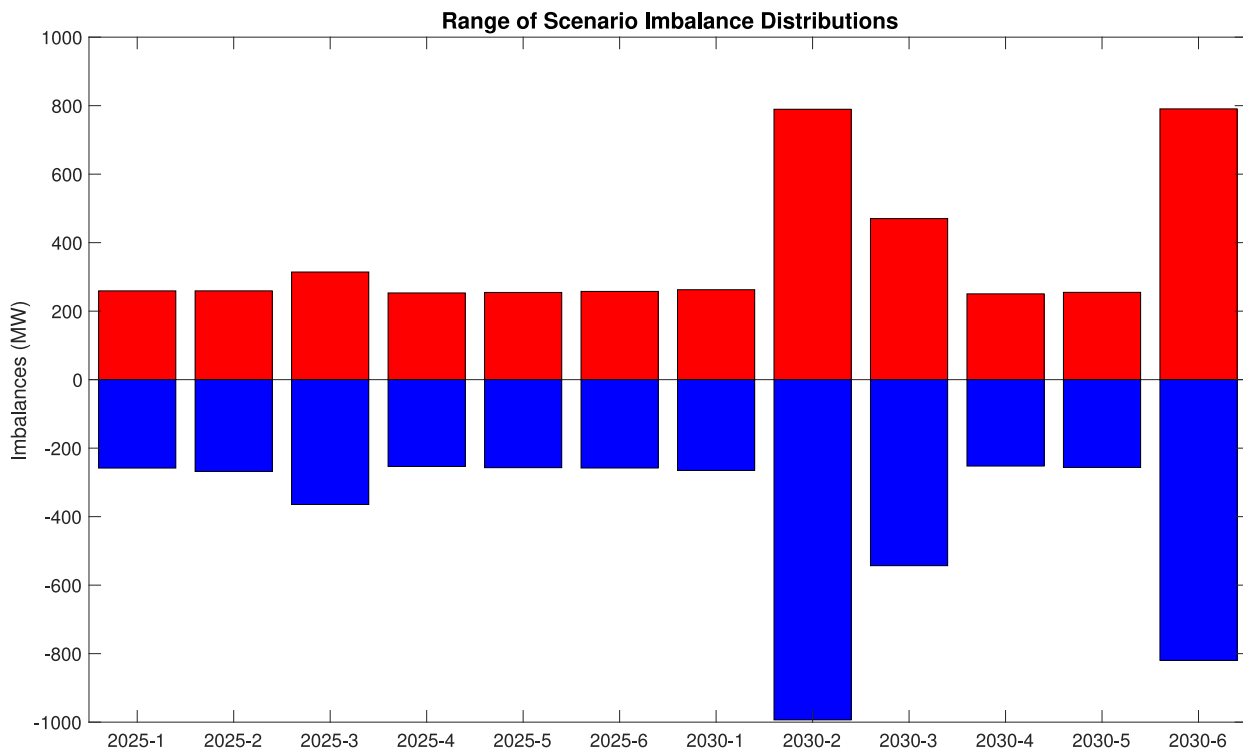


Fig. 50. Imbalance ranges for 2025 and 2030 scenarios.

degraded overall system reliability in real life because it is not clear at which absolute imbalance levels disruptive events might occur. The simulated imbalance excursions in all scenarios are comparable to the historical normal operation data.

6.3. Final insights

The above key findings indicate that Scenarios 2030-2, 2030-3 and 2030-6 and to a lesser extent 2025-3 have qualitatively and

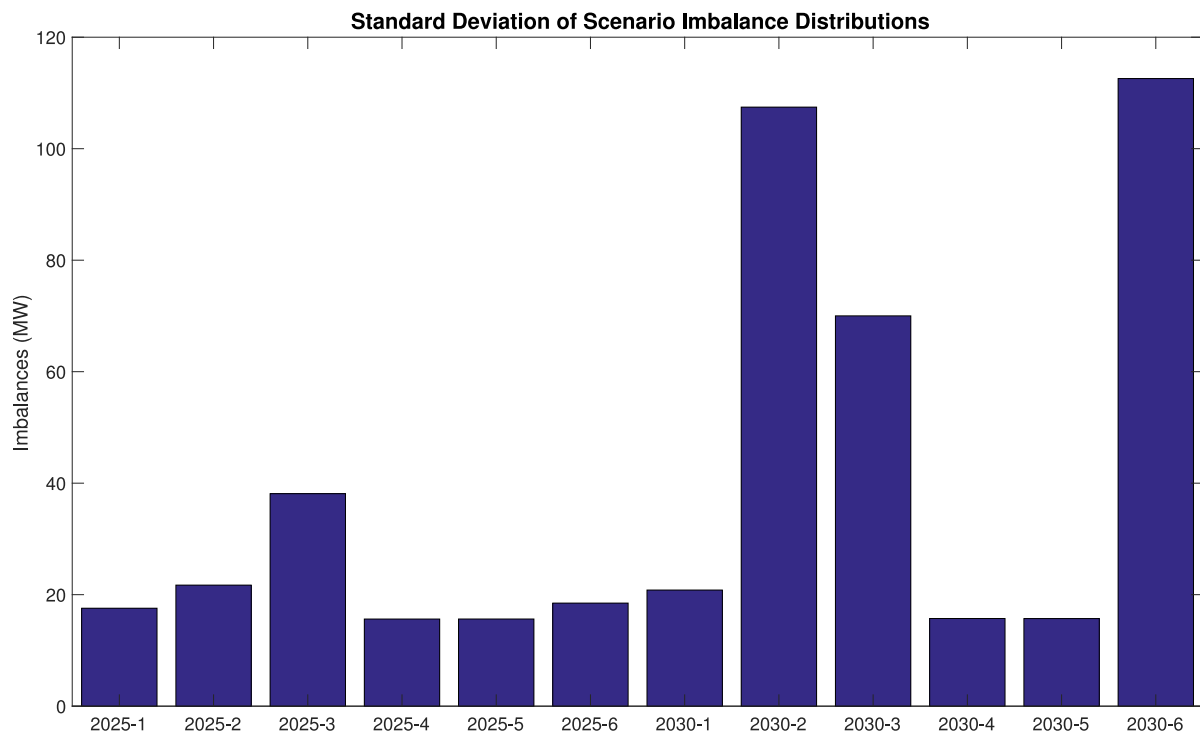


Fig. 51. Imbalance standard deviations for 2025 and 2030 scenarios.

quantitatively different behavior in large part due to the integration of variable energy resources. Consequently, it is important to ask what makes the integration of variable energy resources so different in New England and what actions could potentially serve to bring the balancing performance back to a level similar to that of other scenarios.

The presence of congestion caused by the integration of VERs in remote areas geographically isolates operating reserves in other parts of New England. Simply speaking, because the variable energy resource generation occurs “behind” a congested interface, operating reserves are unable to respond accordingly. Higher interface limits in the form of additional transmission lines would help accommodate these VERs because:

1. it would provide access to load centers that can absorb their power injections;
2. it would provide access to dispatchable resources with additional operating reserves
3. It would reduce the need for and reliance upon curtailment as a mitigating measure.

Removing system transmission constraints would improve the overall system balancing performance. The reduced curtailment levels may also result in a systemic shift in generated energy from dispatchable resources to relatively cheaper semi-dispatchable resources.

These scenarios also prominently show the emergence of curtailment as a balancing performance control lever. Indeed, in the presence of congestion and the absence of other (generation or load) energy resources in remote areas, curtailment often becomes the only control lever. The prominence of curtailment in these scenarios should also inspire deeper reflection. In many cases, curtailment levels are commensurate with the available load following reserves from dispatchable energy resources, and in other cases greatly surpass these values. Furthermore, that the mathematical form of curtailment is nearly equivalent to that of load following reserves should raise the question as to why they are treated differently. The only difference between dispatchable

and semi-dispatchable resources is that the former has a fixed upper capacity limit while the latter has a variable upper capacity limited by forecast. Similarly, curtailment directly contributes to a system’s ramping capability. The *time rate of change* of a curtailment signal is mathematically equivalent to ramping reserves. The values of operating reserves reported in this study should be interpreted in this context. In keeping with the ISO New England mission, a reconciliation of operating reserve and curtailment definitions could serve to clarify our understanding of overall system reliability and provide for an equitable administration of how these values are maintained on the system.

The increased penetration of variable energy resources is likely to require additional regulation reserves. While historically, this type of reserve has come exclusively from dispatchable resources, there is little to suggest that they could not come from semi-dispatchable resources in the future. Indeed, the curtailment signal used in this study did effectively move both upward and downward at the relatively time scale of the 10-minute real-time balancing optimization. If this signal were to become more temporally granular (perhaps with greater telemetry) to a 1-minute level, then it could serve the role of regulation.

In this study, many of the most challenging operational periods occurred during low-load spring and fall months. During these times, nuclear generation units were assumed to “must-run” at full capacity. Balancing performance is likely to improve if this assumption were to be relaxed. In other parts of the world, nuclear generation facilities have been shown to run at less than full capacity and to exhibit modest load following capability. Alternatively, and perhaps more imminently, it is possible to coordinate the scheduled maintenance of these units during these low load periods.

Finally, within these scenarios, energy storage and demand response played relatively minor roles either due to the associated penetration rates and due to the choice of their associated threshold prices. Investigating alternative scenarios in which these types of resources have a more prominent role can serve to rebalance the balancing burden away from curtailment as a primary lever to a broader diversity of energy resources across the

system. Again, a deep reflection of how such resources offer load following, ramping, and regulation reserve capability is needed.

In all, if these considerations are taken into account it is likely that the above scenarios could have a balancing performance that is equal or better than the other eight scenarios studied here.

Acknowledgments

The authors are grateful to ISO New England Inc. for the funding required to complete this work. The authors would also like to thank the ISO New England technical staff for its technical review of the work throughout the duration of the research project.

References

- ABB Inc. Electric Systems Consulting, GridView – An Analytic Tool for Market Simulation & Asset Performance Evaluations. URL <https://library.e.abb.com/public/d25b0020b72d94eac1256fda00488560/GridView%20Presentation.pdf>.
- Aigner, T., Jaehnert, S., Doorman, G.L., Gjengedal, T., 2012. The effect of large-scale wind power on system balancing in northern europe. *IEEE Trans. Sustain. Energy* 3 (4), 751–759. <http://dx.doi.org/10.1109/tste.2012.2203157>.
- Albadi, M., El-Saadany, E., 2011. Comparative study on impacts of wind profiles on thermal units scheduling costs. *IET Renew. Power Gener.* 5 (1), 26. <http://dx.doi.org/10.1049/iet-rpg.2009.0101>.
- Amin, M., 2001. Toward self-healing energy infrastructure systems. *IEEE Comput. Appl. Power* 14 (1), 20–28. <http://dx.doi.org/10.1109/67.893351>.
- Amin, M., 2006. Toward a self-healing energy infrastructure. In: *Power Engineering Society General Meeting*, IEEE, Montreal, Canada, p. 7, pp. BN – 1 4244 0493 2.
- Amin, M., 2008. Challenges in reliability, security, efficiency, and resilience of energy infrastructure: Toward smart self-healing electric power grid. In: *2008 IEEE Power and Energy Society General Meeting - Conversion and Delivery of Electrical Energy in the 21st Century*. In: *BT - 2008 IEEE Power and Energy Society General Meeting*, 20–24 July 2008, 2008 IEEE Power Energy Society General Meeting, IEEE, Pittsburgh, PA, USA, pp. 1–5. <http://dx.doi.org/10.1109/pes.2008.4596791>.
- Amin, S.M., 2011. Smart grid overview issues and opportunities. *Advances and challenges in sensing modeling simulation optimization and control*. *Eur. J. Control* 17 (5–6), 547–567. <http://dx.doi.org/10.3166/EJC.17.547-567>.
- Anon, 2017. Interconnection request queue. [online].
- Anonymous, 2010. NIST Framework and Roadmap for Smart Grid Interoperability Standards Release 1.0: NIST Special Publication 1108. Tech. Rep., Office of the National Coordinator for Smart Grid Interoperability, National Institute of Standards and Technology, United States Department of Commerce, Washington D.C., pp. 1–145.
- Anonymous, Grid, N., Transmission, E., Act, E., Britain, G., Act, P., 2012. The Grid Code. Tech. Rep. 5, National Grid Electricity Transmission plc, Warwick, UK, pp. 1–606.
- ANSI-ISA, 2000. Enterprise-Control System Integration Part 1: Models and Terminology. In: *ISA-95.00.01-2000*, July, Instrument Society of America, pp. 1–142.
- ANSI-ISA, 2005. Enterprise Control System Integration Part 3: Activity Models of Manufacturing Operations Management. Tech. Rep., The International Society of Automation.
- Apt, J., 2007. The spectrum of power from wind turbines. *J. Power Sources* 169 (2), 369–374.
- Beach, R., Muhlemann, A.P., Price, D.H.R., Paterson, A., Sharp, J.A., 2000. Review of manufacturing flexibility. *European J. Oper. Res.* 122 (1), 41–57. [http://dx.doi.org/10.1016/S0377-2217\(99\)00062-4](http://dx.doi.org/10.1016/S0377-2217(99)00062-4).
- Bird, L., Milligan, M., NREL, 2012. Lessons from large-scale renewable energy integration studies preprint. In: *2012 World Renewable Energy Forum*, no. NREL/CP-6A20-54666, Denver, CO, United states, p. 8.
- Bloom, A., Townsend, A., Palchak, D., Novacheck, I., King, J., Barrows, C., Ibanez, E., O'Connell, M., Jordan, G., Roberts, B., Draxl, C., Kenny, G., 2016. Eastern Renewable Generation Integration Study. Tech. Rep. NREL/TP-6A20-64472, National Renewable Energy Laboratory.
- Brooks, D.L., Lo, E.O., Smith, J.W., Pease, J.H., McGree, M., 2002. Assessing the Impact of wind Generation on System Operations At Xcel Energy – North and Bonneville Power Administration. Tech. Rep., North and Bonneville Power Administration, pp. 1–15.
- Brouwer, A.S., van den Broek, M., Seebregts, A., Faaij, A., 2014. Impacts of large-scale intermittent renewable energy sources on electricity systems, and how these can be modeled. *Renew. Sustain. Energy Rev.* 33, 443–466.
- Carpentier, J., 1962. Contribution to the economic dispatch problem. *Bull. Soc. Franc. Electr.* 3 (8), 431–447.
- CIGRE, 2010. Ancillary Services: An Overview of International Practices Technical Brochure 435. Tech. Rep., CIGRE Working Group C5.06.
- Corporation, E., Association, N.P., 2010. Nebraska Statewide Wind Integration Study Nebraska Statewide Wind Integration Study. Tech. Rep. NREL/SR-550-47519, National Renewable Energy Laboratory.
- Coste, W., 2016. 2016 Economic Studies Phase I Assumptions. Tech. Rep., ISO New England Planning Advisory Committee.
- Curtright, A.E., Apt, J., 2008. The character of power output from utility-scale photovoltaic systems. *Prog. Photovolt., Res. Appl.* 16 (September 2007), 241–247. <http://dx.doi.org/10.1002/ppv>.
- Daniel, F., Dimitry, P., Phillip, L., 2015. The Integration Costs of Wind and Solar Power. Tech. Rep. Agora Energiewende.
- De Toni, A., Tonchia, S., 1998. Manufacturing flexibility: a literature review. *Int. J. Prod. Res.* 36 (6), 1587–1617.
- Diaz-Gonzalez, F., Hau, M., Sumper, A., Gomis-Bellmunt, O., Díaz-gonzález, F., 2014. Participation of wind power plants in system frequency control : Review of grid code requirements and control methods. *Renew. Sustain. Energy Rev.* 34, 551–564.
- Easton, B., House, K., Byars, J., 2012. Smart Grid: A Race Worth Winning ? A Report on the Economic Benefits of Smart Grid. Tech. Rep. April, Ernst & Young, London, UK, pp. 1–48.
- Ela, E., Kirby, B., Lannoye, E., Milligan, M., Flynn, D., Zavadil, B., O'Malley, M., 2010. Evolution of operating reserve determination in wind power integration studies. In: *Power and Energy Society General Meeting*, 2010 IEEE. IEEE, pp. 1–8.
- Ela, E., Milligan, M., Kirby, B., 2011. Operating reserves and variable generation. *Contract* 303 (August), 275–3000.
- Ela, E., Milligan, M., Parsons, B., Lew, D., Corbus, D., 2009. The evolution of wind power integration studies: past, present, and future. In: *Power & Energy Society General Meeting*, 2009. PES'09. IEEE. IEEE, pp. 1–8.
- EnerNex, Corporation, E., 2010. Eastern Wind Integration and Transmission Study. Tech. Rep. January, EnerNex Corporation, Knoxville, TN.
- EWIS, 2010. Tech. Rep., ENTSO-E, Brussels, Belgium, pp. 1–90.
- Farid, A.M., Jiang, B., Muzhikyan, A., Youcef-Toumi, K., 2015. The need for holistic enterprise control assessment methods for the future electricity grid. *Renew. Sustain. Energy Rev.* 56 (1), 669–685.
- Farid, A.M., Muzhikyan, A., 2013. The need for holistic assessment methods for the future electricity grid (Best Applied Research Paper Award). In: *GCC CIGRE Power 2013*, Abu Dhabi, UAE, pp. 1–12. URL <http://amfarid.scripts.mit.edu/resources/Conferences/SPG-C13.pdf>.
- Frank, S., Rebennack, S., 2012. A Primer on Optimal Power Flow: Theory, Formulation, and Practical Examples. Working Papers 2012-14, October, pp. 1–42.
- GE Energy, 2010. Western Wind and Solar Integration Study. Tech. Rep. May, GE Energy, Schenectady, New York.
- GE-Energy, 2010. New England Wind Integration Study. Tech. Rep. May, GE Energy and ISO New England, Schenectady, New York, pp. 1–536.
- GE Energy, 2013. PJM Renewable Integration Study (PRIS) Project Review (Task 3a). Tech. Rep., GE Energy, Schenectady, New York.
- Gellings, C., 1985. The concept of demand-side management for electric utilities. *Proc. IEEE* 73 (10), 1468–1470.
- Gellings, C., Functioning, F., Grid, S., 2011. Estimating the Costs and Benefits of the Smart Grid. Tech. Rep., EPRI, Palo Alto, CA, USA, pp. 1–162.
- Georgilakis, P.S., 2008. Technical challenges associated with the integration of wind power into power systems. *Renew. Sustain. Energy Rev.* 12 (3), 852–863. <http://dx.doi.org/10.1016/j.rser.2006.10.007>.
- Giebel, G., Brownsword, R., Kariniotakis, G., Denhard, M., Draxl, C., 2011. The State-Of-The-Art in Short-Term Prediction of Wind Power: A Literature Overview, second ed. ANEMOS.plus, Roskilde, Denmark, pp. 1–109.
- Gomez-Exposito, A., Conejo, A.J., Canizares, C., 2008. *Electric Energy Systems: Analysis and Operation*. CRC Press, Boca Raton, FL.
- Gunasekaran, A., 1998. Agile manufacturing: enablers and an implementation framework. *Int. J. Prod. Res.* 36 (5), 1223–1247.
- Halamay, D.A., Brekken, T.K.A., Simmons, A., McArthur, S., 2011. Reserve requirement impacts of large-scale integration of wind, solar, and ocean wave power generation. *IEEE Trans. Sustain. Energy* 2 (3), 321–328. <http://dx.doi.org/10.1109/tste.2011.2114902>.
- Hannele, H., 2018. Wind integration costs—methodologies and shortfalls. Tech. Rep. VTT Technical Research Center of Finland LTD.
- Hansen, C.W., Papalexopoulos, A.D., 2012. Operational impact and cost analysis of increasing wind generation in the island of crete. *IEEE Syst. J.* 6 (2), 287–295. <http://dx.doi.org/10.1109/jsyst.2011.2163011>.
- Henderson, M.I., 2016. 2016 Economic Studies:S2 Sensitivity Study Draft Results. Tech. Rep., ISO New England Planning Advisory Committee.
- Hoflich, B., Molly, J.P., Neddermann, B., Schorer, T., Callies, D., Knorr, K., Rohrig, K., Sant-Drenan, Y.-M., Bachmann, U., Bauer, R., Konnemann, A., Muller, J., Radtke, H., August, I., Grebe, E., Groninger, S., Neumann, C., Runge, J., Abele, H., Jung, S., Schroth, V., Sener, O., Bopp, S., Nguen, Y., Schmale, M., Siebels, C., Winter, W., Borggreffe, F., Grave, K., Lindenberger, D., Merz, C., Nicolosi, M., Nusler, A., Richter, J., Paulus, M., Samisch, H., Schwill, J., Stadler, I., Dobschinski, J., Faulstich, S., Puchta, M., Sievers, J., 2010. DENA Grid Study II: Integration of Renewable Energy Sources in the German Power Supply Systems from 2015–2020 with an Outlook to 2025. Tech. Rep., German Energy Agency, Berlin, Germany, pp. 1–615.

- Holtinen, H., 2018. Advances in wind integration, recent findings from international collaboration IEAWIND task 25. In: Grand Renewable Energy 2018 International Conference, Yokohama June 18–22, 2018.
- Holtinen, H., Malley, M., Dillon, J., Flynn, D., 2012a. Tech. Rep. International Energy Agency, Helsinki, pp. 1–7.
- Holtinen, H., Milligan, M., Ela, E., Menemenlis, N., Dobschinski, J., Rawn, B., Bessa, R.J., Flynn, D., Gomez-Lazaro, E., Detlefsen, N.K., 2012b. Methodologies to determine operating reserves due to increased wind power. *IEEE Trans. Sustain. Energy* 3 (4), 713–723. <http://dx.doi.org/10.1109/tste.2012.2208207>.
- Holtinen, H., Milligan, M., Kirby, B., Acker, T., Neimane, V., Molinski, T., 2008. Using standard deviation as a measure of increased operational reserve requirement for wind power. *Wind Eng.* 32 (4), 355–377. <http://dx.doi.org/10.1260/0309-524X.32.4.355>.
- Holtinen, H., Orth, A., Abilgaard, H., van Hulle, F., Kiviluoma, J., Lange, B., O'Malley, M., Flynn, D., Keane, A., Dillon, J., Carlini, E.M., Tande, J.O., Estanquero, A., Lazaro, E.G., Soder, L., Milligan, M., Smith, C., Clark, C., 2013. IEA Wind Export Group Report on Recommended Practices Wind Integration Studies. Tech. Rep., International Energy Agency, Paris, France, pp. 1–89.
- IEA, 2017. Natural gas prices in 2016 were the lowest in nearly 20 years. [online] [cited 06/06/2017].
- IEA, 2018. Expert Group Report on Recommended Practices 16. Wind/PV Integration Studies. Tech. Rep., International Energy Agency.
- ISO New England, 2016a. CELT Report: 2016–2025 Forecast Report of Capacity, Energy, Loads, and Transmission. Tech. Rep., ISO New England, URL https://www.iso-ne.com/static-assets/documents/2016/05/2016_celt_report.xls.
- ISO New England, 2016b. Renewable Portfolio Standards Spreadsheet. Tech. Rep., ISO New England.
- ISO New England, 2016c. ISO New England's Internal Market Monitor – 2015 Annual Markets Report. Tech. Rep., ISO New England, Holyoke, MA, URL https://www.iso-ne.com/static-assets/documents/2016/05/2015_imm_amr_final_5_25_2016.pdf.
- ISO New England, 2017a. 2015 ISO New England Electric Generator Air Emissions Report. Tech. Rep., ISO New England Inc. System Planning, January. URL https://www.iso-ne.com/static-assets/documents/2017/01/2015_emissions_report.pdf.
- ISO New England, 2017b. 2016 Economic Study: NEPOOL Scenario Analysis. Tech. Rep., ISO New England.
- ISO New England, 2017c. ISO New England Reserve Requirements. Tech. Rep., ISO New England Inc.
- ISO New England, 2017d. Resource mix-ISO new England. [online] [cited 06/07/2017].
- ISO NEWSWIRE, 2018. A regional first: New Englanders used less grid electricity midday than while they were sleeping on april 21. [online] [cited December 9, 2018].
- Jiang, B., Farid, A.M., Youcef-Toumi, K., A comparison of day-ahead wholesale market: Social Welfare vs industrial demand side management. In: IEEE International Conference on Industrial Technology, Sevilla, Spain, pp. 1–7. <http://dx.doi.org/10.1109/ICIT.2015.7125502>.
- Jiang, B., Farid, A.M., Youcef-Toumi, K., 2015b. Demand side management in a day-ahead wholesale market: a comparison of industrial and social welfare approaches. *Appl. Energy* 156 (1), 642–654. <http://dx.doi.org/10.1016/j.apenergy.2015.07.014>.
- Jiang, B., Farid, A.M., Youcef-Toumi, K., 2015c. Impacts of industrial baseline errors on demand side management in day-ahead wholesale markets. In: Proceedings of the ASME Power & Energy 2015: Energy Solutions for Sustainable Future, San Diego, CA, pp. 1–7. <http://engineering.dartmouth.edu/liines/resources/Conferences/SPG-C45.pdf>.
- Jiang, B., Muzhikyan, A., Farid, A.M., Youcef-Toumi, K., 2015d. Impacts of industrial baseline errors in demand side management enabled enterprise control. In: IECON 2015 – 41st Annual Conference of the IEEE Industrial Electronics Society, Yokohama, Japan, pp. 1–6. <http://dx.doi.org/10.1109/IECON.2015.7392637>.
- Johnson, B., Lindsay, J., Myers, K., Woods, P., Yourkowski, C., 2014. Solar integration study report. Tech. Rep. June, Idaho Power, pp. 1–36.
- Kassakian, J.G., Schmalensee, R., Desgroseillers, G., Heidel, T.D., Afridi, K., Farid, A.M., Grochow, J.M., Hogan, W.W., Jacoby, H.D., Kirtley, J.L., Michaels, H.G., Perez-Arriaga, I., Perreault, D.J., Rose, N.L., Wilson, G.L., Abudaldah, N., Chen, M., Donohoo, P.E., Gunter, S.J., Kwok, P.J., Sakhrani, V.A., Wang, J., Whitaker, A., Yap, X.L., Zhang, R.Y., Massachusetts Institute of Technology, 2011. The Future of the Electric Grid: An Interdisciplinary MIT Study. MIT Press, Cambridge, MA, pp. 1–280, URL http://web.mit.edu/mitei/research/studies/documents/electric-grid-2011/Electric_Grid_Full_Report.pdf.
- Kosanke, K., Vernadat, F., Zelm, M., 1999. CIMOSA: Enterprise engineering and integration. *Comput. Ind.* 40 (2–3), 83–87.
- Lapalus, E., Fang, S., Rang, C., van Gerwen, R., 1995. Manufacturing integration. *Comput. Ind.* 27 (2), 155–165.
- Lew, D., Brinkman, G., Ibanez, E., Florita, A., Heaney, M., Hodge, B., Hummon, M., King, J., 2013. The Western Wind and Solar Integration Study Phase 2 The Western Wind and Solar Integration Study Phase 2. Tech. Rep. NREL/TP-5500-55588, National Renewable Energy Laboratory.
- Luickx, P., Delarue, E., D'haeseleer, W., 2009. Effect of the generation mix on wind power introduction. *IEEE Renew. Power Gener.* 3 (3), 267. <http://dx.doi.org/10.1049/iet-rpg.2008.0061>.
- Martin, P.G., 2012. The Need for Enterprise Control, vol. Nov/Dec. InTech, pp. 1–5.
- McArthur, S.D.J., Taylor, P.C., Ault, G.W., King, J.E., Athanasiadis, D., Alimisis, V.D., Czaplewski, M., 2012. The autonomic power system - network operation and control beyond smart grids. In: 2012 3rd IEEE PES Innovative Smart Grid Technologies Europe, (ISGT Europe). In: IEEE PES Innovative Smart Grid Technologies Conference Europe, IEEE, Berlin, Germany, pp. 1–7. <http://dx.doi.org/10.1109/isgteurope.2012.6465807>.
- Mohseni, M., Islam, S.M., 2012. Review of international grid codes for wind power integration: Diversity, technology and a case for global standard. *Renew. Sustain. Energy Rev.* 16 (6), 3876–3890. <http://dx.doi.org/10.1016/j.rser.2012.03.039>.
- Monteiro, C., Bessa, R., Miranda, V., Botterud, A., Wang, J., Conzelmann, G., 2009. Wind Power Forecasting: State-of-the-Art 2009 Decision and Information Sciences Division. Tech. Rep. November 6, Argonne National Laboratory, Illinois, pp. 1–216, URL http://www.osti.gov/energycitations/product.biblio.jsp?osti_id=968212.
- Moreno-Munoz, A., de la Rosa, J., Posadillo, R., Pallares, V., 2008. Short term forecasting of solar radiation. In: Industrial Electronics, 2008. ISIE 2008. IEEE International Symposium on, pp. 1537–1541. <http://dx.doi.org/10.1109/isie.2008.4676880>.
- Muzhikyan, A., Farid, A.M., Mezher, T., 2016. The impact of wind power geographical smoothing on operating reserve requirements. In: IEEE American Control Conference, Boston, MA, USA, pp. 1–6.
- Muzhikyan, A., Farid, A.M., Youcef-Toumi, K., 2013. Variable energy resource induced power system imbalances: A generalized assessment approach. In: IEEE Conference on Technologies for Sustainability, Portland, Oregon, pp. 1–8. <http://dx.doi.org/10.1109/SusTech.2013.6617329>.
- Muzhikyan, A., Farid, A.M., Youcef-Toumi, K., 2013. Variable energy resource induced power system imbalances: Mitigation by increased system flexibility, spinning reserves and regulation. In: IEEE Conference on Technologies for Sustainability, pp. Portland, Oregon, pp. 1–7. <http://dx.doi.org/10.1109/SusTech.2013.6617292>.
- Muzhikyan, A., Farid, A.M., Youcef-Toumi, K., 2014a. A power grid enterprise control method for energy storage system integration. In: IEEE Innovative Smart Grid Technologies Conference Europe, Istanbul, Turkey, pp. 1–6. <http://dx.doi.org/10.1109/ISGTEurope.2014.7028898>.
- Muzhikyan, A., Farid, A.M., Youcef-Toumi, K., 2014b. An enhanced method for the determination of load following reserves. In: American Control Conference, 2014, Portland, Oregon, 2014, pp. 1–8. <http://dx.doi.org/10.1109/ACC.2014.6859254>.
- Muzhikyan, A., Farid, A.M., Youcef-Toumi, K., 2015a. An enterprise control assessment method for variable energy resource induced power system imbalances Part 1: Methodology. *IEEE Trans. Ind. Electron.* 62 (4), 2448–2458. <http://dx.doi.org/10.1109/TIE.2015.2395391>.
- Muzhikyan, A., Farid, A.M., Youcef-Toumi, K., 2015b. An enterprise control assessment method for variable energy resource induced power system imbalances Part 2: Results. *IEEE Trans. Ind. Electron.* 62 (4), 2459–2467. <http://dx.doi.org/10.1109/TIE.2015.2395380>.
- Muzhikyan, A., Farid, A.M., Youcef-Toumi, K., 2015c. An enhanced method for determination of the regulation reserves. In: IEEE American Control Conference, Los Angeles, CA, USA, pp. 1–8. <http://dx.doi.org/10.1109/ACC.2015.7170866>.
- Muzhikyan, A., Farid, A.M., Youcef-Toumi, K., 2015d. An enhanced method for determination of the ramping reserves. In: IEEE American Control Conference, Los Angeles, CA, USA, pp. 1–8. <http://dx.doi.org/10.1109/ACC.2015.7170863>.
- Muzhikyan, A., Farid, A.M., Youcef-Toumi, K., 2016a. An a priori analytical method for determination of operating reserves requirements. *Int. J. Energy Power Syst.* 86 (3), 1–11. <http://dx.doi.org/10.1016/j.ijepes.2016.09.005>.
- Muzhikyan, A., Farid, A.M., Youcef-Toumi, K., 2016b. Relative merits of load following reserves and energy storage market integration towards power system imbalances. *Int. J. Electr. Power Energy Syst.* 74 (1), 222–229. <http://dx.doi.org/10.1016/j.ijepes.2015.07.013>.
- NERC, 2012. Reliability standards for the bulk electric systems of north america. In: NERC Reliability Standards Complete Set. Tech. Rep., NERC–North American Electric Reliability Corporation, pp. 1–10, URL http://www.nerc.com/files/Reliability_Standards_Complete_Set_1Dec08.pdf.
- PACIFICORP, 2010. Project Method for 2010 Wind Integration Cost Study. Tech. Rep., PacificCorp.
- Pels, H., Wortmann, J., Zwegers, A., 1997. Flexibility in manufacturing: an architectural point of view. *Comput. Ind.* 33 (2–3), 271–283.
- Podmore, R., Robinson, M.R., 2010. The role of simulators for smart grid development. *IEEE Trans. Smart Grid* 1 (2), 205–212. <http://dx.doi.org/10.1109/tsg.2010.2055905>.
- Rebours, Y.G., Kirschen, D.S., Trotignon, M., Rossignol, S., 2007. A survey of frequency and voltage control ancillary services—Part I: Technical features. *IEEE Trans. Power Syst.* 22 (1), 350–357.

- Report, F., Bertsh, J., Growitsch, C., Lorenczik, S., Nagl, S., 2012. Flexibility Options in European Electricity Markets in High RES-E Scenarios Study on behalf of the International Energy Agency (IEA). Tech. Rep. October, Institute of Energy Economics, Cologne, Germany, pp. 163–186.
- Robitaille, A., Kamwa, I., Oussedik, A.H., de Montigny, M., Menemenlis, N., Huneault, M., Forcione, A., Mailhot, R., Bourret, J., Bernier, L., 2012. Preliminary impacts of wind power integration in the hydro-quebec system. *Wind Eng.* 36 (1), 35–52. <http://dx.doi.org/10.1260/0309-524x.36.1.35>.
- Rourke, S.J., 2015. New England's energy resource mix is changing rapidly. [online].
- Sanchez, L.M., Nagi, R., 2001. A review of agile manufacturing systems. *Int. J. Prod. Res.* 39 (16), 3561–3600. <http://dx.doi.org/10.1080/00207540110068790>.
- Schavemaker, P., Van der Sluis, L., Books24x7 Inc., 2008. Electrical Power System Essentials. Wiley, Chichester, England; Hoboken, NJ, URL <http://www.loc.gov/catdir/enhancements/fy0810/2008007359-d.html>, <http://www.loc.gov/catdir/enhancements/fy0810/2008007359-t.html>.
- Shlatz, E., Frantzis, L., McClive, T., Karlson, G., Acharya, D., Lu, S., Etingov, P., Diao, R., Ma, J., Samaan, N., Chadliev, V., Smart, M., Salgo, R., Sorensen, R., Allen, B., Idelchik, B., Ellis, A., Stein, J., Hanson, C., Makarov, Y.V., Guo, X., Hafen, R.P., Jin, C., Kirkham, H., 2011. Large-Scale PV Integration Study. Tech. Rep., Navigant Consulting, Las Vegas, NV, USA, pp. 1–172.
- Soder, L., Holttinen, H., Issues, G.E., 2008. On methodology for modelling wind power impact on power systems. *Int. J. Glob. Energy Issues (Switzerland)*, 29 (1–2), 181–198.
- Stott, B., Jardim, J., Alsaç, O., 2009. DC Power flow revisited. *IEEE Trans. Power Syst.* 24 (3), 1290–1300.
- Ummels, B.C., 2009. Power System Operation with Large-Scale Wind Power in Liberalised Environments (Ph.D. thesis). Technical University of Delft, pp. 1–193.
- Ummels, B.C., Gibescu, M., Pelgrum, E., Kling, W.L., Brand, A.J., 2007. Impacts of wind power on thermal generation unit commitment and dispatch. In: Gibescu, M. (Ed.), *IEEE Trans. Energy Convers.* 22 (1), 44–51. <http://dx.doi.org/10.1109/TEC.2006.889616>, URL <http://ieeexplore.ieee.org/lpdocs/epic03/wrapper.htm?arnumber=4106021>.
- University of Hawaii, Anonymous, 2011. Oahu Wind Integration Study. Tech. Rep. February, University of Hawaii, Hawaii Natural Energy Institute, School of Ocean and Earth Science and Technology, Oahu, HA, pp. 1–229.
- UVIG, 2017. 2017 Spring Technical Workshop. Tech. Rep., Utility Variable-Generation Integration Group.
- van Welie, G., 2018. ISO New england identifies fuel-security risk as the power system undergoes rapid transformation. May, [online] [cited November 19, 2018].
- von Meier, A., 2006. Electric power systems: a conceptual introduction. Wiley Survival Guides in Engineering and Science. IEEE Press : Wiley-Interscience, Hoboken, N.J., p. xv, 309 p.
- Wang, C., Lu, Z., Qiao, Y., 2012. A consideration of the wind power benefits in day-ahead scheduling of wind-coal intensive power systems Caixiawang, student member, ieee, zongxiang lu, member, ieee, and. *IEEE Trans. Power Syst.* 1–10. <http://dx.doi.org/10.1109/TPWRS.2012.2205280>.
- Williams, T., Rathwell, G., Li, H., 2001. A Handbook on Master Planning and Implementation for Enterprise Integration Programs. Purdue University Institute for Interdisciplinary Engineering Studies, pp. 1–342.
- Wood, A., Wollenberg, B., 2014. Power Generation, Operation, and Control, third ed. John Wiley & Sons, Hoboken, NJ, USA.
- Wu, F., Moslehi, K., Bose, A., 2005. Power system control centers: Past, present, and future. *Proc. IEEE* 93 (11), 1890–1908. <http://dx.doi.org/10.1109/JPROC.2005.857499>.
- Yan, Y., Qian, Y., Sharif, H., Tipper, D., 2013. A survey on smart grid communication infrastructures: Motivations, requirements and challenges. *IEEE Commun. Surv. Tutor.* 15 (1), 5–20. <http://dx.doi.org/10.1109/surv.2012.021312.00034>.